Neural Plasticity

Imaging Neural Plasticity following Brain Injury

Guest Editors: Lijun Bai, Lin Ai, and Kevin K. W. Wang

Imaging Neural Plasticity following Brain Injury

Neural Plasticity

Imaging Neural Plasticity following Brain Injury

Guest Editors: Lijun Bai, Lin Ai, and Kevin K. W. Wang

Editorial Board

Contents

Hindawi Publishing Corporation
Neural Plasticity
Volume 2017, Article ID 2083294, 2 pages
http://dx.doi.org/10.1155/2017/2083294

Editorial

Imaging Neural Plasticity following Brain Injury

Lijun Bai,[1,2] Lin Ai,[3] and Kevin K. W. Wang[4]

[1] *The Key Laboratory of Biomedical Information Engineering, Ministry of Education, Department of Biomedical Engineering, School of Life Science and Technology, Xi'an Jiaotong University, Xi'an 710049, China*
[2] *Athinoula A. Martinos Center for Biomedical Imaging, Department of Radiology, Massachusetts General Hospital, Harvard Medical School, Charlestown, MA, USA*
[3] *Department of Nuclear Medicine, Beijing Tiantan Hospital, Capital Medical University, Beijing, China*
[4] *Program for Neurotrauma, Neuroproteomics and Biomarker Research, Departments of Psychiatry and Neuroscience, University of Florida, Gainesville, FL, USA*

Correspondence should be addressed to Lijun Bai; bailj4152615@gmail.com

Received 11 January 2017; Accepted 11 January 2017; Published 28 February 2017

The human brain possesses a superior capacity to reorganize and profound plasticity after focal lesions following brain injury such as trauma, ischemia, and degenerative disorders. The concept of plasticity describes the mechanisms that rearrange cerebral organization following a brain injury. The development of sophisticated noninvasive neuroimaging techniques over the past decade provides a unique opportunity to examine brain plasticity in humans and invaluable insights into the mechanisms underlying neuroplasticity. Unifying pathogenesis of brain injury by neuroimaging techniques can be beneficial to develop therapeutic strategies with broad applicability for disease prevention and an opportunity to decrease morbidity and mortality from these disorders in human beings.

In this special issue on imaging neural plasticity following brain injury, we compiled a series of articles that represent novel primary research and explore brain plasticity following brain injury. T. Wang et al. ("Impairments in brain Perfusion, Metabolites, Functional Connectivity, and Cognition in Severe Asymptomatic Carotid Stenosis Patients: An Integrated MRI Study") investigate the brain impairments following asymptomatic carotid stenosis by utilizing an integrated MRI including pulsed Arterial Spin Labeling (pASL) 22 MRI, Proton MR Spectroscopy (MRS) and resting-state functional MRI (R-fMRI). They found that hypoperfusion in the left frontal lobe, lower NAA/Cr ratio in the left hippocampus, and decreased connectivity to the posterior cingulate cortex in the anterior part of the default mode network might partly contribute to the cognition impairment in these patients.

X. Fan et al. ("Distinctive Structural and Effective Connectivity Changes of Semantic Cognition Network across Left and Right Mesial Temporal Lobe Epilepsy Patients") explore the distinctive brain structural and effective connectivity changes within the semantic cognition network by comparing left and right mesial temporal lobe epilepsy (mTLE) patients and these patients to matched healthy controls. Since seizure attacks were rather targeted than random for patients with hippocampal sclerosis (HS), gray matter atrophy of left mTLE was more serve than that of right mTLE across the whole brain and especially within the contralateral semantic cognition network. This study suggested that left HS patients had a higher vulnerability to seizure attacks, reflecting the compensation strategy. The altered effective connectivity between subregions of the ATL may be the possible reason to explain the more severe name-finding impairment but good comprehension ability.

H. Yan et al. ("Altered Effective Connectivity of Hippocampus-Dependent Episodic Memory Network in mTBI Survivors") examined the altered effective interaction in mild traumatic brain injury (TBI) survivors' episodic memory network. Results presented that mild TBI induced increased bilateral and decreased ipsilateral effective connectivity in the episodic memory network compared with normal controls.

This study provided some evidence to note the overrecruitment of the right anterior PFC caused dysfunction of the strategic component of episodic memory, which caused deteriorating episodic memory in mTBI survivors.

Z. Guo et al. ("Ipsilesional High Frequency Repetitive Transcranial Magnetic Stimulation Add-On Therapy Improved Diffusion Parameters of Stroke Patients with Motor Dysfunction: A Preliminary DTI Study") aimed to evaluate the effects of high frequency repetitive transcranial magnetic stimulation (HF-rTMS) on stroke patients with motor dysfunction and to investigate the underlying neural mechanism. Fifteen stroke patients were assigned to the rTMS treatment (RT) group and conventional treatment (CT) group. RT group showed better improvement in motor scale and enhanced diffusion metrics in the posterior limb internal capsule, which was associated with motor functions.

S. Zhang et al. ("Alternations in Cortical Thickness and White Matter Integrity in Mild-to-Moderate Communicating Hydrocephalic School-Aged Children Measured by Whole-Brain Cortical Thickness Mapping and DTI") explored the cortical thickness and white matter integrity following mild-to-moderate hydrocephalic in children. They found that decreased cortical thickness in the left middle temporal and left rostral middle frontal gyrus in these children compared with normal controls, and diffusion metrics were also decreased in the right body part of the corpus callosum. This study provides the evidence that structural brain changes can be used to monitor long-term outcomes and follow-up in the mild-to-moderate hydrocephalic of children.

Finally, N. Ilves et al. ("Resting-State Functional Connectivity and Cognitive Impairment in Children with Perinatal Stroke") investigate the dysfunctions in the large-scale resting-state functional networks following perinatal stroke in children and its association with congenital hemiparesis and neurocognitive deficits. Results indicated that there were no differences in severity of hemiparesis between the periventricular venous infarction (PVI) and arterial ischemic stroke (AIS) groups. A significant increase in default mode network connectivity (FDR 0.1) and lower cognitive functions were found in children with AIS compared to the controls and the PVI group. The children with PVI had no significant differences in the resting-state networks compared to the controls and their cognitive functions were normal. They further inferred that changes in the resting-state networks found in children with AIS could possibly serve as the underlying derangements of cognitive brain functions in these children.

Great progress has been made and demonstrated the role of functional connectivity and structural abnormalities underlying brain injury (i.e., stroke, traumatic brain injury, and epilepsy), while there is also unclarity about whether these brain changes can provide a clue (as a biomarker) to establish prognostic models, develop focused treatments, and stratify patients for interventional trials. U. Horn et al. ("MRI-Biomarkers for Hand-Motor Outcome Prediction and Therapy-Monitoring following Stroke") conducted a comprehensive review about MRI-biomarkers on the evaluation of corticospinal integrity and functional recruitment of motor resources. Compared with the functional connectivity parameters, corticospinal integrity evaluation using structural imaging showed robust and high predictive power for patients with different levels of impairment. They further suggested a combination of different measures in an algorithm to classify fine-graded subgroups of patients, because the best therapy approaches will become feasible as the subgroup become more specified.

This special issue provides promising evidence to elucidating neural plasticity associated with a wide range of brain injuries. These articles may enhance further research into examining whether the neuroprognosis of imaging biomarker is beneficial to treatment selection and effectiveness evaluation following brain injury.

Lijun Bai
Lin Ai
Kevin K. W. Wang

Hindawi Publishing Corporation
Neural Plasticity
Volume 2017, Article ID 8738714, 7 pages
http://dx.doi.org/10.1155/2017/8738714

Research Article

Impairments in Brain Perfusion, Metabolites, Functional Connectivity, and Cognition in Severe Asymptomatic Carotid Stenosis Patients: An Integrated MRI Study

Tao Wang,[1] Feng Xiao,[2] Guangyao Wu,[2] Jian Fang,[2] Zhenmeng Sun,[2] Hongliang Feng,[1] Junjian Zhang,[1] and Haibo Xu[2]

[1]*Department of Neurology, Zhongnan Hospital of Wuhan University, Wuhan, China*
[2]*Department of Radiology, Zhongnan Hospital of Wuhan University, Wuhan, China*

Correspondence should be addressed to Junjian Zhang; wdsjkx@163.com and Haibo Xu; xuhaibo1120@hotmail.com

Received 23 September 2016; Revised 15 November 2016; Accepted 7 December 2016; Published 1 February 2017

Academic Editor: Lijun Bai

Carotid artery stenosis without transient ischemic attack (TIA) or stroke is considered as "asymptomatic." However, recent studies have demonstrated that these asymptomatic carotid artery stenosis (aCAS) patients had cognitive impairment in tests of executive function, psychomotor speed, and memory, indicating that "asymptomatic" carotid stenosis may not be truly asymptomatic. In this study, when 19 aCAS patients compared with 24 healthy controls, aCAS patients showed significantly poorer performance on global cognition, memory, and executive function. By utilizing an integrated MRI including pulsed arterial spin labeling (pASL) MRI, Proton MR Spectroscopy (MRS), and resting-state functional MRI (R-fMRI), we also found that aCAS patients suffered decreased cerebral blood flow (CBF) mainly in the Left Frontal Gyrus and had decreased NAA/Cr ratio in the left hippocampus and decreased connectivity to the posterior cingulate cortex (PCC) in the anterior part of default mode network (DMN).

1. Introduction

Carotid artery stenosis without transient ischemic attack (TIA) or stroke is considered as "asymptomatic" [1]. However, recent studies have demonstrated that these asymptomatic carotid artery stenosis (aCAS) patients had cognitive impairment in tests of executive function, psychomotor speed, and memory [2–4]. However, the pathophysiological mechanism of cognition impairment in aCAS patients has not been understood thoroughly.

In the past few years, several imaging techniques have increasingly been used to study cognition impairment in humans, such as pulsed arterial spin labeling (pASL) MRI, Proton MR Spectroscopy (MRS), and resting-state functional MRI (R-fMRI) [5–7]. pASL MRI can be used to detect regional cerebral blood flow (CBF) while MRS can measure relative changes in metabolites, which had been changed at a very early stage of cognitive impairment. R-fMRI evaluates the temporal correlation between the spontaneous blood oxygenation level-dependent (BOLD) fluctuations at resting-state [8]. We tested two parameters, functional connectivity (FC) and amplitude of low-frequency fluctuation (ALFF). FC reflects interregional cooperation while ALFF refers to the intensity of regional brain activity [9, 10]. Since lots of previous studies have reported that the posterior cingulate cortex (PCC) is one of the key nodes of default mode network (DMN) and cognition, the region of interest (ROI) in this study was set at this node [11, 12].

In this study, our first goal was to detect the differences in CBF, metabolites, and intrinsic functional network connectivity between aCAS patients and healthy controls. Secondly, we tried to find whether these differences were related to the cognition differences.

2. Methods

2.1. Participants, Inclusion Criteria, and Exclusion Criteria. We recruited testable aCAS patients from Zhongnan Hospital

affiliated to Wuhan University between January 2015 and June 2016. The inclusion criteria include the following: (1) age from 55 to 80 years; (2) ICA stenotic degree ⩾ 70%; (3) right-hand dominance; (4) being free of stroke, TIA, dementia, or depression; (5) Modified Rankin Scale: score 0 or 1; and (6) no major psychiatric disease or other medical conditions. The exclusion criteria were (1) contralateral internal carotid artery stenosis ⩾ 50%; (2) posterior circulation diseases; (3) MMSE < 26; (4) functional disability (Modified Rankin Scale ≥ 2); (5) severe systemic diseases and neuropsychiatric diseases (such as congestive heart failure and history of stroke); (6) any contraindications for MR scan (e.g., metal implants); and (7) low education level (<6 years). In the meanwhile, we also recruited 24 age and education level matched healthy controls. Written informed consent was obtained from all participants. All the study procedures were approved by the Zhongnan Hospital Review Board.

2.2. Cognition Assessments. Cognition assessments were performed within 7 days of MRI scan. The MMSE and MoCA Beijing Version were utilized to assess the global cognition. The Digit Symbol Test required subjects to translate numbers to symbols in a given time and correct translations within 90 seconds were recorded. The Rey Auditory Verbal Learning Test (RAVLT) was applied to evaluate the memory and verbal learning ability. The participant should try to recall the words as much as he/she can remember. This procedure was repeated five times and then followed a delayed recall after thirty minutes. The total number of the words immediately recalled during the first five repeats and the sum of the delayed recall were record accordingly. In the Verbal Memory Test, participants were required to repeat orally presented lists of numbers, beginning with a 2 number sequence, and each correct performance was followed by 1 additional number. In the forward span, participants were asked to retell the span in forward order. In the backward span, participants were asked to retell the span in reverse order.

2.3. Brain Imaging Collection. MRI images were acquired using a 3.0 Tesla Siemens scanner at Zhongnan Hospital. pASL perfusion images were collected using Q2TIPS II technique. Scan parameters were TR = 2500 ms, TE = 11 ms, FOV = 240 × 240 mm^2, matrix = 64 × 64, FA = 90°, and slice thickness = 6 mm. ^{1}H MRS chemical shift imaging (CSI) was conducted according to the following protocol: TR = 1600 ms, TE = 135 ms, FOV = 160 × 160 mm^2, matrix = 16 × 16, and voxel size = 10 × 10 × 16 mm^3. R-fMRI were acquired using EPI sequence: Repetition Time = 2000 ms, Echo Time = 30 ms, Flip Angle = 90°, number of slices: 33, slice thickness: 3.8 mm, gap: 1 mm, data matrix: 64 × 64, and Field of View = 240 × 240 mm^2.

2.4. Image Processing

2.4.1. pASL. relCBF were automatically generated by Siemens workstation and then were normalized to EPI template provided by Statistical Parametric Mapping 8 (SPM8). The final voxel size was 3 × 3 × 3 mm^3. Each subject's relCBF map was transformed into standard MNI space using these transformation parameters. These normalized relCBF maps were then smoothed with 8 mm FWHM isotropic Gaussian kernel. SPM8 were then used to identify significant different regions between two groups.

2.4.2. MRS. Since previous study had demonstrated that abnormal level of hippocampus metabolites may mediate cognitive performance, we selected 4–6 voxels from both hippocampi using workstation Spectroscopy software [13]. Then the concentrations of *N*-acetyl-aspartate (2.02 ppm), choline (3.22 ppm), creatine (3.02 ppm), the ratio of NAA/Cr, and the ratio of Cho/Cr were measured in each selected voxel.

2.4.3. R-fMRI Preprocessing. R-fMRI preprocessing was performed with Data Processing Assistant for resting-state fMRI (DPABI 2.1). The first 10 volumes were abandoned. Then, the images were corrected for slice timing and realigned. (Subjects with a maximum displacement in the x, y, or z direction of more than 1 mm or more than 1° of angular rotation about any axis for any of the 230 volumes were excluded from this study. No subject was excluded according to this criterion.) Afterward, images were normalized into standard MNI space and smoothed with 8 mm FWHM isotropic Gaussian kernel.

2.4.4. ALFF. ALFF calculation was performed with resting-state fMRI Data Analysis Toolkit (REST 1.8). One-sample t-test was performed using SPM8 in each group to detect the regions with higher-than-mean ALFF. These mALFF images were then performed for two-sample t-test to determine between-group differences. Significant different regions were shown on MNI templates. The two-sample t-test results were restricted within the mask made from the results of one-sample t-tests performed for two groups.

2.4.5. Functional Connectivity. All images were filtered with a 0.01–0.08 Hz band-pass filter to reduce the noise before FC analysis. The ROI was located in the bilateral PCC (centered MNI coordinates: 0, −56, 25, r = 10 mm) [14]. The mean ROI signal was counted by averaging all voxels in bilateral PCC. The ROI time course was used to perform correlation analysis with all other voxels in the brain. To normalize the correlation coefficients, Fisher z-transform was then applied. One-sample t-test was performed using SPM8 in each group to detect the regions with significant connectivity to the PCC. These z-FC images were then performed for two-sample t-test to determine between-group differences. Significant different regions were shown on MNI templates. The two-sample t-test results were restricted within the mask made from the results of one-sample t-tests performed for two groups.

2.5. Statistical Analysis. We used IBM SPSS 20.0 and SPM8 to perform statistical analyses. Continuous variables were assessed with Mann–Whitney test or two-sample t-test. Categorical variables were assessed with Chi-squared or Fisher exact test if the expected number was ≤5. Significance was defined as $P < 0.05$. Education and age were defined as covariates in all tests involving cognition. After the analysis

Table 1: Basic demographics and cognitive test scores of enrolled subjects.

Characteristics	Patients ($n = 19$)	Controls ($n = 24$)	P value
Age (years)	68.0 ± 5.6	64.5 ± 7.3	0.08
Male : female	15 : 4	19 : 5	1.00
Education (years)	9.9 ± 3.3	10.9 ± 3.4	0.21
Hypertension	19	18	0.70
Diabetes mellitus	4	4	1.00
Hypercholesterolemia	13	12	0.64
Stenotic side			
Left	7	N/A	
Right	12	N/A	
MMSE	26.8 ± 0.7	27.4 ± 0.7	0.02
MoCA	23.3 ± 1.2	24.2 ± 1.6	0.02
Verbal memory test			
Forward digit span	5.8 ± 1.0	6.5 ± 0.9	0.04
Backward digit span	3.8 ± 0.8	4.5 ± 0.8	0.02
Rey Auditory Verbal Learning test			
Immediate recall	31.0 ± 4.5	35.8 ± 5.6	<0.01
Delayed recall	4.6 ± 1.6	6.5 ± 1.1	<0.01
Digit Symbol Test	28.0 ± 4.7	31.5 ± 5.5	0.03

Table 2: CBF difference between two groups and their location.

Number of voxels	Peak MNI coordinate			Peak MNI coordinate region	Peak T value
	X	Y	Z		
1 603	−24	30	−3	Left Inferior Frontal Gyrus, Brodmann area 11	−3.91

Table 3: Significant NAA/Cr difference in the left hippocampus between two groups.

	aCAS	Controls	P value
NAA/Cr	1.6 ± 0.1	1.7 ± 0.1	0.02

of pASL, ALFF, and FC, regions with significant differences between two groups were defined as ROIs; then Spearman analysis was performed to detect the relationship between these MRI differences and cognition scores.

3. Results

3.1. Patient Characteristics and Neuropsychological Evaluation. We enrolled 19 aCAS patients and 24 healthy controls. No significant difference was found in educational years, gender ratio, age, or vascular risk factors. Compared with the controls, aCAS patients had significantly poorer performances on global cognition (represented by MMSE and MoCA), memory (represented by Verbal Memory Test and Rey Auditory Verbal Learning Test), and executive function (represented by Digit Symbol Test) (Table 1).

3.2. Difference in CBF between Two Groups. aCAS patients showed decreased CBF in the Left Inferior Frontal Gyrus when compared with healthy controls (Table 2, Figure 1(a)). The result was corrected using the AlphaSim program, with a setting at $P < 0.01$ and number of voxels > 489, which corresponded to a corrected $P < 0.025$.

3.3. Difference in MRS Finding between Two Groups. In the study of MRS in both hippocampi, we only found that the NAA/Cr in the left hippocampus had significant difference between two groups (Table 3).

3.4. Significant ALFF Differences between Two Groups. Significantly decreased ALFF in the Left and Right Supra Medial Frontal Lobes were found in aCAS patients. The aCAS patients also showed increased ALFF in Cerebellum (Table 4 and Figure 1(b)). The result was corrected using the AlphaSim program, with a setting at $P < 0.01$ and number of voxels > 277, which corresponded to a corrected $P < 0.01$.

3.5. Differences of FC to PCC between aCAS Patients and Healthy Controls. Compared with controls, the aCAS patients showed decreased connectivity to the PCC mainly in the Right Supra and Medial Frontal Gyrus. No region showing increased FC to the PCC was found (Table 5 and Figure 1(c)). The result was corrected using the AlphaSim program, with a setting at $P < 0.01$ and number of voxels > 203, which corresponded to a corrected $P < 0.025$.

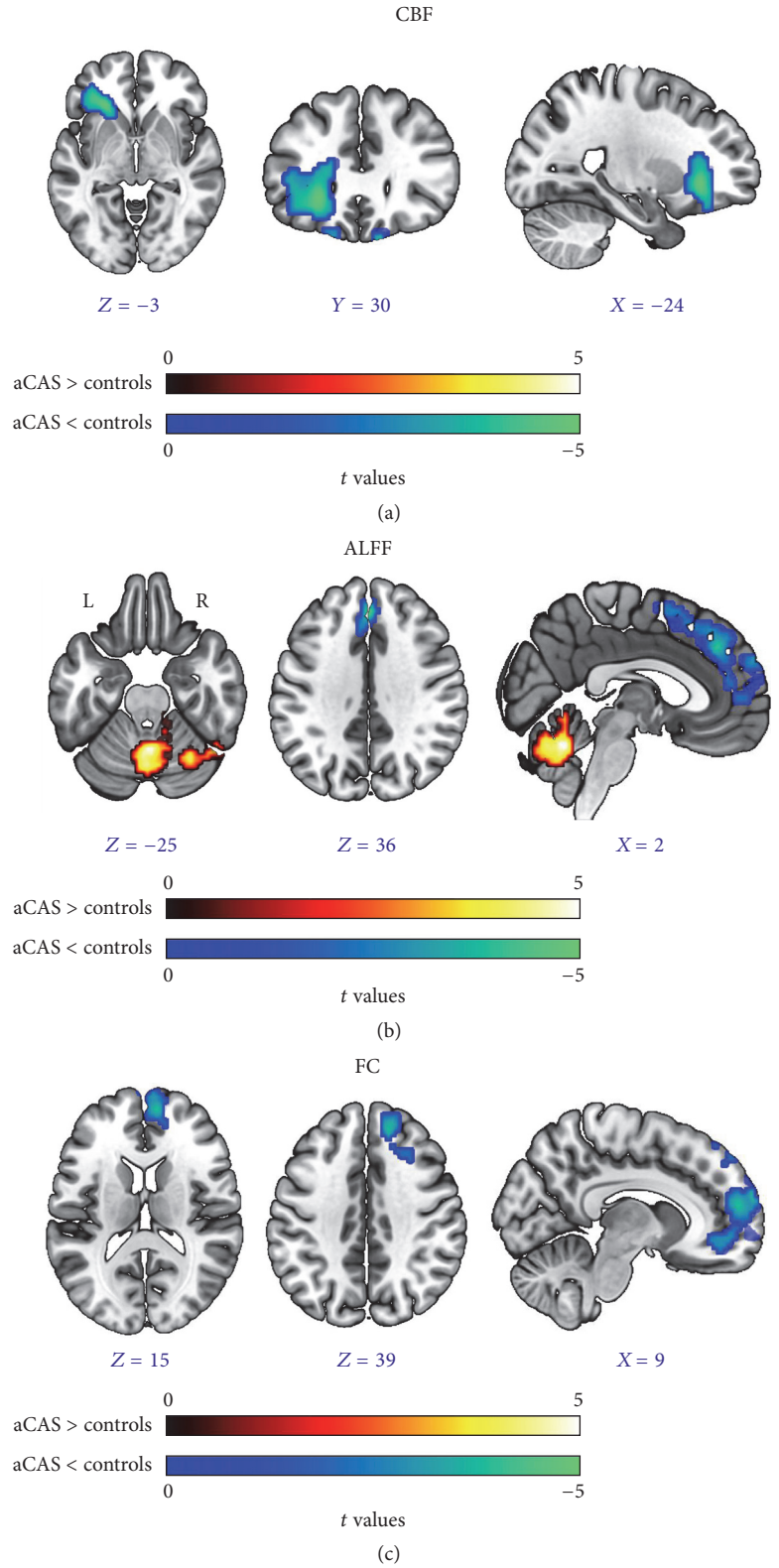

Figure 1: CBF, ALFF, and FC differences between two groups. (a) CBF differences between two groups. (b) Differences of ALFF between two groups. (c) FC differences between aCAS patients and controls. The color bar in (a), (b), and (c) represents t values.

Table 4: Significant ALFF differences between two groups with their location.

	Number of voxels	Peak MNI coordinate			Peak MNI coordinate region	Peak T value
		X	Y	Z		
1	708	0	−57	−24	Cerebellum	5.23
2	356	0	39	36	Left and Right Supra Medial Frontal Lobes	−6.67

Table 5: Significant connectivity differences to the PCC between two groups with their location.

	Number of voxels	Peak MNI coordinate			Peak MNI coordinate region	Peak T value
		X	Y	Z		
1	286	9	57	15	Frontal_Medial_R	−4.20
2	220	15	42	39	Frontal_Sup_R	−4.00

3.6. Relationship between Imaging Findings and Cognition Scores. No significant correlation between MRI findings and cognition scores was found ($P > 0.05$ for all).

4. Discussion

Consistent with previous studies [2, 4], we found that aCAS patients had significantly poorer performances on global cognition (represented by MMSE and MoCA), memory (represented by Verbal Memory Test and Rey Auditory Verbal Learning Test), and executive function (represented by Digit Symbol Test) when compared with the controls. Therefore, aCAS patients should be no longer considered as "asymptomatic." Results from the integrated MRI study could mainly be divided into three parts. Firstly, aCAS patients suffered from decreased CBF mainly in the Left Frontal Lobe when compared with healthy controls. Secondly, aCAS patients had lower NAA/Cr ratio in the left hippocampus. Thirdly, aCAS patients had both decreased ALFF and decreased connectivity to the PCC in the Right Supra and Medial Frontal Gyrus.

This study also showed the adverse effect of decreased cerebral blood flow on cognition. Cerebral hypoperfusion is one of the most important pathophysiological mechanisms of vascular cognitive impairment in vascular diseases [15, 16]. Abnormality of neuron electric activities and protein synthesis can partly explain the correlation between cerebral hypoperfusion and cognition impairment. What is more, reduced CBF was mainly located in the Left Frontal Lobe, which consists of key regions that mediate cognitive function.

NAA is an exclusive amino acid in neuron, and the level of NAA can reflect the neuronal viability [17]. The level of Cho has been found to be related to membrane synthesis and degeneration [18]. Abnormality of these signals had been demonstrated in a number of central nervous system diseases [19, 20]. Similar to our previous study [13], we found that aCAS patients had lower NAA/Cr ratio in the left hippocampus.

In recent years, an increasing number of studies have demonstrated that cognitive function performance are not dependent on individual brain region, but dependent on regions, thereby forming networks [21]. A number of studies have already demonstrated this in patients with neurodegenerative diseases [22, 23]. Among these networks, the default mode network (DMN) has been increasing as noticed in recent years [24]. As demonstrated by functional MRI and PET studies, the most common DMN components are the posterior cingulate cortex, the medial prefrontal cortex, the anterior cingulate cortex, the inferior parietal lobule, and other regions [11, 14]. Although the precise functions of DMN remain largely unclear, studies have shown that it plays an important role in cognition and self-monitoring [25]. Another reason why we selected DMN for analysis was that previous studies have demonstrated that DMN is especially easily affected by hypoperfusion [26].

Of the indexes utilized in R-fMRI, ALFF is a useful index to reflect spontaneous neuronal activity [27–30]. We found that aCAS patients showed decreased ALFF in the Left and Right Supra Medial Frontal Gyrus when compared with healthy controls, which belong to the anterior part of DMN. Since the anterior part of DMN is especially associated with executive function, the cognitive disturbances of aCAS patients could be partly due to the decreased activities of these regions [31–33]. Increased ALFF in the Cerebellum was also found in aCAS patients, and we speculate that the increased ALFF in these regions might reflect compensation due to the low perfusion damage.

We also compared the FC to the PCC between two groups and found that the aCAS patients showed decreased connectivity mainly in the Right Supra and Medial Frontal Gyrus when compared with healthy controls. There was no region that showed increased connectivity to the PCC. The decreased regions were also overlapped with the anterior part of the DMN. Therefore, the cognitive impairment could also be partially attributed to the decreased FC to the PCC in the anterior part of DMN, although no significant correlation was found.

Our study had limitations that required discussion. Firstly, the sample size was relatively small. Secondly, the cerebral hemisphere of the stenosis side often exhibits greater brain atrophy. In that situation, the proportion of cerebrospinal fluid occupying the ROI for metabolites measurement is higher, thereby reducing the accuracy [34]. Thirdly, the cerebral metabolism was obtained using multivoxel

method, while single-voxel method could provide more accurate measurement [35]. In addition, future studies should also examine the influence of silent infarcts and microbleeds on cognition, as they also affect CBF and subsequent neurocognitive outcomes.

In summary, the aCAS patients showed significantly poorer performance on global cognition, memory, and executive function. By utilizing this integrated MRI, we also found that aCAS patients suffered decreased CBF mainly in the Left Frontal Gyrus and had decreased NAA/Cr ratio in the left hippocampus and decreased connectivity to the PCC in the anterior part of DMN.

Competing Interests

There is no conflict of interests.

Authors' Contributions

Tao Wang and Feng Xiao contributed equally to this work.

Acknowledgments

The authors would like to thank Xiaoli Zhong and Xiaohui Chen for MRI technical support. This study was supported by the Science and Technology Support Program of Hubei Province, China (Grant no. 2014BCB044).

References

[1] D. Inzitari, M. Eliasziw, P. Gates et al., "The causes and risk of stroke in patients with asymptomatic internal- carotid-artery stenosis," *New England Journal of Medicine*, vol. 342, no. 23, pp. 1693–1700, 2000.

[2] J. R. Romero, A. Beiser, S. Seshadri et al., "Carotid artery atherosclerosis, MRI indices of brain ischemia, aging, and cognitive impairment: the framingham study," *Stroke*, vol. 40, no. 5, pp. 1590–1596, 2009.

[3] L. K. Sztriha, D. Nemeth, T. Sefcsik, and L. Vecsei, "Carotid stenosis and the cognitive function," *Journal of the Neurological Sciences*, vol. 283, no. 1-2, pp. 36–40, 2009.

[4] I. M. Popovic, A. Lovrencic-Huzjan, A. Simundic, A. Popovic, V. Seric, and V. Demarin, "Cognitive performance in asymptomatic patients with advanced carotid disease," *Cognitive And Behavioral Neurology*, vol. 24, no. 3, pp. 145–151, 2011.

[5] V. J. Schmithorst, L. Hernandez-Garcia, J. Vannest, A. Rajagopal, G. Lee, and S. K. Holland, "Optimized simultaneous ASL and BOLD functional imaging of the whole brain," *Journal of Magnetic Resonance Imaging*, vol. 39, no. 5, pp. 1104–1117, 2014.

[6] S. Delli Pizzi, R. Franciotti, J.-P. Taylor et al., "Thalamic involvement in fluctuating cognition in dementia with lewy bodies: magnetic resonance evidences," *Cerebral Cortex*, vol. 25, no. 10, pp. 3682–3689, 2015.

[7] S. Hirsiger, V. Koppelmans, S. Mérillat et al., "Structural and functional connectivity in healthy aging: associations for cognition and motor behavior," *Human Brain Mapping*, vol. 37, no. 3, pp. 855–867, 2016.

[8] W. Li, P. G. Antuono, C. Xie et al., "Changes in regional cerebral blood flow and functional connectivity in the cholinergic pathway associated with cognitive performance in subjects with mild Alzheimer's disease after 12-week donepezil treatment," *NeuroImage*, vol. 60, no. 2, pp. 1083–1091, 2012.

[9] D. Zhang and M. E. Raichle, "Disease and the brain's dark energy," *Nature Reviews Neurology*, vol. 6, no. 1, pp. 15–28, 2010.

[10] X.-N. Zuo, C. Kelly, J. S. Adelstein, D. F. Klein, F. X. Castellanos, and M. P. Milham, "Reliable intrinsic connectivity networks: test-retest evaluation using ICA and dual regression approach," *NeuroImage*, vol. 49, no. 3, pp. 2163–2177, 2010.

[11] M. De Luca, C. F. Beckmann, N. De Stefano, P. M. Matthews, and S. M. Smith, "fMRI resting state networks define distinct modes of long-distance interactions in the human brain," *NeuroImage*, vol. 29, no. 4, pp. 1359–1367, 2006.

[12] M. L. Ries, T. W. Schmitz, T. N. Kawahara, B. M. Torgerson, M. A. Trivedi, and S. C. Johnson, "Task-dependent posterior cingulate activation in mild cognitive impairment," *NeuroImage*, vol. 29, no. 2, pp. 485–492, 2006.

[13] D. Sun, J. Zhang, Y. Fan et al., "Abnormal levels of brain metabolites may mediate cognitive impairment in stroke-free patients with cerebrovascular risk factors," *Age and Ageing*, vol. 43, no. 5, pp. 681–686, 2014.

[14] M. D. Greicius, B. Krasnow, A. L. Reiss, and V. Menon, "Functional connectivity in the resting brain: a network analysis of the default mode hypothesis," *Proceedings of the National Academy of Sciences of the United States of America*, vol. 100, no. 1, pp. 253–258, 2003.

[15] B. P. Austin, V. A. Nair, T. B. Meier et al., "Effects of hypoperfusion in Alzheimers disease," *Journal of Alzheimer's Disease*, vol. 26, supplement 3, pp. 123–133, 2011.

[16] D. J. Moser, L. L. Boles Ponto, I. N. Miller et al., "Cerebral blood flow and neuropsychological functioning in elderly vascular disease patients," *Journal of Clinical and Experimental Neuropsychology*, vol. 34, no. 2, pp. 220–225, 2012.

[17] D. L. Birken and W. H. Oldendorf, "N-Acetyl-L-Aspartic acid: a literature review of a compound prominent in 1H-NMR spectroscopic studies of brain," *Neuroscience and Biobehavioral Reviews*, vol. 13, no. 1, pp. 23–31, 1989.

[18] B. L. Miller, "A review of chemical issues in 1H NMR spectroscopy: N-acetyl-L-aspartate, creatine and choline," *NMR in Biomedicine*, vol. 4, no. 2, pp. 47–52, 1991.

[19] E. Gonzalez-Toledo, R. E. Kelley, and A. Minagar, "Role of magnetic resonance spectroscopy in diagnosis and management of multiple sclerosis," *Neurological Research*, vol. 28, no. 3, pp. 280–283, 2006.

[20] Y. Handa, M. Kaneko, T. Matuda, H. Kobayashi, and T. Kubota, "In vivo proton magnetic resonance spectroscopy for metabolic changes in brain during chronic cerebral vasospasm in primates," *Neurosurgery*, vol. 40, no. 4, pp. 773–781, 1997.

[21] M. Mesulam, "Defining neurocognitive networks in the BOLD new world of computed connectivity," *Neuron*, vol. 62, no. 1, pp. 1–3, 2009.

[22] F. Andrew Kozel, U. Rao, H. Lu et al., "Functional connectivity of brain structures correlates with treatment outcome in major depressive disorder," *Frontiers in Psychiatry*, vol. 2, article no. 7, 2011.

[23] C. Xie, J. Goveas, Z. Wu et al., "Neural basis of the association between depressive symptoms and memory deficits in nondemented subjects: resting-state fMRI study," *Human Brain Mapping*, vol. 33, no. 6, pp. 1352–1363, 2012.

[24] M. E. Raichle, A. M. MacLeod, A. Z. Snyder, W. J. Powers, D. A. Gusnard, and G. L. Shulman, "A default mode of brain function,"

Proceedings of the National Academy of Sciences, vol. 98, no. 2, pp. 676–682, 2001.

[25] R. N. Spreng, R. A. Mar, and A. S. N. Kim, "The common neural basis of autobiographical memory, prospection, navigation, theory of mind, and the default mode: a quantitative meta-analysis," *Journal of Cognitive Neuroscience*, vol. 21, no. 3, pp. 489–510, 2009.

[26] X. Liang, Q. Zou, Y. He, and Y. Yang, "Coupling of functional connectivity and regional cerebral blood flow reveals a physiological basis for network hubs of the human brain," *Proceedings of the National Academy of Sciences of the United States of America*, vol. 110, no. 5, pp. 1929–1934, 2013.

[27] M. J. Hoptman, X.-N. Zuo, P. D. Butler et al., "Amplitude of low-frequency oscillations in schizophrenia: a resting state fMRI study," *Schizophrenia Research*, vol. 117, no. 1, pp. 13–20, 2010.

[28] X.-Q. Huang, S. Lui, W. Deng et al., "Localization of cerebral functional deficits in treatment-naive, first-episode schizophrenia using resting-state fMRI," *NeuroImage*, vol. 49, no. 4, pp. 2901–2906, 2010.

[29] Y. Liu, P. Liang, Y. Duan et al., "Abnormal baseline brain activity in patients with neuromyelitis optica: a resting-state fMRI study," *European Journal of Radiology*, vol. 80, no. 2, pp. 407–411, 2011.

[30] Y. Yin, L. Li, C. Jin et al., "Abnormal baseline brain activity in posttraumatic stress disorder: a resting-state functional magnetic resonance imaging study," *Neuroscience Letters*, vol. 498, no. 3, pp. 185–189, 2011.

[31] J. A. Alvarez and E. Emory, "Executive function and the frontal lobes: a meta-analytic review," *Neuropsychology Review*, vol. 16, no. 1, pp. 17–42, 2006.

[32] S. J. Gilbert, G. Bird, R. Brindley, C. D. Frith, and P. W. Burgess, "Atypical recruitment of medial prefrontal cortex in autism spectrum disorders: an fMRI study of two executive function tasks," *Neuropsychologia*, vol. 46, no. 9, pp. 2281–2291, 2008.

[33] D. M. Amodio and C. D. Frith, "Meeting of minds: the medial frontal cortex and social cognition," *Nature Reviews Neuroscience*, vol. 7, no. 4, pp. 268–277, 2006.

[34] D. Ishigaki, K. Ogasawara, Y. Yoshioka et al., "Brain temperature measured using proton MR spectroscopy detects cerebral hemodynamic impairment in patients with unilateral chronic major cerebral artery steno-occlusive disease: comparison with positron emission tomography," *Stroke*, vol. 40, no. 9, pp. 3012–3016, 2009.

[35] A. Di Costanzo, F. Trojsi, M. Tosetti et al., "Proton MR spectroscopy of the brain at 3 T: an update," *European Radiology*, vol. 17, no. 7, pp. 1651–1662, 2007.

Hindawi Publishing Corporation
Neural Plasticity
Volume 2017, Article ID 5167973, 6 pages
http://dx.doi.org/10.1155/2017/5167973

Research Article

Alterations in Cortical Thickness and White Matter Integrity in Mild-to-Moderate Communicating Hydrocephalic School-Aged Children Measured by Whole-Brain Cortical Thickness Mapping and DTI

Siyu Zhang,[1,2] Xinjian Ye,[1] Guanghui Bai,[1] Yuchuan Fu,[1] Chuanwan Mao,[1] Aiqin Wu,[1] Xiaozheng Liu,[1] and Zhihan Yan[1]

[1]*China-USA Neuroimaging Research Institute, Radiology Department of The Second Affiliated Hospital and Yuying Children's Hospital, Wenzhou Medical University, Wenzhou, Zhejiang, China*
[2]*Radiology Department, Meizhou People's Hospital, Meizhou, Guangdong, China*

Correspondence should be addressed to Xiaozheng Liu; lxz_2088@hotmail.com and Zhihan Yan; zhihanyan@hotmail.com

Received 28 September 2016; Revised 9 December 2016; Accepted 27 December 2016; Published 16 January 2017

Academic Editor: Lijun Bai

Follow-up observation is required for mild-to-moderate hydrocephalic patients because of the potential damage to brain. However, effects of mild-to-moderate hydrocephalus on gray and white matter remain unclear in vivo. Using structural MRI and diffusion tensor imaging (DTI), current study compared the cortical thickness and white matter integrity between children with mild-to-moderate communicating hydrocephalus and healthy controls. The relationships between cortical changes and intelligence quota were also examined in patients. We found that cortical thickness in the left middle temporal and left rostral middle frontal gyrus was significantly lower in the hydrocephalus group compared with that of controls. Fractional anisotropy in the right corpus callosum body was significantly lower in the hydrocephalus group compared with that of controls. In addition, there was no association of cortical thinning or white matter fractional anisotropy with intelligence quota in either group. Thus, our findings provide clues to that mild-to-moderate hydrocephalus could lead to structural brain deficits especially in the middle temporal and middle frontal gyrus prior to the behavior changes.

1. Introduction

Hydrocephalus is a pathologic condition in which excessive cerebrospinal fluid (CSF) accumulates in the ventricular system because of obstruction along CSF pathways or an imbalance between CSF production and reabsorption [1, 2]. The enlarged ventricles and associated increase in intracranial pressure can cause damage to various brain regions, including the gray matter (GM) and white matter (WM). Surgical treatment is presently the main therapeutic option for severe hydrocephalus. However, follow-up observation is required for mild-to-moderate hydrocephalic patients because of risk of operation [3, 4].

Although conventional MRI techniques, including T1 weighted image (T1WI) or T2 weighted image (T2WI), can detect major structural abnormalities, they cannot detect more subtle GM and WM abnormalities, such as cortical thickness and ultrastructural changes, in hydrocephalic patients during follow-up observation. By contrast, 3-dimensional fast spoiled gradient-recalled sequence can provide high-resolution T1WI data that allowed us to observe and measure cortical thickness. DTI provides quantitative information on anisotropic diffusion properties in WM and has been used to investigate WM damage and recovery in various neurologic and pathologic disorders [5–8]. Changes of cortical thickness were reported in a variety of diseases [9–11]. Severe hydrocephalus also leads to compression of the cerebral cortex, with reduction of overall brain mass and cortical thickness, particularly in the parietal and occipital regions [12–14]. In animal studies, an increasing degree

of ventriculomegaly is associated with more marked thinning of the cerebral cortex [15]. However, to our knowledge, there are very few studies examining both GM and WM abnormalities in school-aged children with mild-to-moderate hydrocephalus, which is important because mild-to-moderate hydrocephalus may have a negative impact on children and reduce their quality of life in the future.

In the present study, we performed MRI studies on school-aged children with mild-to-moderate communicating hydrocephalus to identify regional changes of cortical thickness and WM fractional anisotropy (FA) and assessed the correlation between cortical changes and intelligence quota (IQ).

2. Materials and Methods

2.1. Subjects. This study included 15 treatment-naive patients with communicating hydrocephalic (mean age = 9.76 ± 1.80 years; duration of illness = 1.77 ± 0.68 years; sex ratio = 6 female/9 male). All hydrocephalus subjects were recruited from patients who visited The Second Affiliated Hospital of Wenzhou Medical University from December 2013 to June 2015. The inclusion criteria were (1) age between 6 and14 years, (2) IQ within the normal range, (3) no evidence of obstruction in CSF flow and no GRASS MRI finding of other diseases, (4) Evan's index between 0.33 and 0.50, (5) duration of illness more than 1 year, (6) no history of other intracranial or other related diseases (e.g., meningitis, head trauma, epilepsy, nephritic, congenital heart disease, and diabetes mellitus), (7) right-handed, and (8) no claustrophobia [3, 4]. The control group consisted of 20 healthy comparison subjects with age (9.50 ± 1.96 years), gender (8 female/12 male), IQ, family condition, and education level matched with patient group. Healthy control subjects were recruited through poster advertisements. Demographic and IQ data are summarized in Table 1. Informed consent was obtained from all subjects and their guardian for study participation.

Table 1: Demographics and IQ of two groups.

	Hydrocephalus group (N = 15)	Control group (N = 20)	P value
Gender			0.73
Male	9	12	
Female	6	8	
Age (years)	9.67 ± 1.80	9.50 ± 1.96	0.80
Duration of illness (years)	1.77 ± 0.68	—	—
Evan's index	0.35 ± 0.02	0.26 ± 0.01	<0.01
Linguistic IQ	91.47 ± 19.37	87.50 ± 8.68	0.47
Performance IQ	96.13 ± 13.93	92.60 ± 12.38	0.43
Full scale IQ	93.00 ± 17.33	88.90 ± 9.59	0.42

The data were presented as mean ± SD.

2.2. Intelligence Assessments. The Wechsler Intelligence Scale for Children-Chinese Revised, which demonstrates high reliability and validity, was used to assess general intellectual ability of all subjects and the linguistic IQ and performance IQ, and senior medical staff that majored on intelligence assessment calculated full scale IQ.

2.3. Imaging Data Acquisition. MRI data were obtained on a 3.0 Tesla system (GE Signa HDxt) with an 8-channel phase array head coil. High-resolution T1WI was acquired with a volumetric 3-dimensional fast spoiled gradient-recalled sequence (slice thickness = 1.0 mm, slice gap = 0.5 mm, TR = 9 ms, TE = 4 ms, FOV = 240 × 240 mm^2, matrix = 256 × 256, and in-plane resolution = 0.94 × 0.94 mm^2). DTI images were acquired with a diffusion-weighted spin-echo sequence (slice thickness = 4.0 mm, TR = 8000 ms, TE = 90 ms, FOV = 240 × 240 mm^2, matrix = 128 × 128, in-plane resolution = 1.88 × 1.88 mm^2, and flip angle = 90°; diffusion weighting was applied with a b value = 1000 s/mm^2 along 36 independent nonlinear orientations, and 1 additional image with no diffusion weighting was acquired).

2.4. Imaging Processing. High-resolution T1WI analysis was performed using the FreeSurfer package (http://surfer.nmr.mgh.harvard.edu/). Cortical thickness was measured as the difference between the position of equivalent vertices in the pial and GM/WM surfaces, by utilizing both intensity and continuity information from the entire 3-dimensional MR volume in the segmentation and deformation procedures. The reliability of the method was previously validated against histological analysis on postmortem brains and manual measurements, and the test-retest reliability is high [16–19]. Briefly, the main steps included motion correction using FSL FLIRT and automated registration to Talairach space, segmentation of the subcortical GM and WM structures, intensity normalization and removal of nonbrain voxels, and tessellation of GM and WM boundaries and automated topology correction and surface deformation to optimally place the GM/WM and GM/CSF borders defined at the location with the greatest shift in signal intensity [16, 20–24]. Following registration of all subjects' cortical reconstructions to a common average surface, the surface maps were interpolated and analyzed. This procedure is capable of detecting submillimeter differences between groups [16].

DTI image processing was performed using the FSL package (http://fsl.fmrib.ox.ac.uk/fsl/fslwiki/). Data were inspected for movement artifacts using FSL-MCFLIRT (<1° rotation and <1 mm translation) and then corrected for eddy current-induced distortions. Brain extraction and calculation of diffusion parameter maps were performed using FSL. FA maps for each participant were registered into a standard brain template (FMRIB58_FA, part of the FSL suite) using the nonlinear spatial transformation tool FNIRT. A mean FA image was then compiled by averaging aligned FA maps from each participant. To generate a mean FA skeleton representing the centers of all tracts common to the group, the map threshold was then set for voxels showing FA values ≥ 0.2. Aligned FA maps for each participant were projected onto the standard skeletonized FA image (FMRIB58_FA-skeleton,

Table 2: Changes in cortical thickness in hydrocephalus patients.

	Region size (mm^2)	Cortical thickness (mm)		Talairach coordinate		
		Hydrocephalus group	Control group	Tal$X$	Tal$Y$	Tal$Z$
Left rostral middle frontal	1402.96	2.88 ± 0.26	2.92 ± 0.18	−34.6	48.2	6.3
Left middle temporal	1122.09	2.37 ± 0.22	2.44 ± 0.25	−61.5	−40.8	−3.2

The data were presented as mean ± SD.

Table 3: Changes in FA values in hydrocephalus patients.

	Region size (voxels)	FA		MNI coordinate		
		Hydrocephalus group	Control group	X	Y	Z
Right corpus Callosum body	836	0.51 ± 0.07	0.63 ± 0.09	11	−11	31

The data were presented as mean ± SD. FA: fractional anisotropy. MNI: Montreal Neurological Institute.

packaged in FSL) by searching the area around the skeleton in the direction perpendicular to each tract, finding the highest local FA value, and assigning this value to the skeleton [25].

2.5. Statistical Analysis. In the graphical interface of FreeSurfer (QDEC [Query, Design, Estimate, Contrast]), structural parameters were smoothed with full width at half maximum at 10 mm, mesh surface-base, and concomitant variable of age. Cortical thickness was compared between the two groups, corrected using the Monte Carlo simulation (corrected threshold = 1.3, $P < 0.05$), to find regions with significant group differences.

Using tract based spatial statistics tools, voxelwise spatial statistical analysis comparing the hydrocephalus and control groups was performed using the "randomize" program within FSL, which involves permutation testing [26]. The mean FA skeleton was used as a mask (threshold at a mean FA value of 0.2), and the number of permutations was set to 5000. Thresholding was performed using threshold-free cluster enhancement, a new method for finding significant clusters in MRI data without having to define them as binary units [27]. Clusters were assessed for multiple comparisons using the familywise error rate ($P < 0.05$).

To evaluate the relationship between cortical changes and IQ, we extracted the mean value of cortical thickness of regions with significant intergroup differences. A 2-sample t-test was performed to compare age and IQ of the hydrocephalus and control groups, while Chi-square test was performed to compare gender ratio (SPSS v19.0 software). Bivariate correlations were performed between cortical thickness, FA changes, and IQ for each group.

3. Results

3.1. Group Differences in Demographics. There were no significant differences in age ($P = 0.80$) or gender composition ($P = 0.73$) between the hydrocephalus and control groups (Table 1).

3.2. Group Differences in Cortical Thickness. Compared with the control group, hydrocephalus patients had a lower cortical thickness in the left middle temporal gyrus (area = 1122.09 mm^2; Talairach coordinates = −61.5, −40.8, −3.2; $P < 0.05$; and mean thickness = 2.37 ± 0.22 [hydrocephalus group] and 2.44 ± 0.25 [control group]) and in the left rostral middle frontal gyrus (area = 1402.96 mm^2; Talairach coordinates = −34.6, 48.2, 6.3; $P < 0.05$; and mean thickness = 2.88 ± 0.26 [hydrocephalus group] and 2.92±0.18 [control group]). There were no brain regions with increased cortical thickness in hydrocephalus patients (Figure 1, Table 2).

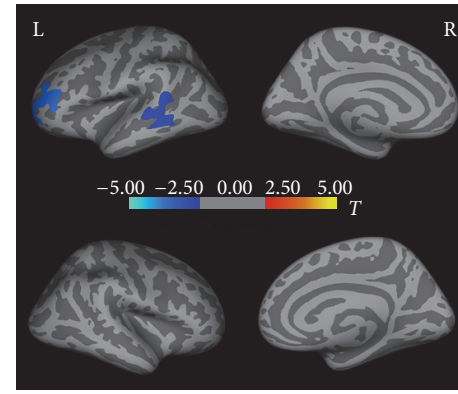

Figure 1: Differences in cortical thickness between hydrocephalus group and control group. Significance was determined by Monte Carlo simulation. Less cortical thickness in hydrocephalus group than in control group is indicated by blue/cool color. $P < 0.05$. L: left hemisphere. R: right hemisphere.

3.3. Group Differences in FA. Compared with the control group, hydrocephalus patients had a lower FA in the right corpus callosum body (region size = 836 voxels; MNI coordinates = 11, −11, 31; $P < 0.05$; and mean FA = 0.51 ± 0.07 [hydrocephalus group] and 0.63±0.09 [control group]). There were no brain regions with increased FA in hydrocephalus patients (Figure 2, Table 3).

3.4. Cortical and FA Changes with IQ. In the control group, there were a trend towards a decrease in cortical thickness in the left middle temporal gyrus with increasing linguistic IQ and full scale IQ and a trend towards an increase in cortical thickness in other regions with increasing linguistic

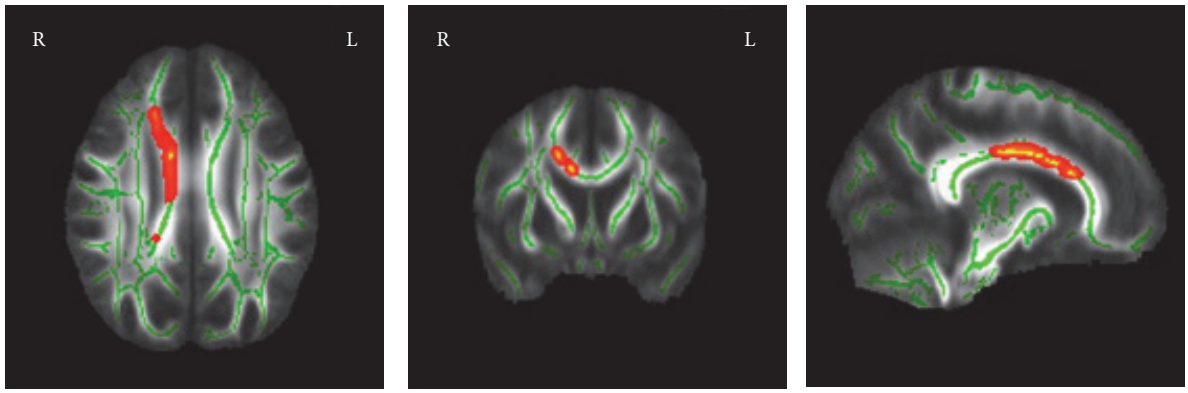

Figure 2: Differences in FA values between hydrocephalus group and control group. Significance was determined by t-test. Less FA values in hydrocephalus group than in control group are indicated by red/warm color. $P < 0.05$. L: left hemisphere. R: right hemisphere.

Table 4: Relationship between mean cortical thickness of the left middle temporal and IQ.

	Hydrocephalus group		Control group	
	r[a]	p	r	p
Linguistic IQ	0.368	0.177	−0.235	0.319
Performance IQ	0.051	0.858	0.046	0.849
Full scale IQ	0.255	0.359	−0.098	0.680

[a]+: increase. −: decrease.

Table 5: Relationship between mean cortical thickness of the left rostral middle frontal and IQ.

	Hydrocephalus group		Control group	
	r[a]	p	r	p
Linguistic IQ	0.360	0.188	0.030	0.900
Performance IQ	0.268	0.334	0.256	0.276
Full scale IQ	0.330	0.230	0.160	0.501

[a]+: increase. −: decrease.

IQ, performance IQ, and full scale IQ. In both the control and the hydrocephalus groups, there were a trend towards an increase in cortical thickness in the left rostral middle frontal gyrus with increasing linguistic IQ, performance IQ, and full scale IQ and a trend towards a decrease in FA in the right corpus callosum body with increasing linguistic IQ. Further, in the hydrocephalus group, there was a trend towards a decrease in full scale IQ. By contrast, there was no association of cortical thinning or decreased FA with IQ in either group (Tables 4–6).

4. Discussion

Unlike the widespread cortical deficits of the whole brain in patients with severe hydrocephalus, school-aged children with mild-to-moderate communicating hydrocephalus showed significant cortical thinning in the left middle temporal gyrus and left rostral middle frontal gyrus and decreased FA in the right corpus callosum body, though the two groups showed no difference of IQ. Furthermore, there was no correlation between the mean cortical thickness nor the FA and IQ in either group. These findings suggest that the gray matter of left temporal and frontal lobe and white matter of corpus callosum are the most vulnerable regions in children with mild-to-moderate communicating hydrocephalus, which may happen before the behavior changes.

Table 6: Relationship between mean FA of the right corpus callosum body and IQ.

	Hydrocephalus group		Control group	
	r[a]	p	r	p
Linguistic IQ	−0.230	0.409	−0.049	0.838
Performance IQ	0.054	0.847	0.235	0.318
Full scale IQ	−0.137	0.627	0.124	0.603

[a]+: increase. −: decrease.

Widespread cortical thinning was previously reported in animal models and children with severe hydrocephalus [13, 15, 28, 29]. This is consistent with the pathology studies, which revealed moderate-to-severe neuronal swelling of the whole brain in hydrocephalus patients, with marked enlargement of the extracellular space in the adjacent neuropil, synaptic plasticity and degeneration, damage to myelinated axons, and myelination delay. Astrocytes also display evidence of edema and phagocytic activity [29, 30]. These pathological changes in the cerebral cortex of human hydrocephalus patients are considered to result from an initial mechanical injury because of the high CSF pressure, followed by secondary changes associated with increased interstitial edema, ischemia, and oxidative stress [31]. However, the evidences for the gay and matter changes in children with mild-to-moderate communicating hydrocephalus are rare. Our findings in vivo showed that the regional decreased gray matter does happen in the left temporal and frontal lobe.

The decreased FA in the right corpus callosum body of infants and children with severe hydrocephalus was also reported in previous studies [32–37]. DTI studies in acute hydrocephalus patients revealed increased FA in the WM areas lateral to the ventricles, which recovered after surgery,

suggesting white matter compression as the possible cause of this observed change, and decreased FA in the corpus callosum, with no changes after surgery, suggesting that the corpus callosum may be easier to undergo neuronal degeneration [32]. In addition, infants with hydrocephalus showed significantly lower FA in the corpus callosum, but not in the internal capsule [33]. Pathological studies on the corpus callosum in acute and chronic hydrocephalus patients suggest a potential causative role of neuronal degeneration during hydrocephalus [36, 37]. Current studies provided further evidences in vivo that the white matter deficits were prominent in the right corpus callosum body. Compared to the previous studies in patients with severe hydrocephalus, our research focused on mild-to-moderate communicating hydrocephalic children who had shorter duration and lower-level hydrocephalus than those of previous studies [13, 15, 28, 29, 32–37]. These findings suggest that the corpus callosum is the most vulnerable white matter tract under hydrocephalus, which happens early in the course of the illness.

We acknowledge several potential limitations of our study. First, our results were derived from a limited number of participants, which may have had an adverse effect on the power of statistical analysis. Second, a confounding factor is the relationship between age of onset and disease duration, which is difficult to resolve in a cross-sectional design. Thus, further longitudinal studies with more patients are required to confirm the changes in cortical thickness and WM ultrastructure in children with mild-to-moderate communicating hydrocephalus. A third limitation is that the Wechsler Intelligence Scale for Children-Chinese Revised is a basic and very ordinary intelligence scale for children, which may be the reason why no association of cortical thinning and decreased FA with IQ was found. Therefore, more detailed intelligence scales may be required to detect specific differences. In addition, we use Evan's index instead of cerebrospinal fluid pressure as crucial indicator for noninvasiveness. However, the accuracy of Evan's index is still not very ideal and more reference indexes will be helpful for noninvasive indicators [3]. Meanwhile, our study lacked functional MRI information and behavior assessments, which needs to be studied further.

5. Conclusions

By studying the school-aged children with mild-to-moderate communicating hydrocephalus, our findings provide evidences that the gray matter of left temporal and frontal lobe and white matter of corpus callosum are the most vulnerable regions in mild-to-moderate hydrocephalus, which happens even before the behavior changes. Thus, structural analysis by MRI can be used to monitor long-term outcomes and follow-up observation in mild-to-moderate hydrocephalic patients.

Abbreviations

CSF: Cerebrospinal fluid
GM: Gray matter
WM: White matter
MRI: Magnetic resonance imaging
T1WI: T1 weighted image
T2WI: T2 weighted image
3-DFSPGR: 3-Dimensional fast spoiled gradient-recalled
DTI: Diffusion tensor imaging
FA: Fractional anisotropy
IQ: Intelligence quota
TR: Repetition time
TE: Echo time
FOV: Field of view
MNI: Montreal Neurological Institute
SD: Standard deviations.

Competing Interests

The authors declare that they have no competing interests regarding the publication of this paper.

Authors' Contributions

Siyu Zhang and Xinjian Ye contributed equally to this study.

Acknowledgments

The authors thank Dr. Chunlei Liu, Department of Electrical Engineering and Computer Sciences, and Helen Wills Neuroscience Institute University of California, Berkeley, CA 94720, USA, and Dr. Su Lui, Huaxi MR Research Center, Department of Radiology, West China Hospital, Sichuan University, Chengdu Sichuan, China, for their helpful comments. The work was supported by the grants from the National Key Research and Development Plan of China (2016YFC0100300); the General Project of the Department of Science and Technology of Zhejiang Province (2017ZD024 and 2017KY109); and the Natural Science Foundation of Zhejiang Province (LY15H180010 and LY16H180009).

References

[1] H. L. Rekate, "A contemporary definition and classification of hydrocephalus," *Seminars in Pediatric Neurology*, vol. 16, no. 1, pp. 9–15, 2009.

[2] M. R. Del Bigio, "Neuropathological changes caused by hydrocephalus," *Acta Neuropathologica*, vol. 85, no. 6, pp. 573–585, 1993.

[3] M. G. Kartal and O. Algin, "Evaluation of hydrocephalus and other cerebrospinal fluid disorders with MRI: an update," *Insights into Imaging*, vol. 5, no. 4, pp. 531–541, 2014.

[4] H. L. Rekate, "A consensus on the classification of hydrocephalus: its utility in the assessment of abnormalities of cerebrospinal fluid dynamics," *Child's Nervous System*, vol. 27, no. 10, pp. 1535–1541, 2011.

[5] D. J. Werring, C. A. Clark, G. J. Barker, A. J. Thompson, and D. H. Miller, "Diffusion tensor imaging of lesions and normal-appearing white matter in multiple sclerosis," *Neurology*, vol. 52, no. 8, pp. 1626–1632, 1999.

[6] F. Zelaya, N. Flood, J. B. Chalk et al., "An evaluation of the time dependence of the anisotropy of the water diffusion tensor in acute human ischemia," *Magnetic Resonance Imaging*, vol. 17, no. 3, pp. 331–348, 1999.

[7] G. Jiang, X. Yin, C. Li et al., "The plasticity of brain gray matter and white matter following lower limb amputation," *Neural Plasticity*, vol. 2015, Article ID 823185, 10 pages, 2015.

[8] K. O. Lim, M. Hedehus, M. Moseley, A. de-Crespigny, E. V. Sullivan, and A. Pfefferbaum, "Compromised white matter tract integrity in schizophrenia inferred from diffusion tensor imaging," *Archives of General Psychiatry*, vol. 56, no. 4, pp. 367–374, 1999.

[9] M. A. Eckert, V. W. Berninger, K. I. Vaden Jr., M. Gebregziabher, and L. Tsu, "Gray matter features of reading disability: a combined meta-analytic and direct analysis approach," *eNeuro*, vol. 3, no. 1, 2016.

[10] W. Zhang, W. Deng, L. Yao et al., "Brain structural abnormalities in a group of never-medicated patients with long-term schizophrenia," *The American Journal of Psychiatry*, vol. 172, no. 10, pp. 995–1003, 2015.

[11] M. Artzi, S. I. Shiran, M. Weinstein et al., "Cortical reorganization following injury early in life," *Neural Plasticity*, vol. 2016, Article ID 8615872, 9 pages, 2016.

[12] M. Dennis, C. R. Fitz, C. T. Netley et al., "The intelligence of hydrocephalic children," *Archives of Neurology*, vol. 38, no. 10, pp. 607–615, 1981.

[13] J. M. Fletcher, S. R. McCauley, M. E. Brandt et al., "Regional brain tissue composition in children with hydrocephalus. Relationships with cognitive development," *Archives of Neurology*, vol. 53, no. 6, pp. 549–557, 1996.

[14] J. P. McAllister II, M. I. Cohen, K. A. O'Mara, and M. H. Johnson, "Progression of experimental infantile hydrocephalus and effects of ventriculoperitoneal shunts: an analysis correlating magnetic resonance imaging with gross morphology," *Neurosurgery*, vol. 29, no. 3, pp. 329–340, 1991.

[15] F. E. Olopade, M. T. Shokunbi, and A.-L. Sirén, "The relationship between ventricular dilatation, neuropathological and neurobehavioural changes in hydrocephalic rats," *Fluids and Barriers of the CNS*, vol. 9, no. 1, article 19, 2012.

[16] B. Fischl and A. M. Dale, "Measuring the thickness of the human cerebral cortex from magnetic resonance images," *Proceedings of the National Academy of Sciences of the United States of America*, vol. 97, no. 20, pp. 11050–11055, 2000.

[17] H. D. Rosas, A. K. Liu, S. Hersch et al., "Regional and progressive thinning of the cortical ribbon in Huntington's disease," *Neurology*, vol. 58, no. 5, pp. 695–701, 2002.

[18] D. H. Salat, R. L. Buckner, A. Z. Snyder et al., "Thinning of the cerebral cortex in aging," *Cerebral Cortex*, vol. 14, no. 7, pp. 721–730, 2004.

[19] X. Han, J. Jovicich, D. Salat et al., "Reliability of MRI-derived measurements of human cerebral cortical thickness: the effects of field strength, scanner upgrade and manufacturer," *NeuroImage*, vol. 32, no. 1, pp. 180–194, 2006.

[20] A. M. Dale, B. Fischl, and M. I. Sereno, "Cortical surface-based analysis: I. Segmentation and surface reconstruction," *NeuroImage*, vol. 9, no. 2, pp. 179–194, 1999.

[21] B. Fischl, D. H. Salat, E. Busa et al., "Whole brain segmentation: automated labeling of neuroanatomical structures in the human brain," *Neuron*, vol. 33, no. 3, pp. 341–355, 2002.

[22] B. Fischl, M. I. Sereno, and A. M. Dale, "Cortical surface-based analysis. II: inflation, flattening, and a surface-based coordinate system," *NeuroImage*, vol. 9, no. 2, pp. 195–207, 1999.

[23] B. Fischl, A. Van Der Kouwe, C. Destrieux et al., "Automatically parcellating the human cerebral cortex," *Cerebral Cortex*, vol. 14, no. 1, pp. 11–22, 2004.

[24] F. Ségonne, A. M. Dale, E. Busa et al., "A hybrid approach to the skull stripping problem in MRI," *NeuroImage*, vol. 22, no. 3, pp. 1060–1075, 2004.

[25] S. M. Smith, M. Jenkinson, H. Johansen-Berg et al., "Tract-based spatial statistics: voxelwise analysis of multi-subject diffusion data," *NeuroImage*, vol. 31, no. 4, pp. 1487–1505, 2006.

[26] T. E. Nichols and A. P. Holmes, "Nonparametric permutation tests for functional neuroimaging: a primer with examples," *Human Brain Mapping*, vol. 15, no. 1, pp. 1–15, 2002.

[27] S. M. Smith and T. E. Nichols, "Threshold-free cluster enhancement: addressing problems of smoothing, threshold dependence and localisation in cluster inference," *NeuroImage*, vol. 44, no. 1, pp. 83–98, 2009.

[28] A. Wünschmann and M. Oglesbee, "Periventricular changes associated with spontaneous canine hydrocephalus," *Veterinary Pathology*, vol. 38, no. 1, pp. 67–73, 2001.

[29] M. Negi, D. Kobayashi, J. Kumagai et al., "An autopsy case of congenital hydrocephalus and severe thinning of the cerebral cortex in a 4-year-old boy," *Neuropathology*, vol. 30, no. 5, pp. 559–563, 2010.

[30] O. J. Castejón, "Submicroscopic pathology of human and experimental hydrocephalic cerebral cortex," *Folia Neuropathologica*, vol. 48, no. 3, pp. 159–174, 2010.

[31] O. J. Castejon, "Transmission electron microscope study of human hydrocephalic cerebral cortex," *Journal of Submicroscopic Cytology and Pathology*, vol. 26, no. 1, pp. 29–39, 1994.

[32] Y. Assaf, L. Ben-Sira, S. Constantini, L. C. Chang, and L. Beni-Adani, "Diffusion tensor imaging in hydrocephalus: initial experience," *American Journal of Neuroradiology*, vol. 27, no. 8, pp. 1717–1724, 2006.

[33] W. Yuan, F. T. Mangano, E. L. Air et al., "Anisotropic diffusion properties in infants with hydrocephalus: a diffusion tensor imaging study," *American Journal of Neuroradiology*, vol. 30, no. 9, pp. 1792–1798, 2009.

[34] W. Yuan, R. C. McKinstry, J. S. Shimony et al., "Diffusion tensor imaging properties and neurobehavioral outcomes in children with hydrocephalus," *American Journal of Neuroradiology*, vol. 34, no. 2, pp. 439–445, 2013.

[35] T. Koyama, K. Marumoto, K. Domen, and H. Miyake, "White matter characteristics of idiopathic normal pressure hydrocephalus: a diffusion tensor tract-based spatial statistic study," *Neurologia Medico-Chirurgica*, vol. 53, no. 9, pp. 601–608, 2013.

[36] Y. Ding, J. P. McAllister II, B. Yao, N. Yan, and A. I. Canady, "Axonal damage associated with enlargement of ventricles during hydrocephalus: a silver impregnation study," *Neurological Research*, vol. 23, no. 6, pp. 581–587, 2001.

[37] M. R. Del Bigio, M. J. Wilson, and T. Enno, "Chronic hydrocephalus in rats and humans: white matter loss and behavior changes," *Annals of Neurology*, vol. 53, no. 3, pp. 337–346, 2003.

Hindawi Publishing Corporation
Neural Plasticity
Volume 2016, Article ID 6353845, 12 pages
http://dx.doi.org/10.1155/2016/6353845

Research Article

Altered Effective Connectivity of Hippocampus-Dependent Episodic Memory Network in mTBI Survivors

Hao Yan,[1,2,3] Yanqin Feng,[3] and Qian Wang[4]

[1]*Neuroimaging Laboratory, School of Biomedical Engineering, Shenzhen University Health Science Center, Shenzhen 518060, China*
[2]*Key Laboratory of Optoelectronic Devices and Systems of Ministry of Education and Guangdong Province, College of Optoelectronic Engineering, Shenzhen University, Shenzhen 518060, China*
[3]*Departments of Linguistics and Psychology, Xidian University, Xi'an 710071, China*
[4]*School of Foreign Languages, Northwestern Polytechnical University, Xi'an 710029, China*

Correspondence should be addressed to Hao Yan; yanhao@xidian.edu.cn

Received 14 September 2016; Accepted 14 November 2016

Academic Editor: Kevin K. W. Wang

Traumatic brain injuries (TBIs) are generally recognized to affect episodic memory. However, less is known regarding how external force altered the way functionally connected brain structures of the episodic memory system interact. To address this issue, we adopted an effective connectivity based analysis, namely, multivariate Granger causality approach, to explore causal interactions within the brain network of interest. Results presented that TBI induced increased bilateral and decreased ipsilateral effective connectivity in the episodic memory network in comparison with that of normal controls. Moreover, the left anterior superior temporal gyrus (aSTG, the concept forming hub), left hippocampus (the personal experience binding hub), and left parahippocampal gyrus (the contextual association hub) were no longer network hubs in TBI survivors, who compensated for hippocampal deficits by relying more on the right hippocampus (underlying perceptual memory) and the right medial frontal gyrus (MeFG) in the anterior prefrontal cortex (PFC). We postulated that the overrecruitment of the right anterior PFC caused dysfunction of the strategic component of episodic memory, which caused deteriorating episodic memory in mTBI survivors. Our findings also suggested that the pattern of brain network changes in TBI survivors presented similar functional consequences to normal aging.

1. Introduction

Traumatic brain injury (TBI) is a heterogeneous phenomenon with a variety of external force causes, severities, and anatomical injuries. The most common causes of TBI include falls, sports-related injuries, and motor vehicle accidents. TBI severity ranges from mild to severe with brain functional deficits for survivors manifesting across motor, sensory, cognitive, psychological, and socioemotional domains.

The temporal lobes are the most vulnerable areas to acute injury in TBI, in part related to their location near the base of the skull and the free edge of the tentorium [1–3]. Hippocampal atrophy in TBI, which has been demonstrated to be related to injury severity [4], is likely to reflect an aggregated effects of trauma-induced cellular loss that develops over time. Protracted neuronal loss of the hippocampus has been well documented in human postmortem studies [5] and in an extensive experimental animal literature that records cell loss [6–8]. Longitudinal studies showed that hippocampal volumes will decline over a prolonged period from 1 week (largest decline) to 2.5 years [9, 10].

The hippocampus is critical for episodic memory [11, 12], which contains personally experienced events situated in subjective time and space [13]. It has been proposed that both remembering past and imagining novel scenarios rely on an intact hippocampus as the physiologic basis for memory formation and consolidation in a coherent scene [14]. Recent evidence suggests that amnesic patients with hippocampal damage have difficulty not only projecting back in time to

mentally simulate the past (retrospection), but also projecting forward in time to mentally simulate novel and specific future scenarios (prospection) [15, 16]. It has also been documented that some TBI survivors seem to live in a timeless world, in a sort of perpetual present experiencing difficulties in traveling back and forward into subjective time [17]. For example, TBI survivors may fail to recall specific events from the personal past [18, 19], may be incompetent in conscious recollection of personal events [19, 20], and may present disturbances in the ability to imagine future (episodic future thinking) [21]. It was putative that the prolonged hippocampal damage may impair the episodic memory system in TBI survivors. However, there was no quantitative MRI study examining how deteriorating structural abnormality of the hippocampus affected episodic memory network in TBI survivors. It prompted us to examine brain connectivity changes of the hippocampus-dependent network in TBI.

Brain connectivity is now being explored by depicting neuronal coupling between brain regions through various techniques [22–24], among which resting state fMRI (rsfMRI) analysis not only has the noninvasive advantage but also possesses additional gains: resting state networks (RSNs) are highly organized in space, reproducible from subject to subject, and allow the search for significant baseline fluctuations to obtain task-free functional network information [25]. To examine cognitive changes specifically, we highlighted how responses in individual brain regions can be effectively combined through functional connectivity. Effective connectivity quantifies directed relationships between brain regions and controls for confounds that limit functional connectivity—features that facilitate insight into functional integration [26]. It overcomes important pitfalls of functional connectivity that limit our understanding of neuronal coupling, such as involvement of functional connection of other cognitive processes, observational noise, or neuronal fluctuations [27]. One popular approach to make effective connectivity analysis is Granger causality analysis (GCA). Coefficient-based GCA is a directed functional connectivity method [28]. It uses multivariate autoregressive models of time series data to illustrate the amount of variance in one region explained by the signal history in another region and quantifies the magnitude and direction of influence of one region time series on another [29]. By examining altered effective interaction in TBI survivors' episodic memory network, we sought to enrich its neural connectivity pathology which is of high importance for accurate diagnosis and early intervention.

The current study planned to focus on mild traumatic brain injury (mTBI) survivors. mTBI is most popular, as it accounts for the overwhelming majority of the head-injured population treated in emergency departments [30]. A recent WHO systematic review suggests that the annual incidence of mild TBI is probably over 600/100,000 [31]. Moreover, moderate and severe TBI consumes most resources per individual, yet mTBI's magnitude and societal ramifications are often underestimated [31]. With the label of "mild," patients do not seek medical attention, are not systematically assessed, or are lost to medical follow-up [32]. However, many of these injuries may result in long-term difficulties. It has been estimated that 40–80% of mTBI survivors experience postconcussive syndrome, a constellation of physical, cognitive, and behavioral difficulties [33] that may persist up to 2 years after TBI [34]. Along with the significant number of mTBI, these negative outcomes underline the value of accurate identification and adequate management [35]. Further, according to a cohort study with standardized tests of language skills, severe TBI group displayed greater improvement in scores from the acute period to 12 months after TBI. However, scores for the mild-moderate TBI groups remained quite stable over time [36]. To keep subjects more homogeneous and reduce intersubject variabilities, we only focused on patients over 3 months to 14 months after TBI.

2. Methods

2.1. Participants. Two groups of participants were included in this study. The TBI group was composed of 19 patients (16 males, mean age 38.21 ± 13.42 years) with mild TBI. Screening for mild TBI was based on the World Health Organization's Collaborating Center for Neurotrauma Task Force. Inclusion criteria were (i) conscious survivors at the time of testing; (ii) a favorable outcome (Glasgow Coma Score of 13–15) according to Glasgow outcome scale (GOS); (iii) loss of consciousness (if present) < 30 min, posttraumatic amnesia (if present) < 24 h, and/or other transient neurological abnormalities such as focal signs, seizure, and intracranial lesion not requiring surgery; (iv) an age range of 19–61 years at the time of injury. Exclusion criteria for participants included documented history of neurological disease or long-standing psychiatric condition, preexisting speech and language disorders, drug or alcohol abuse, head injury, and neurological conditions such as brain tumor, stroke, dementia, and Parkinson's. The present study reports data from the 3- and 14-month postinjury assessments. The adult normal control (NC) group consisted of 19 age- and sociocultural level (indexed by the number of years of education) matched healthy controls (13 males, mean age 36.58 ± 7.86 years). All subjects gave written, informed consent after the experimental procedures had been fully explained, and all research procedures were approved by the Ethical Committee of the First Affiliated Hospital of Medical College of Xi'an Jiaotong University and conducted in accordance with the Declaration of Helsinki.

2.2. Data Acquisition. The MRI scans were acquired with a 1.5 T MRI scanner (Siemens). A custom-built head holder was used to prevent head movements. Alertness during the scan was confirmed immediately afterward. The MRI protocol involved the high-resolution T1-weighted 3D MPRAGE sequence (echo time (TE) = 2.8 ms, repetition time (TR) = 1900 ms, inversion time (TI) = 1000 ms, flip angle = 8°, slice thickness = 1 mm, field of view (FOV) = 256 mm × 256 mm, and matrix size = 256 × 256), and the single-shot, gradient-recalled echo planar imaging (EPI) sequence with 30 slices covering the whole brain (TR = 2000 ms, TE = 24 ms, flip angle = 90°, FOV = 224 mm × 224 mm, matrix size = 64 × 64, and voxel size = 3.5 mm × 3.5 mm × 4.0 mm). Standard T1,

T2, and susceptibility weighted imaging for each patient were examined by two independent neurologists to classify the presence of microbleeds and structural contusion within the clinical group. The scanning datasets were validated visually, and scans were discarded if they did not meet quality control (QC) standards (e.g., regarding artifacts, noise, excessive motion, and missing data). Participants were instructed to stay awake with eyes closed.

2.3. Data Processing. Firstly, we adopted functional connectivity analysis to examine brain function and cooperation at a network level by identifying regions that makes up the network of interest. It reflects the degree of signal synchrony between anatomically distant brain regions during resting state. Secondly, we employed multivariate Granger causality analysis (GCA) to quantify the magnitude and direction of influence between network components determined by the functional connectivity analysis step [37].

We used the FMRIB (Oxford Centre for Functional MRI of the Brain, UK) Software Library (FSL) version 6.0 (https://www.fmrib.ox.ac.uk/fsl/) to preprocess raw data and the MATLAB package named REST (resting state fMRI data analysis Toolkit) to make functional connectivity (FC) analysis [38]. The first ten volumes of each functional time course were discarded to allow for steady state stabilization of BOLD fMRI signals. Then, we preprocessed all images firstly through motion correction with MCFLIRT [39] to calculate six head movement parameters, making sure that no participant had head motion with more than 2.0 mm maximum displacement in any direction or 2.0° of any angular motion throughout the course of the scan. Slice timing correction was based on the slice acquisition parameters (slicetimer, FSL), and spatial normalization registered each participant's functional MRI data to its structural MRI data by using Data Processing Assistant for Resting State fMRI (DPARSF), which were then applied to the standard space image MNI-152 atlas (Montreal Neurological Institute, Montreal, QC, Canada) using a 12 parameter affine registration and high-resolution imaging of each subject using 6 parameter affine registrations. REST was then used for linear trend removal and temporal band-pass filtering (0.01, 0.08 Hz) to remove low and high-frequency signal fluctuations. The preprocessed data were spatially smoothed by a Gaussian kernel of 6 mm FWHM (full width at half maximum).

It has been claimed that the left hippocampus represents sequential aspects of episodic experiences and temporal aspects of autobiographical memory, whereas the right hippocampus in humans plays a greater role in spatial processing [40, 41]. The left hippocampus was therefore identified as the seed region of interest (ROI). Our functional connectivity analysis was based on an AAL atlas threshold. For each participant, the mean time course within this ROI was used as the reference time course. A seed functional connectivity analysis was then performed in a whole brain voxel-wise manner with the averaged time courses of the left hippocampus, the white matter, the CSF, and the six head motion parameters as covariates (REST). Individual r-maps were normalized to Z-maps by using Fisher's Z transformation. All Fisher's Z-maps were entered into a two-sided one-sample t-test to detect regions showing significant functional connectivity with the left hippocampus. Between-group FC differences were determined by two-sample t-test detecting the regions showing significantly different FC strength with the left hippocampus.

The whole brain hippocampal network results are reported at $p < 0.05$ (FDR corrected) and with cluster > 10 voxels. The statistics were color-coded and mapped in MNI space, while brain regions were estimated from Talairach and Tournoux after adjustments for differences between MNI and Talariach coordinates with a nonlinear transform. ROIs for further multivariate Granger causality analysis (mGCA) were defined as regions that showed significant functional connectivity with the left hippocampus in the episodic memory network in healthy controls.

The Granger causality is an optimal candidate for its data-driven nature and is widely used in fMRI studies [42]. The entire time series of BOLD signal intensities from ROIs, averaged across voxels within each ROI among subjects of the same group, were normalized to form a single vector per ROI. The mGCA uses directed transfer function (DTF) [43], computed from a multivariate autoregressive model of the time series in the selected ROIs. In this study, we also adopted the weighted DTF with partial coherence to emphasize direct connections and inhibit mediated influences [43, 44]. To assess the significance of path weights, a null distribution was obtained by generating 2500 sets of surrogate data and calculating the DTF [43, 44]. For instance, Fourier transform was applied to each regional time series, and the phase of the transformed signal was randomized. Inverse Fourier transform was then applied to generate one instance of surrogate data. Test statistics were then computed by fitting the VAR model to the surrogate data. In addition, a difference of influence (doi) term was used to assess links that showed a dominant direction of influence to limit potentially spurious links caused by hemodynamic blurring. The doi was compared with the null distribution for a one-tailed test of significance with a p value of 0.01 (FDR corrected for multiple comparisons). The stringent threshold was chosen to avoid potentially spurious causal links introduced by low temporal resolution and hemodynamic blurring in the fMRI signal [37].

The high degree nodes were considered to be hubs of network [45]. We calculated "In-degree" (number of Granger causal afferent connections to a node) to find the central targets of network, "Out-degree" (number of Granger causal efferent connections from a node) to find the central sources [46, 47], and "In + Out degree" to find network hubs. Further, three kinds of hubs of the network were defined if the sum of "In-degree," "Out-degree," or "In + Out degree" of a node was at least 1 standard deviation (SD) greater than the average degree of all nodes in the network respectively [48, 49]. Between-group degree difference was carried out by the two-sample t-test analysis of the "In-degree," "Out-degree," and "In + Out degree" of each ROI in each individual, respectively. Connection density difference was determined by calculating between-group difference about the numbers of significantly causal interactions in each individual.

Between-group differences in the causal connectivity graphs were determined using permutation tests to get a data-driven nonparametric approach [50]. Permutation tests constructed a distribution of a test statistic by freely resampling the dDTF values without replacement. The key and only assumption for permutation tests is data exchangeability which means the distributions of two group data are identical under the null hypothesis [51]. Here, we randomly permuted the dDTF values to two new groups. As a result, an empirical distribution of the data sets was constructed using test statistic values for all possible permutations. The true doi obtained with the correct pairs of subjects was then compared with the obtained distribution. Thus, p value was calculated by dividing the frequency of permutations presenting more extreme test statistic value by the number of all permutations (10000 times). We consider doi with a $p \leq 0.05$ as reliable.

3. Results

3.1. Functional Connectivity Analysis. Whole brain functional connectivity maps for the mTBI group, healthy controls, and their contrast results are illustrated in Figure 1 and listed in Table 1. These maps illustrate significant functional connectivity between the left hippocampus and a widespread set of brain regions belonging to the episodic memory system. In common, the hippocampal network of both groups covered bilateral inferior frontal gyrus (IFG, BA47), bilateral medial frontal gyrus (MeFG, BA10/11), left inferior temporal gyrus (ITG, BA21/20), bilateral middle temporal gyrus (MTG, BA 21/22), left fusiform gyrus (BA20/37), bilateral parahippocampal gyrus (PHG), left anterior part of the superior temporal gyrus (STG, BA38), the middle portion of the left STG (BA 41/22), bilateral anterior cingulate cortex (ACC), and left posterior cingulate cortex (PCC). The hippocampus-dependent FC network of the mTBI group additionally involved the bilateral posterior parts of STG (BA39) and left supramarginal gyrus (BA40), as well as the right ITG, right fusiform gyrus, right anterior and middle parts of right STG, and right PCC. By contrast, functional connectivity between the left hippocampus and the right middle/posterior STG (BA22/41 and BA39) were significantly stronger in mTBI survivors than in normal controls. However, functional connectivity between the left hippocampus and other components in the hippocampal network was not significantly stronger in normal controls than that in mTBI survivors. We then determined regions in the hippocampus-dependent functionally connected network in healthy controls as ROIs to form a canonical network and evaluated effective connectivity of the episodic memory network by means of mGCA.

3.2. Effective Connectivity Analysis. A causal connectivity graph was constructed using the thickness of connecting lines to indicate strengths of causal influences (see Figures 2(a) and 2(c)). For both mTBI survivors and healthy controls, causal influences within the episodic memory network presented strongly covarying relations (Figures 2(a) and 2(b)). Results from mGCA analysis showed that causal interactions became denser for the mTBI group than that of the NC group. However, connection density between the two groups was not significantly different from each other ($p = 0.84$). Causal interaction results manifested obvious laterality effect across two groups. For the NC group, significant causal interaction mainly existed between ROIs in the left hemisphere. For example, strong causal outflow originated from the left hippocampus to left anterior STG (aSTG), from the left PHG to left aSTG, and from the left PCC to left PHG. Besides, bidirectional interactions in the left hemisphere between the left hippocampus and left PHG and between the left IFG and left MeFG were significant too. However, we also observed two cross-hemisphere causal connectivity, such as from the left MeFG to right MeFG, from the left aSTG to the right IFG, and from the right PHG to left hippocampus (see Figure 2(b)). For the mTBI group, in the contrary, significant causal interaction mainly existed across hemispheres, mainly flowing out from the right hemisphere. For example, strong causal outflow originated from the right MeFG to left MeFG and from the right hippocampus to left aSTG, as well as bidirectional interactions between the left IFG and right MeFG and between the left aSTG and right MTG. Also significant interhemisphere causal connectivity originating from the left hippocampus to left PHG and left PCC and from the left IFG to left aSTG was detected (see Figure 2(d)). The only overlapped causal interaction in both the mTBI and NC groups was bidirectional connectivity between the right hippocampus and right PHG.

Node degree analysis showed that, in healthy controls, there were three hubs in the hippocampus-dependent episodic memory network, such as the left hippocampus, left PHG, and left aSTG. Specifically, central target hubs (flow-in hubs) were the left MeFG, left hippocampus, and left PHG, while the left PHG and left aSTG were the central source hubs (flow-out hubs). In the mTBI survivors, all three kinds of network hubs shifted from the left to the right hemisphere. Specifically, network hubs were the right MeFG and right hippocampus, the central target hub was the right hippocampus, and central source hubs were the left PHG, left aSTG, and right MeFG. Between-group differences of the "In-degree," "Out-degree," and "In + Out degree" values of each ROI were not significantly different (p value ranging from 0.09 to 0.96).

Between-group analysis also showed increased driving effect between nodes in bilateral structures (see Figure 3). In detail, increased interhemisphere causal effects were found in the interactions from the left fusiform gyrus to right IFG (NC mean ± SD versus mTBI mean ± SD: 0.0052 ± 0.0061 versus 0.0169 ± 0.0205, $p = 0.02$), from the right MTG to left fusiform gyrus (0.0014 ± 0.0016 versus 0.0044 ± 0.0054, $p = 0.01$), and from the right hippocampus to left MTG (0.0049±0.0110 versus 0.0169±0.0230, $p = 0.04$) and bilateral interaction between the right MeFG and left MTG (0.0030 ± 0.0050 versus 0.0096±0.0114, $p = 0.02$; 0.0031±0.0045 versus 0.0099 ± 0.0205, $p = 0.01$). Increased intrahemisphere causal connectivity was also identified from the left fusiform to the left STG (0.0035 ± 0.0059 versus 0.0113 ± 0.0171, $p = 0.04$) and from the left MTG to left MeFG (0.0036 ± 0.0049 versus 0.0148 ± 0.0263, $p = 0.03$). No decreased driving effect was

Table 1: Functionally connected brain areas with the left hippocampus in normal controls and mTBI survivors (voxel level: $p < 0.05$, FDR corrected).

	Normal controls					mTBI					mTBI versus normal controls				
	Talairach			t	V	Talairach			t	V	Talairach			t	V
	x	y	z	value	voxels	x	y	z	value	voxels	x	y	z	value	voxels
Frontal cortex															
Inferior frontal gyrus BA47															
L	−45	17	−11	5.00	37	−42	14	−11	5.74	82					
R	24	8	−18	4.48	84	33	29	−12	8.25	123					
Medial frontal gyrus BA10/11															
L	0	37	−12	4.35	20	0	49	−8	6.55	103					
R	3	46	−10	4.09	18	3	49	−8	6.69	65					
Temporal cortex															
Inferior temporal gyrus BA21/20															
L	−50	−50	−10	6.08	72	−56	−9	−12	5.97	135					
R						36	−2	−35	5.00	73					
Middle temporal gyrus BA 21/22															
L	−50	2	−25	5.51	300	−36	1	−33	7.35	476					
R	50	2	−18	4.00	20	53	5	−10	6.24	383					
Fusiform gyrus BA20/37															
L	−36	−10	−22	5.56	167	−36	−13	−22	8.39	246					
R						42	−44	−15	6.48	182					
Parahippocampal gyrus															
L	−24	−12	−15	26.91	518	−21	−12	−15	23.79	628					
R	27	−24	−9	8.75	193	24	−1	10	11.00	477					
Hippocampus															
R	30	−24	−9	7.14	130	36	−9	−12	10.72	183					
Superior temporal gyrus BA38															
L	−30	10	−31	5.72	181	−33	−1	−13	8.76	255					
R						27	4	−33	8.66	284					
Superior temporal gyrus BA22/41															
L	−42	−27	−6	4.60	34	−53	−9	−10	7.13	439					
R						48	−11	3	8.14	417	62	−40	13	8.18	51
Superior temporal gyrus BA39															
L						−45	−52	16	5.17	37					
R						48	−52	11	6.62	39	48	−52	11	6.13	17
Parietal cortex															
Supramarginal gyrus BA40															
L						−56	−49	19	4.60	13					
R															

Table 1: Continued.

	Normal controls					mTBI					mTBI versus normal controls				
	Talairach			t	V	Talairach			t	V	Talairach			t	V
	x	y	z	value	voxels	x	y	z	value	voxels	x	y	z	value	voxels
Subcortical cortex															
ACC															
L	−3	0	−8	5.93	40	−3	3	−3	4.34	41					
R	3	32	−7	3.45	23	3	34	−9	4.00	79					
PCC															
L	−18	−40	10	5.38	21	−15	−43	8	5.12	48					
R						12	−34	18	4.24	28					

BA: Brodmann area; ACC: anterior cingulate cortex; PCC: posterior cingulate cortex.

detected by comparing the mTBI group with that the NC group.

4. Discussion

Resting state fMRI maps have been shown to reveal the full distribution of memory-related regions, as they coincide with regions showing activation across a variety of task-based memory studies [52]. The current study sought for covarying areas with the left hippocampus and determined the hippocampus-dependent neural network of episodic memory in mTBI survivors with reference to previous findings. Further effective connectivity analysis of this hippocampal network by GCA revealed significant findings, such as contralateral shift of source, target and network hubs, weakened ipsilateral causal interactions, and increased causal interactions across the two hemispheres, which reflected the neural compensatory mechanism of mTBI survivors.

4.1. An Extended Hippocampal Network in mTBI Survivors. The hippocampus-dependent neural network identified in the current study was consistent with previous findings. Specifically, functional connectivity was observed between the hippocampus and many regions of the brain, including the IFG, the MeFG (anterior prefrontal gyrus), the anterior part of STG, the MTG, the ITG, the parahippocampus, and the PCC/retrosplenial cortex [14, 52–55]. These structures are also known to be involved in the default mode network (DMN). As part of episodic memory network [56], the DMN is an interconnected and anatomically defined brain system that preferentially activates in states of relative rest but deactivate during tasks [57]. As expected, mTBI survivors compensated for hippocampal deficits by relying on an intensified and extended functionally connected network. Along with the heavier manipulation of the hippocampal neural network, both the anterior and posterior parts of right STG were overrecruited by mTBI survivors. It was consistent with many neuroimaging studies concerning episodic memory, which have reported that functional brain activity in elders increases in the right hemisphere [58]. Recruitment of the right hemisphere reflected that mTBI patients compensated for decreased functional connectivity of one brain region through recruiting additional brain resources in the contralateral hemisphere to perform a cognitive task. By means of GCA, directed relationships with different linking weights within the episodic memory network provided more information.

4.2. A Contralateral Shift of Network Hubs. Causal interaction analysis between ROIs determined by functional connectivity analysis found that hubs of patients' episodic memory network displayed a contralateral shift. In NC, network hubs were the left hippocampus and the PHG (also flow-in hubs, with a dominant role of receiving information) as well as the left aSTG (as a flow-out hub, with a dominant role of sending information). These areas constituted an interactive model of episodic memory in which the anterior STG and hippocampus/PHG were information integration centers for semantic and episodic memory in the declarative memory system.

As a macromodel based on neuropsychological data which presents an interactive construction of memory systems, the MNESIS model (short for Memory NEoStructural Inter-Systemic model) specifies the dynamic and reconstructive nature of memory by highlighting a hierarchical order of three long-term representation systems of perceptual memory (the lowest level), semantic memory, and episodic memory (the highest level) and adds two retroactive processes of memory semanticization and perceptual memory transfer during experience reliving [59]. The perceptual representation system receives, stores, and makes the basic unit of information about perceptual features of physical objects available to other systems [60]. Semantic memory refers to one's noetic awareness of the existence of the world and objects, events and other regularities in it, independent of self, autonoetic awareness and time [60]. When semantic information of the memory, which has no contextual richness but present a schematic version of the memory, is established, retrieval processes are required to reactivate its

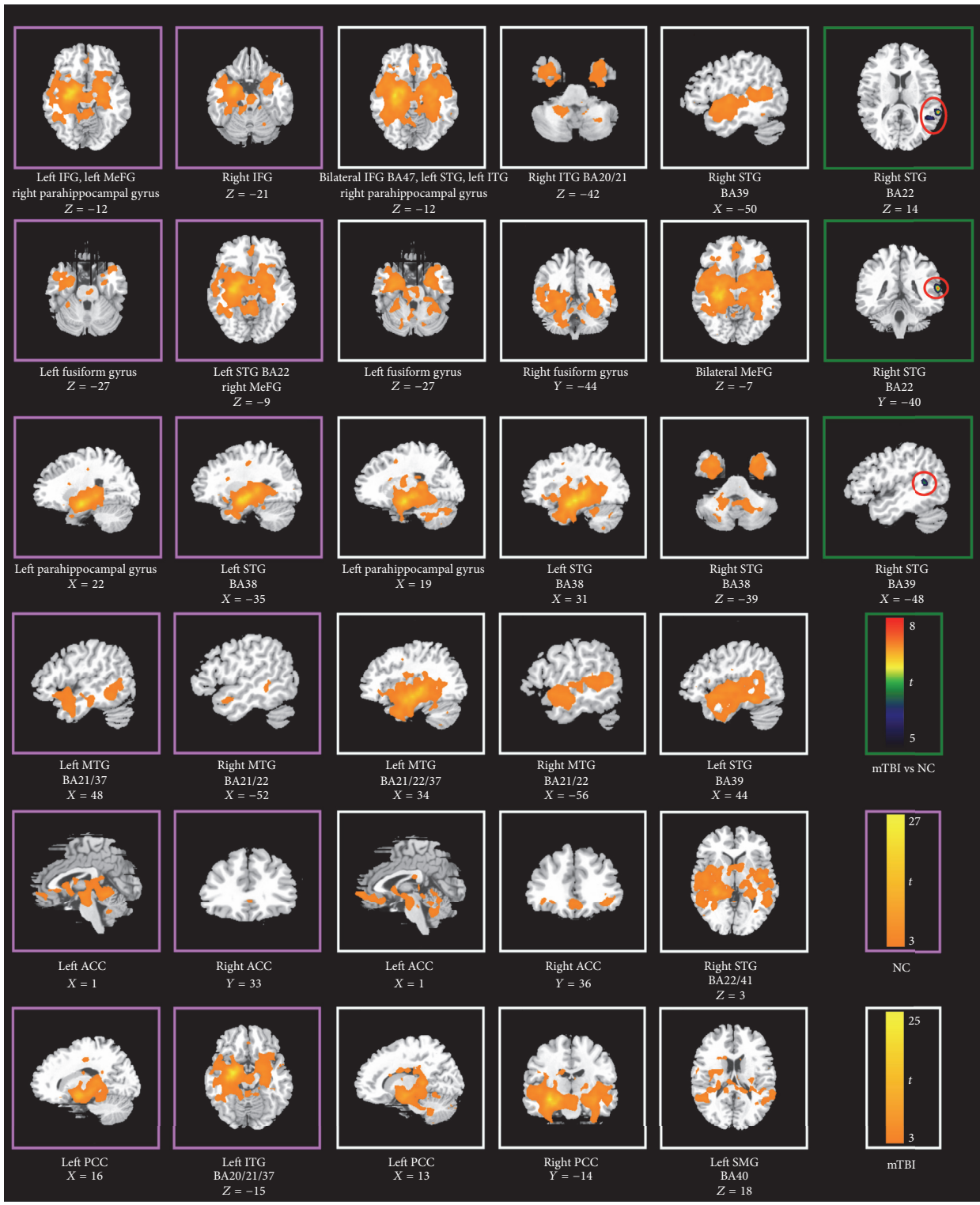

Figure 1: Functional connected hippocampal networks concerning episodic memory in normal controls and mTBI survivors, as well their differences. (i) Covarying brain areas in two groups and their differences were presented in the pink box, white box, and green box, respectively. (ii) BA: Brodmann area; IFG: inferior frontal gyrus; MeFG: medial frontal gyrus; MTG: middle temporal gyrus; ITG: inferior temporal gyrus; STG: superior temporal gyrus; SMG: supramarginal gyrus; ACC: anterior cingulate cortex; PCC: posterior cingulate cortex.

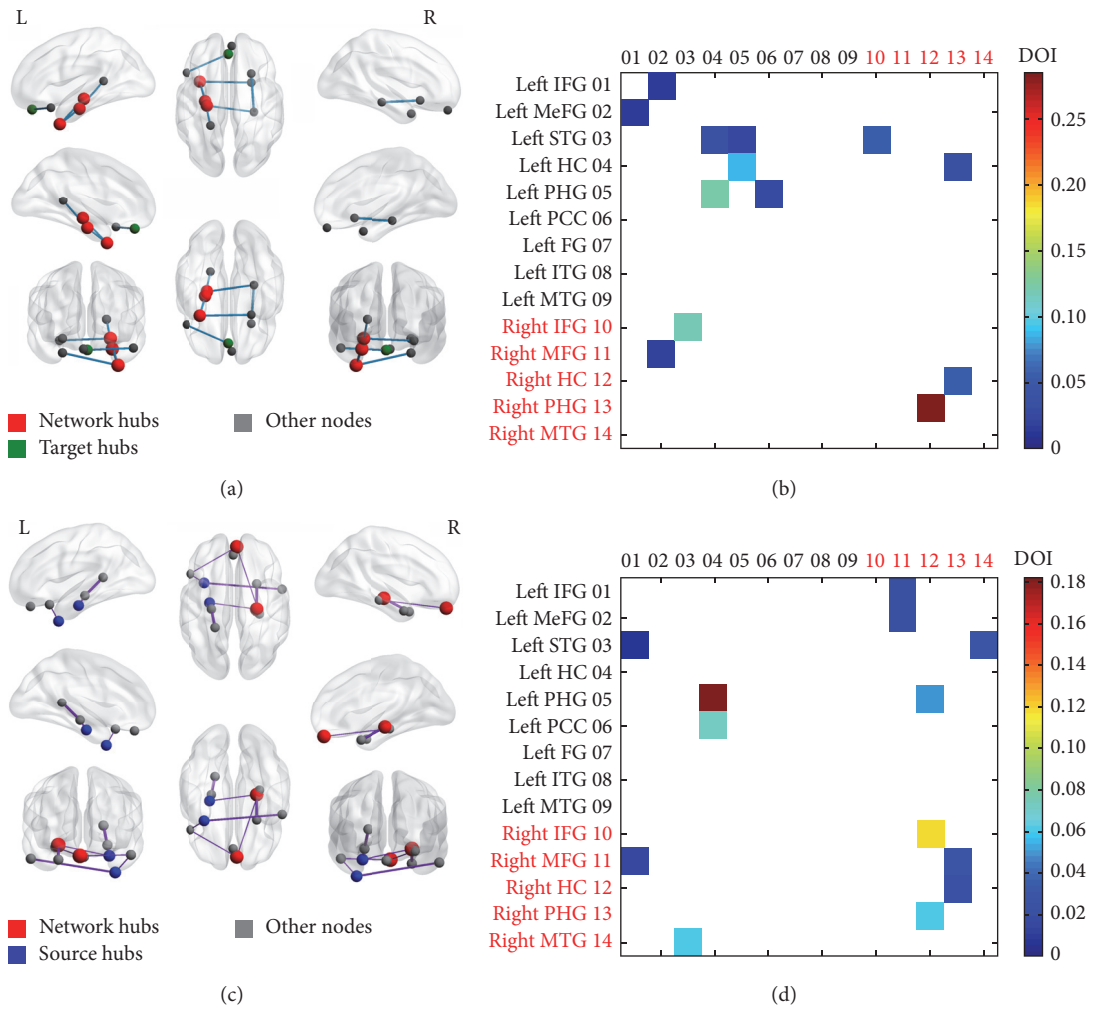

Figure 2: Causal influence of effectively connected episodic memory network in normal controls and mTBI survivors. (i) Connection density in normal controls and mTBI was not significantly different; (ii) significant causal interaction mainly existed between ROIs in the left hemisphere in normal controls, while mTBI survivors presented significant cross-hemisphere connection originating from the right hemisphere; (iii) nodes of source hubs (flow-out hubs), target hubs (flow-in hubs), and network hubs were displayed by different colors, but only the network hub color was presented if their function overlapped (a, c); (iv) significant causal interactions from nodes in x-axis to nodes in y-axis among all possible causal interactions were presented in (b, d); (v) relative strengths of path weights (in arbitrary units) were indicated by the width of lines; (vi) IFG:inferior frontal gyrus; MeFG: medial frontal gyrus; MTG-middle temporal gyrus; ITG: inferior temporal gyrus; STG-: superior temporal gyrus; FG: fusiform; HC: hippocampus; PHG: parahippocampal gyrus; ACC: anterior cingulate cortex; PCC: posterior cingulate cortex.

mental representations and return the individual to his or her conscious experience of the event [61]. These personal experiences covered detailed contextual information [62], scene construction [63], and a sense of reliving or autonoetic consciousness [64].

Semantic memory encompasses a rich fund of general knowledge about the world, represented in visual, olfactory, gustatory, tactile, and auditory cortices [65, 66], conducive to the identity of perceptual events. It is proposed that these multiple sensory inputs are converged in the left anterior temporal lobe (ATL), a transmodal representational hub [65], to form a concept. The ATL as a concept formation center in the semantic memory network has been demonstrated by magnetoencephalography, distortion-corrected functional MRI, PET, or repetitive transcranial magnetic stimulation techniques [67]. Meanwhile, the hippocampus is always involved whenever detailed; contextual information is recalled according to the Transformation Hypothesis of memory consolidation [68] and the Binding of Items and Contexts model [69]. Personal experience is represented as a pattern of features that correspond to different facets processed during the encoding of the episode [70]. The hippocampus is more adept at associating multiple attributes of differential forms of memory than other structures [71]. Inputs from regions of the recognition (or context) memory network are not directly involved in memory strength, but converge at the hippocampus to become cohesive memories of individual events via the formation ("binding") of episodic

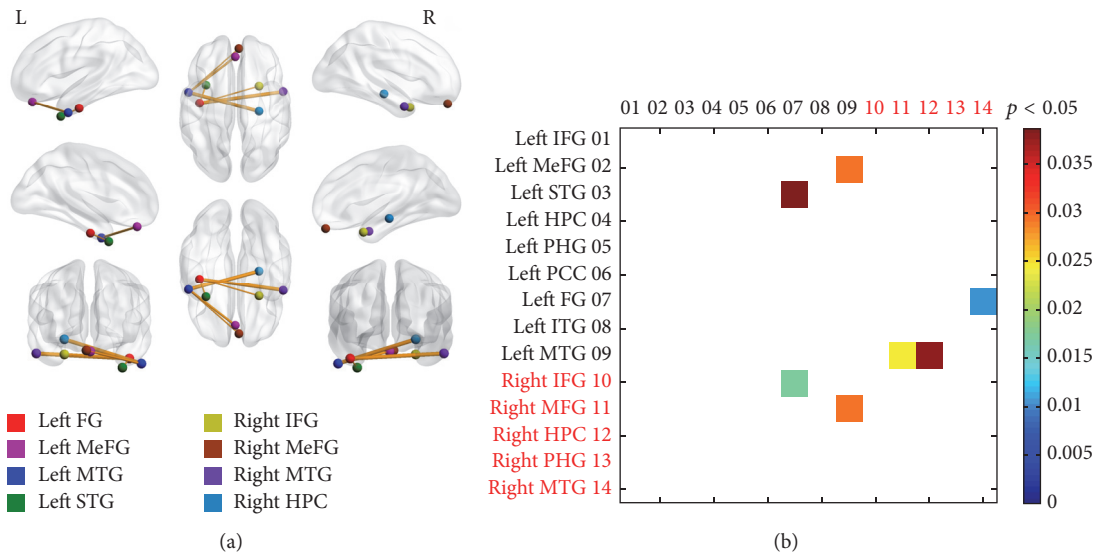

FIGURE 3: Changes of the driving effect in the episodic memory network between mTBI and normal controls. (i) Most increased driving effects were detected between bilateral structures in patients surviving mTBI. (ii) No decreased causal interaction was found in mTBI survivors. (iii) Relative strengths of path weights (in arbitrary units) were indicated by the width of lines.

memory [72, 73]. After binding, the outputs of the hippocampus return to cortical regions from which the inputs arose. Thus, the hippocampus performs complex high-resolution binding of the different qualitative aspects of an event, both at encoding and at retrieval [58]. The parahippocampal area is also an important hub as it enables the communication between the hippocampus and neocortical areas [74]. It has been proposed that the PHG provides contextual information about the "where" and "when" of a target item for memory encoding to the hippocampus to bind new memories and link the memory of that particular episode within a larger network [11, 59, 69], underlining its integrative and maintenance functions.

In mTBI survivors, both the left hippocampus/PHG and anterior STG were no longer network hubs. It indicated that external forces can severely damage human declarative memory. These network hubs in normal controls were replaced by the right hippocampus and right MeFG. It was compatible with the pathological observation that reduced volume of the temporal lobe is commonly found following moderate to severe TBI, due to abrasive contact with bony plates of the skull during the acute injury. The observed compensation mechanism in mTBI was also consistent with previous findings. A latest research, which performs a direct test of the relationship between episodic memory's perceptual richness and hippocampal function, claims that the right hippocampus plays an important role in the recruitment of posterior cortical regions that support the representation of perceptual memory content [75]. In the current study, mTBI survivors enhanced effective connectivity of the right hippocampus with other regions. It reflected that mTBI survivors compensated for episodic memory dysfunction by means of overenrollment of the perceptual memory system.

Meanwhile, greater activation of the right PFC also indicated an optimized compensation mechanism in the mTBI survivors. The PFC is generally thought to be the primary site of scaffolds to compensate for declines in functioning in other regions, due to its versatile and flexible nature [76]. It was suggested that at least some of the age-related overrecruitment in prefrontal cortex may reflect attempted compensation for reduced activation in the hippocampus [77]. A recent review also highlighted that the PFC was heavily activated during memory encoding and retrieval in elderly participants [78]. With reference to neurocognitive models, it was postulated that the strategic component of episodic memory depends primarily on the PFC to constrain memory search and monitor the appropriateness of recovered memories [79]. The intensified interconnection between the right MeFG and other regions in the current study showed that mTBI survivors manipulated the right MeFG to a greater degree to make up for the left hippocampus deficit. We attributed its greater involvement to increased strategic retrieval/recombination demands. However, overactivation of the PFC is not always related to better performance but a poorer memory [80], because recruitment of additional brain regions might come with additional cost [81]. We postulated that overrecruitment of the right MeFG may cause dysfunction of its primary role due to overload. The affected executive control and working memory thus led to failed episodic memory retrieval.

A study analyzing story narratives from 10 participants with TBI reported a normal microlinguistic processing (lexical and syntactic) but impaired macrolinguistic abilities (pragmatic, cohesive, and coherent) in TBI survivors [82]. The authors defined these patients as nonaphasic and suggested that their confused and impoverished language was caused by reduced ability to organize information at the macrolinguistic level (unable to guide comprehension and production of logical relationships, both temporal and causal, between agents and events) [83]. Our primary finding of

a disrupted causal connectivity between the left aSTG (the concept formation center in the semantic memory network) and the hippocampus may provide their research a possible explanation. We demonstrated that it was due to the broken-down interaction of the concept forming center and the context binding center that caused the abnormal macrolinguistic processing but preserved lexical and syntactic competence in TBI survivors. Hence, TBI survivors always presented a confused and impoverished language but no obvious symptoms of other language deficits, such as anomia.

5. Conclusion

Brain injury of the hippocampus was consistently reported to cause a chronic post-TBI episodic memory impairment. By examining altered effective connectivity of the episodic memory network in mTBI survivors, we found that the pattern of brain network changes detected in TBI survivors has similar functional consequences to normal aging [84]. Even though functionally connected regions with the hippocampus were extended, dysfunction of neural network hubs of the aSTG, hippocampus, and PHG in the dominant hemisphere and overrecruitment of the right MeFG lead to an abnormal episodic memory network. Our findings also demonstrated that effective connectivity analysis was more suitable to represent the working mechanism of an episodic memory network than functional connectivity analysis. To the best of our knowledge, this is the first in vivo demonstration of the dynamic relationships between nodes in the hippocampal episodic memory network in mTBI survivors.

Competing Interests

There are no competing interests.

Acknowledgments

This paper is supported by the National Natural Science Foundation of China (31400962, 81371201, and 31371026), China Postdoctoral Science Foundation (2015M582400), and the Fundamental Research Funds for the Central Universities (RW150401).

References

[1] M. Ariza, J. M. Serra-Grabulosa, C. Junqué et al., "Hippocampal head atrophy after traumatic brain injury," *Neuropsychologia*, vol. 44, no. 10, pp. 1956–1961, 2006.

[2] E. D. Bigler, "Anterior and middle cranial fossa in traumatic brain injury: relevant neuroanatomy and neuropathology in the study of neuropsychological outcome," *Neuropsychology*, vol. 21, no. 5, pp. 515–531, 2007.

[3] B. Levine, N. Kovacevic, E. I. Nica et al., "The Toronto traumatic brain injury study: injury severity and quantified MRI," *Neurology*, vol. 70, no. 10, pp. 771–778, 2008.

[4] P. M. Vespa, D. L. McArthur, Y. Xu et al., "Nonconvulsive seizures after traumatic brain injury are associated with hippocampal atrophy," *Neurology*, vol. 75, no. 9, pp. 792–798, 2010.

[5] W. L. Maxwell, K. Dhillon, L. Harper et al., "There is differential loss of pyramidal cells from the human hippocampus with survival after blunt head injury," *Journal of Neuropathology and Experimental Neurology*, vol. 62, no. 3, pp. 272–279, 2003.

[6] W. S. Carbonell and M. S. Grady, "Regional and temporal characterization of neuronal, glial, and axonal response after traumatic brain injury in the mouse," *Acta Neuropathologica*, vol. 98, no. 4, pp. 396–406, 1999.

[7] D. M. Geddes, M. C. LaPlaca, and R. S. Cargill II, "Susceptibility of hippocampal neurons to mechanically induced injury," *Experimental Neurology*, vol. 184, no. 1, pp. 420–427, 2003.

[8] J. E. S. Pierce, D. H. Smith, J. Q. Trojanowski, and T. K. McIntosh, "Enduring cognitive, neurobehavioral and histopathological changes persist for up to one year following severe experimental brain injury in rats," *Neuroscience*, vol. 87, no. 2, pp. 359–369, 1998.

[9] M. A. Warner, T. S. Youn, T. Davis et al., "Regionally selective atrophy after traumatic axonal injury," *Archives of Neurology*, vol. 67, no. 11, pp. 1336–1344, 2010.

[10] K. Ng, D. J. Mikulis, J. Glazer et al., "Magnetic resonance imaging evidence of progression of subacute brain atrophy in moderate to severe traumatic brain injury," *Archives of Physical Medicine and Rehabilitation*, vol. 89, no. 12, pp. S35–S44, 2008.

[11] H. Eichenbaum, A. P. Yonelinas, and C. Ranganath, "The medial temporal lobe and recognition memory," *Annual Review of Neuroscience*, vol. 30, pp. 123–152, 2007.

[12] L. R. Squire, C. E. L. Stark, and R. E. Clark, "The medial temporal lobe," *Annual Review of Neuroscience*, vol. 27, pp. 279–306, 2004.

[13] E. Tulving, D. L. Schacter, D. R. McLachlan, and M. Moscovitch, "Priming of semantic autobiographical knowledge: a case study of retrograde amnesia," *Brain and Cognition*, vol. 8, no. 1, pp. 3–20, 1988.

[14] D. Hassabis and E. A. Maguire, "Deconstructing episodic memory with construction," *Trends in Cognitive Sciences*, vol. 11, no. 7, pp. 299–306, 2007.

[15] D. Hassabis, D. Kumaran, S. D. Vann, and E. A. Maguire, "Patients with hippocampal amnesia cannot imagine new experiences," *Proceedings of the National Academy of Sciences of the United States of America*, vol. 104, no. 5, pp. 1726–1731, 2007.

[16] E. Race, M. M. Keane, and M. Verfaellie, "Medial temporal lobe damage causes deficits in episodic memory and episodic future thinking not attributable to deficits in narrative construction," *The Journal of Neuroscience*, vol. 31, no. 28, pp. 10262–10269, 2011.

[17] C. Coste, B. Navarro, C. Vallat-Azouvi, M. Brami, P. Azouvi, and P. Piolino, "Disruption of temporally extended self-memory system following traumatic brain injury," *Neuropsychologia*, vol. 71, pp. 133–145, 2015.

[18] R. G. Knight and K. O'Hagan, "Autobiographical memory in long-term survivors of severe traumatic brain injury," *Journal of Clinical and Experimental Neuropsychology*, vol. 31, no. 5, pp. 575–583, 2009.

[19] P. Piolino, B. Desgranges, L. Manning, P. North, C. Jokic, and F. Eustache, "Autobiographical memory, the sense of recollection and executive functions after severe traumatic brain injury," *Cortex*, vol. 43, no. 2, pp. 176–195, 2007.

[20] E. Tulving, "Episodic memory: from mind to brain," *Annual Review of Psychology*, vol. 53, pp. 1–25, 2002.

[21] R. S. Rosenbaum, A. Gilboa, and M. Moscovitch, "Case studies continue to illuminate the cognitive neuroscience of memory,"

Annals of the New York Academy of Sciences, vol. 1316, no. 1, pp. 105–133, 2014.

[22] K. Friston, "Causal modelling and brain connectivity in functional magnetic resonance imaging," *PLoS Biology*, vol. 7, no. 2, article no. e33, 2009.

[23] S. M. Smith, K. L. Miller, G. Salimi-Khorshidi et al., "Network modelling methods for FMRI," *NeuroImage*, vol. 54, no. 2, pp. 875–891, 2011.

[24] O. Sporns, "Contributions and challenges for network models in cognitive neuroscience," *Nature Neuroscience*, vol. 17, no. 5, pp. 652–660, 2014.

[25] B. B. Biswal, M. Mennes, X. N. Zuo et al., "Toward discovery science of human brain function," *Proceedings of the National Academy of Sciences of the United States of America*, vol. 107, pp. 4734–4739, 2010.

[26] H.-J. Park and K. Friston, "Structural and functional brain networks: from connections to cognition," *Science*, vol. 342, no. 6158, Article ID 1238411, 2013.

[27] K. J. Friston, "Functional and effective connectivity: a review," *Brain Connectivity*, vol. 1, no. 1, pp. 13–36, 2011.

[28] G. Chen, J. P. Hamilton, M. E. Thomason, I. H. Gotlib, Z. S. Saad, and R. W. Cox, "Granger causality via vector auto-regression tuned for FMRI data analysis," in *Proceedings of the 17th Annual Scientific Meeting and Exhibition (ISMRM '09)*, vol. 17, p. 1718, International Society for Magnetic Resonance in Medicine, Honolulu, Hawaii, USA, April 2009.

[29] V. L. Morgan, B. P. Rogers, H. H. Sonmezturk, J. C. Gore, and B. Abou-Khalil, "Cross hippocampal influence in mesial temporal lobe epilepsy measured with high temporal resolution functional magnetic resonance imaging," *Epilepsia*, vol. 52, no. 9, pp. 1741–1749, 2011.

[30] F. Tagliaferri, C. Compagnone, M. Korsic, F. Servadei, and J. Kraus, "A systematic review of brain injury epidemiology in Europe," *Acta Neurochirurgica*, vol. 148, no. 3, pp. 255–268, 2006.

[31] J. D. Cassidy, L. J. Carroll, P. M. Peloso et al., "Incidence, risk factors and prevention of mild traumatic brain injury: results of the WHO Collaborating Centre Task Force on Mild Traumatic Brain Injury," *Journal of Rehabilitation Medicine*, vol. 36, no. 43, pp. 28–60, 2004.

[32] P. Dischinger, K. Read, T. Kerns et al., "Causes and outcomes of mild traumatic brain injury: an analysis of CIREN data," *Annual Proceedings—Association for the Advancement of Automotive Medicine*, vol. 47, pp. 577–589, 2003.

[33] J. D. Corrigan, M. Wolfe, W. J. Mysiw, R. D. Jackson, and J. A. Bogner, "Early identification of mild traumatic brain injury in female victims of domestic violence," *Clinical Journal of Women's Health*, vol. 1, no. 4, pp. 184–190, 2001.

[34] E. J. O'Shaughnessy, R. S. Fowler Jr., and V. Reid, "Sequelae of mild closed head injuries," *Journal of Family Practice*, vol. 18, no. 3, pp. 391–394, 1984.

[35] L. J. Carroll, J. D. Cassidy, L. Holm, J. Kraus, and V. G. Coronado, "Methodological issues and research recommendations for mild traumatic brain injury: the who collaborating centre task force on mild traumatic brain injury," *Journal of Rehabilitation Medicine*, no. 43, pp. 113–125, 2004.

[36] V. A. Anderson, S. A. Morse, G. Klug et al., "Predicting recovery from head injury in young children: a prospective analysis," *Journal of the International Neuropsychological Society*, vol. 3, no. 6, pp. 568–580, 1997.

[37] A. Roebroeck, E. Formisano, and R. Goebel, "Mapping directed influence over the brain using Granger causality and fMRI," *NeuroImage*, vol. 25, no. 1, pp. 230–242, 2005.

[38] X.-W. Song, Z.-Y. Dong, X.-Y. Long et al., "REST: a toolkit for resting-state functional magnetic resonance imaging data processing," *PLoS ONE*, vol. 6, no. 9, Article ID e25031, 2011.

[39] M. Jenkinson, P. Bannister, M. Brady, and S. Smith, "Improved optimization for the robust and accurate linear registration and motion correction of brain images," *NeuroImage*, vol. 17, no. 2, pp. 825–841, 2002.

[40] R.-P. Behrendt, "Conscious experience and episodic memory: hippocampus at the crossroads," *Frontiers in Psychology*, vol. 4, article 304, 2013.

[41] A. Talati and J. Hirsch, "Functional specialization within the medial frontal gyrus for perceptual go/no-go decisions based on 'what,' 'when,' and 'where' related information: an fMRI study," *Journal of Cognitive Neuroscience*, vol. 17, no. 7, pp. 981–993, 2005.

[42] O. Demirci, M. C. Stevens, N. C. Andreasen et al., "Investigation of relationships between fMRI brain networks in the spectral domain using ICA and Granger causality reveals distinct differences between schizophrenia patients and healthy controls," *NeuroImage*, vol. 46, no. 2, pp. 419–431, 2009.

[43] R. Stilla, G. Deshpande, S. LaConte, X. Hu, and K. Sathian, "Posteromedial parietal cortical activity and inputs predict tactile spatial acuity," *Journal of Neuroscience*, vol. 27, no. 41, pp. 11091–11102, 2007.

[44] G. Deshpande, K. Sathian, and X. Hu, "Effect of hemodynamic variability on Granger causality analysis of fMRI," *NeuroImage*, vol. 52, no. 3, pp. 884–896, 2010.

[45] E. Bullmore and O. Sporns, "Complex brain networks: graph theoretical analysis of structural and functional systems," *Nature Reviews Neuroscience*, vol. 10, no. 3, pp. 186–198, 2009.

[46] D. Sridharan, D. J. Levitin, and V. Menon, "A critical role for the right fronto-insular cortex in switching between central-executive and default-mode networks," *Proceedings of the National Academy of Sciences of the United States of America*, vol. 105, no. 34, pp. 12569–12574, 2008.

[47] M. C. Stevens, G. D. Pearlson, and V. D. Calhoun, "Changes in the interaction of resting-state neural networks from adolescence to adulthood," *Human Brain Mapping*, vol. 30, no. 8, pp. 2356–2366, 2009.

[48] W. Liao, J. Ding, D. Marinazzo et al., "Small-world directed networks in the human brain: multivariate Granger causality analysis of resting-state fMRI," *NeuroImage*, vol. 54, no. 4, pp. 2683–2694, 2011.

[49] Z. Liu, Y. Zhang, L. Bai et al., "Investigation of the effective connectivity of resting state networks in Alzheimer's disease: a functional MRI study combining independent components analysis and multivariate Granger causality analysis," *NMR in Biomedicine*, vol. 25, no. 12, pp. 1311–1320, 2012.

[50] A. P. Holmes, R. C. Blair, J. D. G. Watson, and I. Ford, "Nonparametric analysis of statistic images from functional mapping experiments," *Journal of Cerebral Blood Flow and Metabolism*, vol. 16, no. 1, pp. 7–22, 1996.

[51] T. E. Nichols and A. P. Holmes, "Nonparametric permutation tests for functional neuroimaging: a primer with examples," *Human Brain Mapping*, vol. 15, no. 1, pp. 1–25, 2002.

[52] J. L. Vincent, A. Z. Snyder, M. D. Fox et al., "Coherent spontaneous activity identifies a hippocampal-parietal memory network," *Journal of Neurophysiology*, vol. 96, no. 6, pp. 3517–3531, 2006.

[53] M. D. Greicius, B. Krasnow, A. L. Reiss, and V. Menon, "Functional connectivity in the resting brain: a network analysis of the default mode hypothesis," *Proceedings of the National Academy of Sciences of the United States of America*, vol. 100, no. 1, pp. 253–258, 2003.

[54] A. R. Laird, S. B. Eickhoff, K. Li, D. A. Robin, D. C. Glahn, and P. T. Fox, "Investigating the functional heterogeneity of the default mode network using coordinate-based meta-analytic modeling," *Journal of Neuroscience*, vol. 29, no. 46, pp. 14496–14505, 2009.

[55] D. L. Schacter, D. R. Addis, and R. L. Buckner, "Remembering the past to imagine the future: the prospective brain," *Nature Reviews Neuroscience*, vol. 8, no. 9, pp. 657–661, 2007.

[56] I. Shapira-Lichter, N. Oren, Y. Jacob, M. Gruberger, and T. Hendler, "Portraying the unique contribution of the default mode network to internally driven mnemonic processes," *Proceedings of the National Academy of Sciences of the United States of America*, vol. 110, no. 13, pp. 4950–4955, 2013.

[57] A. Anticevic, M. W. Cole, J. D. Murray, P. R. Corlett, X.-J. Wang, and J. H. Krystal, "The role of default network deactivation in cognition and disease," *Trends in Cognitive Sciences*, vol. 16, no. 12, pp. 584–592, 2012.

[58] E. D. Leshikar, A. H. Gutchess, A. C. Hebrank, B. P. Sutton, and D. C. Park, "The impact of increased relational encoding demands on frontal and hippocampal function in older adults," *Cortex*, vol. 46, no. 4, pp. 507–521, 2010.

[59] F. Eustache, A. Viard, and B. Desgranges, "The MNESIS model: memory systems and processes, identity and future thinking," *Neuropsychologia*, vol. 87, pp. 96–109, 2016.

[60] E. Tulving, "Episodic memory and common sense: how far apart?" *Philosophical Transactions of the Royal Society B: Biological Sciences*, vol. 356, no. 1413, pp. 1505–1515, 2001.

[61] E. Tulving, *Elements of Episodic Memory*, Oxford University Press, London, UK, 1983.

[62] A. P. Yonelinas, "The hippocampus supports high-resolution binding in the service of perception, working memory and long-term memory," *Behavioural Brain Research*, vol. 254, pp. 34–44, 2013.

[63] E. A. Maguire and S. L. Mullally, "The hippocampus: a manifesto for change," *Journal of Experimental Psychology: General*, vol. 142, no. 4, pp. 1180–1189, 2013.

[64] D. C. Rubin and S. Umanath, "Event memory: a theory of memory for laboratory, autobiographical, and fictional events," *Psychological Review*, vol. 122, no. 1, pp. 1–23, 2015.

[65] T. T. Rogers, M. A. Lambon Ralph, P. Garrard et al., "Structure and deterioration of semantic memory: a neuropsychological and computational investigation," *Psychological Review*, vol. 111, no. 1, pp. 205–235, 2004.

[66] K. Patterson, P. J. Nestor, and T. T. Rogers, "Where do you know what you know? The representation of semantic knowledge in the human brain," *Nature Reviews Neuroscience*, vol. 8, no. 12, pp. 976–987, 2007.

[67] M. A. Lambon Ralph, "Neurocognitive insights on conceptual knowledge and its breakdown," *Philosophical Transactions of the Royal Society B: Biological Sciences*, vol. 369, no. 1634, Article ID 20120392, 2014.

[68] G. Winocur, M. Moscovitch, and B. Bontempi, "Memory formation and long-term retention in humans and animals: convergence towards a transformation account of hippocampal-neocortical interactions," *Neuropsychologia*, vol. 48, no. 8, pp. 2339–2356, 2010.

[69] R. A. Diana, A. P. Yonelinas, and C. Ranganath, "Imaging recollection and familiarity in the medial temporal lobe: a three-component model," *Trends in Cognitive Sciences*, vol. 11, no. 9, pp. 379–386, 2007.

[70] L. J. Gottlieb, J. Wong, M. De Chastelaine, and M. D. Rugg, "Neural correlates of the encoding of multimodal contextual features," *Learning and Memory*, vol. 19, no. 12, pp. 605–614, 2012.

[71] L. R. Squire, A. S. Van Der Horst, S. G. R. McDuff, J. C. Frascino, R. O. Hopkins, and K. N. Mauldin, "Role of the hippocampus in remembering the past and imagining the future," *Proceedings of the National Academy of Sciences of the United States of America*, vol. 107, no. 44, pp. 19044–19048, 2010.

[72] R. P. C. Kessels, D. Hobbel, and A. Postma, "Aging, context memory and binding: a comparison of 'what, where and when' in young and older adults," *International Journal of Neuroscience*, vol. 117, no. 6, pp. 795–810, 2007.

[73] F. Lekeu, P. Marczewski, M. Van Der Linden et al., "Effects of incidental and intentional feature binding on recognition: a behavioural and PET activation study," *Neuropsychologia*, vol. 40, no. 2, pp. 131–144, 2002.

[74] E. M. Aminoff, K. Kveraga, and M. Bar, "The role of the parahippocampal cortex in cognition," *Trends in Cognitive Sciences*, vol. 17, no. 8, pp. 379–390, 2013.

[75] M. St-Laurent, M. Moscovitch, and M. P. McAndrews, "The retrieval of perceptual memory details depends on right hippocampal integrity and activation," *Cortex*, vol. 84, pp. 15–33, 2016.

[76] D. C. Park and P. Reuter-Lorenz, "The adaptive brain: aging and neurocognitive scaffolding," *Annual Review of Psychology*, vol. 60, pp. 173–196, 2009.

[77] A. H. Gutchess, R. C. Welsh, T. Hedden et al., "Aging and the neural correlates of successful picture encoding: frontal activations compensate for decreased medial-temporal activity," *Journal of Cognitive Neuroscience*, vol. 17, no. 1, pp. 84–96, 2005.

[78] C. Grady, "The cognitive neuroscience of ageing," *Nature Reviews Neuroscience*, vol. 13, no. 7, pp. 491–505, 2012.

[79] A. Gilboa, C. Alain, D. T. Stuss, B. Melo, S. Miller, and M. Moscovitch, "Mechanisms of spontaneous confabulations: a strategic retrieval account," *Brain*, vol. 129, no. 6, pp. 1399–1414, 2006.

[80] R. Cabeza, N. D. Anderson, J. K. Locantore, and A. R. McIntosh, "Aging gracefully: compensatory brain activity in high-performing older adults," *NeuroImage*, vol. 17, no. 3, pp. 1394–1402, 2002.

[81] P. A. Reuter-Lorenz and K. A. Cappell, "Neurocognitive aging and the compensation hypothesis," *Current Directions in Psychological Science*, vol. 17, no. 3, pp. 177–182, 2008.

[82] S. Carlomagno, S. Giannotti, L. Vorano, and A. Marini, "Discourse information content in non-aphasic adults with brain injury: a pilot study," *Brain Injury*, vol. 25, no. 10, pp. 1010–1018, 2011.

[83] A. Marini, V. Galetto, E. Zampieri, L. Vorano, M. Zettin, and S. Carlomagno, "Narrative language in traumatic brain injury," *Neuropsychologia*, vol. 49, no. 10, pp. 2904–2910, 2011.

[84] D. Tromp, A. Dufour, S. Lithfous, T. Pebayle, and O. Després, "Episodic memory in normal aging and Alzheimer disease: insights from imaging and behavioral studies," *Ageing Research Reviews*, vol. 24, pp. 232–262, 2015.

Hindawi Publishing Corporation
Neural Plasticity
Volume 2016, Article ID 2306406, 11 pages
http://dx.doi.org/10.1155/2016/2306406

Research Article

Resting-State Functional Connectivity and Cognitive Impairment in Children with Perinatal Stroke

Nigul Ilves,[1] Pilvi Ilves,[1,2] Rael Laugesaar,[3,4] Julius Juurmaa,[1] Mairi Männamaa,[5,6] Silva Lõo,[7] Dagmar Loorits,[2] Tiiu Tomberg,[2] Anneli Kolk,[3,8] Inga Talvik,[9] and Tiina Talvik[3,4]

[1]*Department of Radiology, University of Tartu, Tartu, Estonia*
[2]*Radiology Clinic of Tartu University Hospital, Tartu, Estonia*
[3]*Department of Pediatrics, University of Tartu, Tartu, Estonia*
[4]*Children's Clinic of Tartu University Hospital, Tartu, Estonia*
[5]*Department of Development and Rehabilitation Centre of Children and Adolescents, Children's Clinic of Tartu University Hospital, Tartu, Estonia*
[6]*Institute of Psychology, University of Tallinn, Tallinn, Estonia*
[7]*Department of Pediatric Neurology, University of Helsinki and Helsinki University Hospital, Helsinki, Finland*
[8]*Department of Neurology and Neurorehabilitation, Children's Clinic of Tartu University Hospital, Tartu, Estonia*
[9]*Tallinn Children's Hospital, Tallinn, Estonia*

Correspondence should be addressed to Pilvi Ilves; pilvi.ilves@kliinikum.ee

Received 10 August 2016; Revised 25 October 2016; Accepted 1 November 2016

Academic Editor: Lijun Bai

Perinatal stroke is a leading cause of congenital hemiparesis and neurocognitive deficits in children. Dysfunctions in the large-scale resting-state functional networks may underlie cognitive and behavioral disability in these children. We studied resting-state functional connectivity in patients with perinatal stroke collected from the Estonian Pediatric Stroke Database. Neurodevelopment of children was assessed by the Pediatric Stroke Outcome Measurement and the Kaufman Assessment Battery. The study included 36 children (age range 7.6–17.9 years): 10 with periventricular venous infarction (PVI), 7 with arterial ischemic stroke (AIS), and 19 controls. There were no differences in severity of hemiparesis between the PVI and AIS groups. A significant increase in default mode network connectivity (FDR 0.1) and lower cognitive functions ($p < 0.05$) were found in children with AIS compared to the controls and the PVI group. The children with PVI had no significant differences in the resting-state networks compared to the controls and their cognitive functions were normal. Our findings demonstrate impairment in cognitive functions and neural network profile in hemiparetic children with AIS compared to children with PVI and controls. Changes in the resting-state networks found in children with AIS could possibly serve as the underlying derangements of cognitive brain functions in these children.

1. Introduction

Perinatal stroke leads to congenital hemiparesis [1–6]; however, these children may also have neurocognitive deficits, language impairment, behavioral disorders, and epilepsy [2–4, 7–14]. Previous outcome studies of perinatal stroke have been mainly focused on an isolated clinical function: either motor function [1, 2, 4, 7, 9, 15] or cognitive function [3, 5, 8, 13–16].

Perinatal ischemic stroke is a group of heterogeneous conditions in which there is a focal disruption of the cerebral blood flow secondary to arterial or venous thrombosis or embolization during the perinatal period [17]. Based on clinical-radiographical findings, there are two main subtypes of perinatal stroke: arterial ischemic stroke (AIS) and periventricular venous infarction (PVI) [3, 4, 9, 18]. The AIS involves arterial occlusion mostly in the middle cerebral artery (MCA) territory [3, 4, 9, 18], comprising large areas

in the parietal, temporal, and frontal cortex and/or in the basal ganglia including the corticospinal tract [2]. The PVI, in contrast, comprises purely subcortical areas, predominantly the periventricular white matter, but also other parts of the descending corticospinal tract [3, 9]. In both types of vascular injury, damage of the corticospinal tract leads to hemiparesis [1, 2, 6].

Previous data about long-term cognitive development mostly apply to children with perinatal AIS [7–10, 13, 14, 16]; however, results vary to a great extent. Cognitive deficit in children with presumed PVI has received less attention and these children are usually investigated together with children with presumed AIS [4, 7, 14].

Task-based functional magnetic resonance imaging (fMRI) is used to investigate separate functions like motor [19] and language [20, 21] functions in stroke children. The fMRI has revealed the functional plasticity of the brain in the case of focal brain damage in perinatal stroke patients [19, 21]. However, task-based studies present several challenges for stroke patients, including motor task-related motion artifacts, inconsistent performance, mirror movements, or individual ability to perform the task altogether [22]. Furthermore, although structural damage from stroke is focal, remote dysfunction can occur in regions connected to the area of lesion [23].

Resting-state fMRI (rs-fMRI) is acquired in the absence of a task, which allows exploring the global functional organization of the brain and how it is altered in brain damage. It is now well established that many resting-state networks (RSN) are robust, that is, consistent across subjects, and involve the sensory (visual, auditory, and somatosensory) and motor regions of the brain, as well as a number of associative "control" networks (default, dorsal stream, frontoparietal, and ventral stream) [24, 25]. A framework based on connectivity and neural communication across the brain regions provides us with a view of the brain as organized in an ensemble of functional networks in adults [25, 26] and in children [27, 28]. However, there exist differences in functional connectivity in global RSN between infants and young children, on one hand, and adults, on the other, which are due to brain developmental progression in regional and network specialization [28, 29]. During childhood, changes occur in the hierarchical and regional organization of brain connectivity, and functional connections between distant regions become stronger with advancing maturation [30]. The process of network maturation appears to be parallel with the progress of behavioral maturation and sensorimotor development precedes the development of the systems underlying higher cognition [31]. Furthermore, certain networks, such as the default mode network (DMN), are only slightly functionally connected in childhood but increase in connection strength over time until they are fully developed by adulthood [29]. Thus, an early childhood stroke that affects immature connections might have a stronger impact on functional reorganization compared to a stroke that affects more mature networks [32].

The relationship between functional connectivity, sensory deficits, and structural abnormality remains poorly understood [33]. However, to our knowledge, rs-fMRI data for children with stroke are limited and refer only to the somatosensory system. Dinomais et al. [33] have investigated rs-fMRI in perinatal stroke patients with cortical and periventricular lesions and demonstrated a relationship between functional connectivity and somatosensory impairment. Children who had lesions in the MCA territory displayed significantly less functional connectivity in the somatosensory cortex than children with periventricular lesions [33]. Recently, a small group of children with spastic cerebral palsy [34] and another group of hemiplegic cerebral palsy after cortical and subcortical damage [35] were investigated with rs-fMRI without data about the vascular origin of the damage. Saunders [36] found differences in the motor network in patients with perinatal AIS and PVI compared to controls and suggested that in these children extensive plasticity in the brain occurs after experiencing a stroke, which consequently has an effect on the functional connections between the areas of the brain at rest. There were also significant differences in plasticity between the AIS and PVI groups, suggesting that the functional reorganization of the motor function is different in each of these groups [36].

The aim of the study was to identify differences in resting-state networks and cognitive development in children with perinatal AIS and PVI and to compare the obtained data with the corresponding data for healthy controls.

2. Methods

2.1. Patients. The Estonian Pediatric Stroke Database [5] contains data for 80 children with perinatal stroke, initially collected for an epidemiological study (1994–2003) and prospectively updated through 2015. All radiological images in Estonia are archived in a single all-Estonian Picture Archiving System.

Of the 80 children with perinatal stroke, those with neonatal sinovenous thrombosis ($n = 4$), neonatal hemorrhagic stroke ($n = 7$), or inadequate magnetic resonance imaging ($n = 2$) were excluded.

Ischemic stroke was classified as AIS or PVI using the criteria based on a previous study by Kirton and coworkers [4] and modified by Ilves and coworkers [3, 21]. Patients were only considered eligible for our preliminary study when (a) they had documented unilateral left-hemisphere AIS or PVI (for the sake of homogeneity in the study as perinatal stoke affects more often the left side according to previous studies [18]) but also in our database (68%); (b) they were aged 7–17; and (c) they were able to remain still for about 45 minutes without sedation and to follow instructions during the MRI investigation.

Of the 67 patients with perinatal ischemic stroke, 22 had unilateral left-side PVI and 24 had unilateral left-side AIS. The parents were contacted by phone and were asked to participate in the outcome study. Also, the parents were enquired about the child's ability to undergo the MRI investigation without sedation; otherwise only studies of cognitive and motor outcome were applied. Eleven children with PVI, 10 children with AIS, and 25 ages and sex matched healthy voluntary controls without contraindications for MRI agreed to participate in the rs-fMRI investigation. The control

Table 1: Demographic and neuroimaging data for the children with periventricular venous infarction and arterial ischemic stroke.

Patients number	Sex	Gestational age at birth	Presumed or neonatal stroke	Type of stoke	Age at the time of resting-state functional MRI	Lesion location (left)	Lesion size 1–5
(1)	M	40	Presumed	PVI	15.9 years	F	2
(2)	F	40	Presumed	PVI	7.6 years	F	2
(3)	F	42	Presumed	PVI	10.6 years	F	2
(4)	M	40	Presumed	PVI	13.4 years	F	2
(5)	F	38	Presumed	PVI	14.6 years	Th-F	2
(6)	F	36	Presumed	PVI	14.6 years	P	1
(7)	F	38	Presumed	PVI	9.7 years	BG-Th-F-P	4
(8)	M	37	Presumed	PVI	10.8 years	BG-Th-F-P	4
(9)	F	34	Presumed	PVI	12.7 years	BG-Th-F-P	4
(10)	F	40	Presumed	PVI	8.6 years	F-P	4
(11)	M	42	Neonatal	AIS/PT	10.5 years	Th-P	3
(12)	F	38	Presumed	AIS/AT	15.3 years	F	3
(13)	M	40	Neonatal	AIS/DMI	10.7 years	Th-F-P	5
(14)	M	41	Neonatal	AIS/PT	10.5 years	F-T	5
(15)	M	39	Presumed	AIS/PMI	14.1 years	BG-Th-F-P	5
(16)	M	40	Presumed	AIS/PMI	17.4 years	BG-Th-F-P-T	5
(17)	F	39	Presumed	AIS/DMI	16.3 years	Th-F-P-T	5

Type of stroke: PVI: periventricular venous infarction; AIS: arterial ischemic stroke; PT: posterior trunk of the medial cerebral artery (MCA); AT: anterior trunk of the MCA; PMI: proximal MCA; DMI: distal MCA.
Lesion location: BG: basal ganglion; Th: thalamus; F: frontal cortex; P: parietal cortex; T: temporal cortex; O: occipital cortex.
Lesion size grading system:
(1) ventricular dilatation or atrophy; (2) focal periventricular damage involving one lobe only; (3) focal cortical damage involving one lobe only; (4) focal periventricular damage involving multiple lobes; (5) focal cortical damage involving multiple lobes.

children were recruited from among children of the hospital staff members and their acquaintances and from among their classmates and friends attending regular school without learning difficulties. Written informed consent was obtained from the parents and from the children aged seven years or older for participation in the study in accordance with the Declaration of Helsinki. The study was approved by the Ethics Review Committee on Human Research, University of Tartu (Protocol no. 170/T-17 from 28.04.2008).

One child (1/11) with PVI, three with AIS (3/10), and six controls (6/25) were excluded from the analysis due to artifacts in the acquired MRI sequences or due to a shorter than planned investigation time.

The final rs-fMRI analysis included 36 children, among them 10 with PVI (age range 7.6–15.9 years, 3 boys), 7 with AIS (age range 10.4–17.4 years, 5 boys), and 19 age and sex matched controls (age range 8.1–17.9 years, 9 boys) without significant differences in age or sex between the groups. The individual demographic and neuroimaging data of the children with PVI and AIS are presented in Table 1.

2.2. Neurodevelopmental Assessments and Analysis. All children with PVI had been symptom-free after birth and had received the diagnosis of presumed perinatal stroke after 28 days of life. Four children with AIS were diagnosed after birth and three were diagnosed beyond the neonatal period (presumed AIS).

Clinical evaluation of stroke patients was made by pediatric neurologists (R L, S L) according to Pediatric Stroke Outcome Measurement (PSOM) [37]. The PSOM is a disease-specific outcome measure for children with stroke and comprises 115 test items. It yields a deficit severity score ranging from 0 to 2 (0: no deficit, 0.5: mild deficit, normal function, 1: moderate deficit, impaired function, and 2: severe deficit, missing function) for five subscales: right sensorimotor, left sensorimotor, language production, language comprehension, and cognitive/behavioral performance. Hemiparesis was diagnosed in children who had abnormal tone and reflexes associated with moderate or severe sensorimotor impairment (impaired or missing function), that is, hemiplegic cerebral palsy and congenital hemiparesis.

Cognitive performance was evaluated by a clinical psychologist (M. M.) who was blinded to the data for the stroke vascular subgroup or any rs-fMRI data, using the Kaufman Assessment Battery for Children, Second Edition (K-ABC II) [38]. The battery comprises (a) Fluid-Crystallized Index, a general measure of cognitive ability that includes acquired knowledge; (b) Mental-Processing Index, a measure of mental processing ability that excludes measures of acquired knowledge; and (c) Nonverbal Index, a general measure of nonverbal abilities. In addition, standard scores for five subscales (sequential and simultaneous processing, learning, planning, and knowledge) are provided. The range of possible scores is from 40 to 160 (mean 100, SD 15).

Ischemic lesions were classified by the location and extent as described earlier [3, 22]. Among the children with PVI, five had small periventricular white matter damage in one lobe (patients (1) to (5)), one child had unilateral

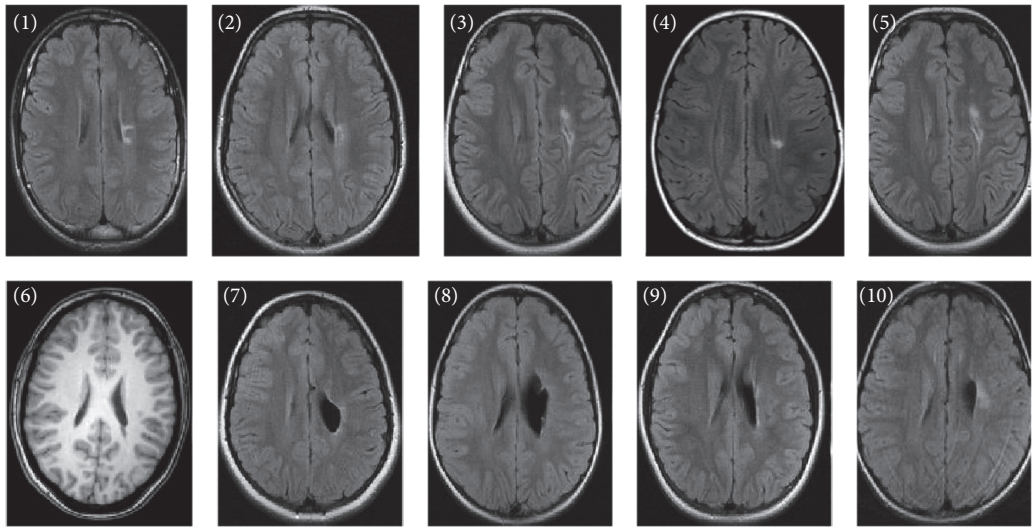

Figure 1: Anatomical fluid attenuated inversion recovery sequence images (patient (6) with T1 weighted image) for each of the patients with periventricular venous infarction according to patient number in Table 1. The single axial slices display maximum lesion volume. The individual injury patterns are detailed in Table 1.

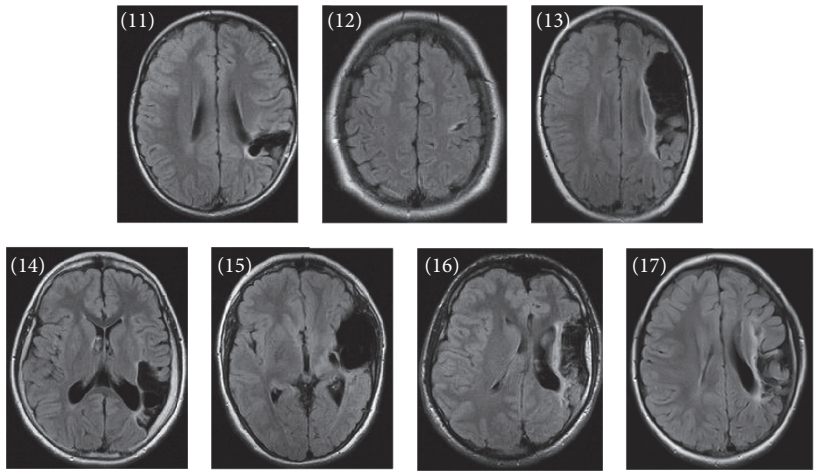

Figure 2: Anatomical fluid attenuated inversion recovery sequence images for each of the patients with arterial ischemic stroke according to patient number in Table 1. The single axial slices display maximum lesion volume. The individual injury patterns are detailed in Table 1.

ventricular enlargement (patient (6)), and four had large left-side periventricular porencephalic damage involving the periventricular area in several lobes (patients (7) to (10)) (Figure 1). Among the children with AIS, there were two with a cortical stroke involving one lobe only (patients (11) and (12)) and five with a large cortical stroke involving several lobes and/or basal ganglia (patients (13) to (17)) (Figure 2). All arterial strokes were located in the MCA region: two in the proximal MCA territory, two in the distal MCA territory, and two in the posterior trunk of MCA and one in the anterior trunk of MCA (Table 1). There were no differences in the size of stroke (defined by involvement of one or several lobes) between the PVI and the AIS children ($p = 0.33$) (Table 1).

2.3. MRI Acquisition. The MRI data were acquired with the Philips 3-T Achieva MR scanner using the 8-channel SENSE head coil 3.0T/8ch (Philips Medical Systems, Best, The Netherlands). The scans were performed without sedation or medication; the participants were asked to stay awake and keep their eyes open.

The scans were acquired using a fixed imaging protocol after the acquisition of an anatomical scan. The T1 weighted slices of the whole head were obtained using a 3D fast field echo sequence (TR = 8.2 ms, TE = 3.8 ms), with a field of view of 256 × 256 mm and an isotropic voxel size of 1 mm. To describe resting-state activity in the brain, 120 volumes of 50 axial $T2^*$-weighted slices of the whole head were acquired using a fast field echo single shot EPI-BOLD sequence

(TR = 3000 ms, TE = 35 ms), with a field of view of 230 × 230 mm and a voxel size of 3 mm isotropic.

The rs-fMRI data were visually inspected for motion and other imaging artifacts; entire scans were excluded from further analysis or, when possible, the scan was rescheduled. During motion correction, the maximum calculated absolute mean displacement was 0.78 mm and the maximum relative mean displacement was 0.29 mm [39].

2.4. Data Preprocessing. The analysis of rs-fMRI was made by a single investigator (N. I.) who was blinded to any clinical information or to the results of the cognitive tests, using the Multivariate Exploratory Linear Decomposition into Independent Components (MELODIC) tool, version 3.14 employing FSL from the FMRIB Software Library (https://www.fmrib.ox.ac.uk/fsl/) [40].

The following preprocessing workflow consisted of the following steps: (a) discarding of the first 2 volumes from each subject for signal stabilization; (b) motion correction using MCFLIRT [41]; (c) brain extraction of BOLD images; (d) spatial smoothing with FWHM 6 mm; (e) high-pass temporal filtering for 150 seconds.

Blood-oxygen level dependent (BOLD) volumes were registered to the T1 weighted structural volumes with 6 degrees of freedom using a boundary-based registration algorithm. Subsequently, the structural images were registered to the MNI-152 standard space with 12 degrees of freedom (T1 standard brain averaged over 152 subjects; Montreal Neurological Institute, Montreal, QC, Canada) [41, 42]. Normalized 4D datasets were subsequently resampled to 4 mm isotropic voxels.

2.5. Extracting Resting-State Networks. The data of the resting-state functions for both the study and control groups were temporarily concatenated and analyzed using probabilistic independent component analysis (PICA) [27]. The concatenated dataset was decomposed into 30 independent components. The components were visually evaluated and compared to previous literature data [24, 25, 27, 43–45] and 13 out of the 30 components were identified as anatomically and functionally relevant separate resting-state networks. The other 17 components reflected artifacts. The criteria for inclusion were signal within a low frequency range of 0.1–0.01 Hz [46, 47], location of connectivity patterns mainly in gray matter, and presence of coherent voxel clusters [48].

The subject-specific statistical maps of all RSN were created using a dual-regression tool from the FMRIB Software Library [24, 49] to test for differences in the identified components between the AIS, PVI, and control groups. Subsequently, groupwise comparison of RSN was carried out using a randomized, permutation-testing tool Version 2.9 from FSL. For each resting-state network, threshold-free cluster enhancement (TFCE) [50] was performed. The resulting statistical maps were thresholded at $p \leq 0.05$ and at $p \leq 0.01$ (TFCE corrected for familywise errors) for revealing group main effects. Inference was only carried out on the subject specific z-maps of 13 relevant RSNs. Between-group effects were thresholded controlling for local false discovery rate (FDR) [49] at $q \leq 0.1$ to reduce susceptibility to type 1 errors when testing multiple resting-state networks.

Statistical evaluation was performed with the statistical package SAS Version 9.1 (SAS Institute INC, Cary, NC). Prior to further analysis, normality of the data was evaluated using the Kolmogorov-Smirnov criterion. To compare the proportions, the Chi-square test and Fisher's exact test (when the expected values were <5) were used. The nonparametric Mann-Whitney U-test was employed to compare the groups of AIS and PVI. Values are presented as means with the 95% confidence interval. The alpha level used to determine significance is $p < 0.05$. All p values are two-sided.

3. Results

3.1. Neurodevelopmental Outcome. The clinical findings and the data of cognitive functions for the children with PVI and AIS are presented in Tables 1 and 2 and the radiological findings are presented in Figures 1 and 2. Total PSOM score was abnormal for all stroke children. The children with AIS had significantly higher total PSOM scores compared to the children with PVI ($p = 0.0486$). All children had mild to severe sensorimotor deficit. However, 4/7 (57%) of the children with AIS and 8/10 (80%) of the children with PVI had moderate to severe hemiparesis; the difference between the PVI and AIS groups was not statistically significant ($p = 0.59$).

Most children with AIS (5/7, 71%) and only one child (1/10, 10%) with PVI had cognitive deficit according to PSOM ($p = 0.035$).

According to the Kaufman Assessment Battery for Children, the children with AIS received significantly lower scores (Figure 3) in all three general ability indexes than the children of the PVI group: FCI (mean 79.7 versus 99.2, $p = 0.013$), MPI (mean 81.1 versus 97.7, $p = 0.017$), and NVI (mean 84.4 versus 105.3, $p = 0.022$). The PVI group outperformed the AIS group also in the subscale scores, while the results were significantly better for the children with PVI in simultaneous information processing (mean 102.3 versus 78.6; $p = 0.015$) and in planning ability (mean 110.2 versus 85.7; $p = 0.017$). The children with AIS performed significantly lower than the controls in all general ability and subscale indexes, except for learning. The overall cognitive development of the children with PVI in our study remained roughly within a normal range. However, children with PVI got lower results, compared to the control group in one general ability score (FCI), and in two subscales (simultaneous and sequential information processing) (Figure 3).

None of the 10 PVI children had epilepsy; however, 5/7 children in the AIS group had epilepsy and received antiepileptic medication ($p = 0.0034$).

3.2. Resting-State Functional Connectivity. Thirteen functionally relevant RSN were found using group PICA (Figure 4). Such networks have been described in previous studies using a similar methodology for adults [24–26, 51] and for children [27, 28, 43]. According to the present study, the networks were stable across the participants of the AIS, PVI,

Table 2: Clinical data and data of cognitive function for the children with periventricular venous infarction and arterial ischemic stroke.

Patients number	Type of stroke	Severity of the right hemiparesis mild/moderate/severe	PSOM	Cognitive dysfunction no/mild/moderate/severe	Seizures Yes/no	FCI score	MPI score	NVI score
(1)	PVI	Mild	0.5	No	No	111	108	127
(2)	PVI	Severe	2.5	No	No	103	97	98
(3)	PVI	Moderate	1.5	No	No	88	86	88
(4)	PVI	Severe	5	Mild	No	73	75	69
(5)	PVI	Moderate	1.5	No	No	104	104	108
(6)	PVI	Moderate	1.5	No	No	109	119	144
(7)	PVI	Moderate	1	No	No	111	97	105
(8)	PVI	Moderate	2	No	No	95	97	100
(9)	PVI	Mild	1	No	No	99	101	113
(10)	PVI	Moderate	1	No	No	99	93	101
(11)	AIS/PT	Mild	2	No	Yes	96	95	102
(12)	AIS/AT	Moderate	1	No	No	89	89	94
(13)	AIS/DMI	Moderate	3.5	Mild	No	79	78	80
(14)	AIS/PT	Mild	3	Mild	Yes	84	80	82
(15)	AIS/PMI	Severe	8	Severe	Yes	53	54	59
(16)	AIS/PMI	Severe	2.5	Mild	Yes	79	92	87
(17)	AIS/DMI	Severe	3	Mild	Yes	78	80	87

Type of stroke: PVI: periventricular venous infarction; AIS: arterial ischemic stroke; PT: posterior trunk of the medial cerebral artery (MCA); AT: anterior trunk of MCA; PMI: proximal MCA; DMI: distal MCA.

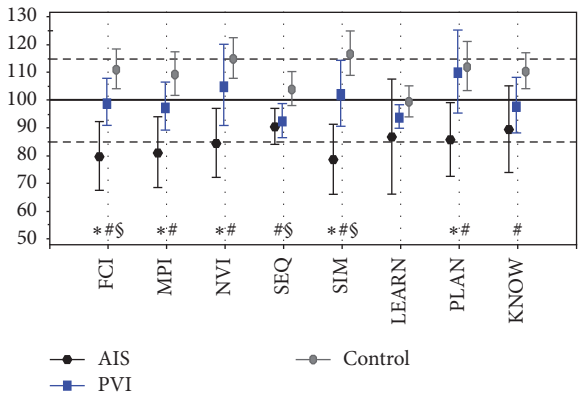

Figure 3: Mean with 95% CI Kaufman Assessment Battery for Children, Second Edition index with the subscale scores for children with periventricular venous infarction (PVI), arterial ischemic stroke (AIS), and controls. The FCI stands for Global Fluid-Crystallized Index (includes all subscales); MPI stands for Mental Processing Index (excludes acquired knowledge); NVI stands for Nonverbal Index; SEQ stands for Sequential Processing; SIM stands for simultaneous processing; LEARN stands for learning; PLAN stands for planning; KNOW stands for knowledge. Standard mean (SD) value for the battery is 100 (85–115). $^{*}p < 0.05$ AIS versus PVI. $^{\#}p < 0.01$ AIS versus controls. $^{\S}p < 0.05$ PVI versus controls.

and control groups. All of these 13 networks were found with independent PICA analysis for each of the PVI, AIS, and control groups.

3.3. Differences in Functional Connectivity between the Stroke and Control Groups. All 13 RSN networks were included in group-level analyses. Testing of the main effects of the group on the subject specific z-maps of these networks (all $p \leq 0.05$ and also $p \leq 0.01$ TFCE corrected for familywise errors) showed significantly increased functional connectivity in the posterior and anterior components of DMN and in the task positive and medial temporal networks in the patients with AIS ($p < 0.01$), compared to the controls. These networks, except for the anterior component of DMN ($p < 0.05$), were even increased in AIS compared to PVI ($p < 0.01$), corrected for familywise errors. However, after FDR correction (local FDR-corrected at $q \leq 0.1$), significantly increased functional connectivity was only found in the DMN posterior component in the left periventricular area of the AIS patients versus the controls (Figure 5).

The control group showed increased functional connectivity in the primary visual, salience, task positive, cerebellum, and sensorimotor networks compared to the AIS group ($p < 0.01$); however, after FDR corrected analysis at $q \leq 0.1$, the difference was not significant.

The PVI group showed increased functional connectivity in the medial visual, auditory, salience, ventral stream, and cerebellum networks compared to the patients with AIS ($p < 0.01$); however, after FDR corrected analysis at $q \leq 0.1$ level, the difference was not significant.

There were no statistical differences between the children of the PVI and control groups in RSN.

4. Discussion

We report differences in the rs-fMRI networks and cognitive functions in children with left-hemisphere perinatal stroke of different vascular origin. More severe dysfunctions in the rs-fMRI RSN networks and cognitive functions occurred in the AIS compared to the PVI children. These results

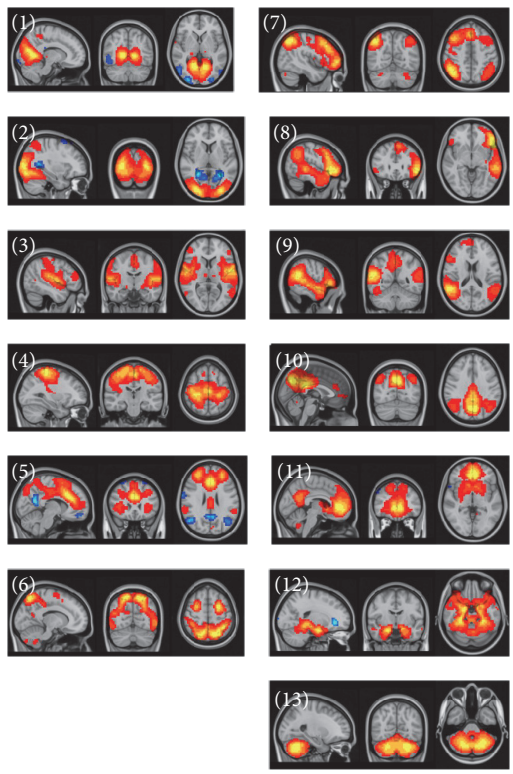

Figure 4: Resting-state networks estimated with ICA. The images are z statistics of the concatenated dataset for the controls and the stroke patients decomposed into the independent network components: primary visual (1), lateral visual cortex (2), auditory cortex (3), sensory-motor cortex (4) network associated with salience processing (5), task positive network involved in higher-order cognition and attention (6), networks implicated in working memory and cognitive attentional processes as right lateral network (7), and left lateral frontoparietal network (8), ventral stream ventral attention system (9), posterior component of the default mode network in the precuneus and parietal regions (10), anterior component of the default mode network in the frontal pole and precuneus (11), medial temporal/the hippocampus amygdala complex (12), and cerebellar network (13).

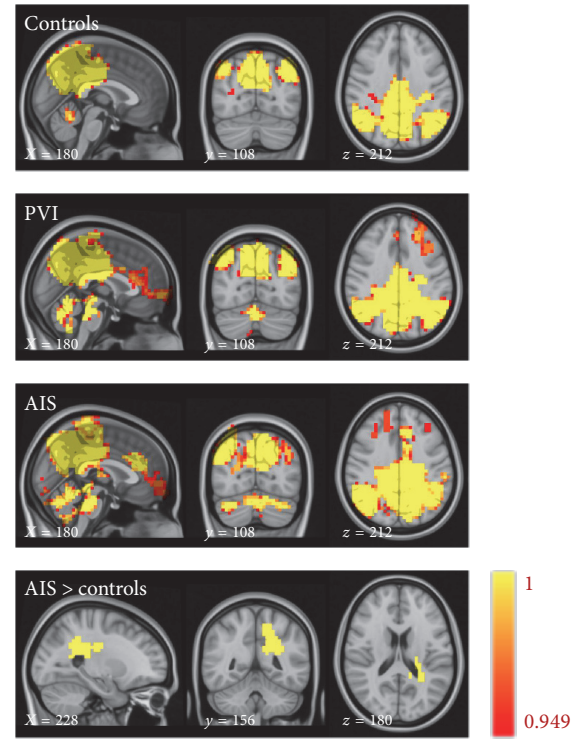

Figure 5: Connectivity maps of the posterior precuneus part of the default mode network for the controls, periventricular venous infarction (PVI), arterial ischemic stroke (AIS), and a map of the areas with increased connectivity in AIS versus control (FDR 0.1). Color map from 0.949 (red) to 1 (yellow).

provide a preliminary insight into large-scale brain network dysfunction that may be the underlying cause of the various motor, cognitive, and behavioral problems in patients with perinatal stroke.

4.1. Neurodevelopmental Outcome. The children with AIS had significantly higher PSOM scores compared to the PVI children. Depending on vascular origin, different pathogenetic mechanisms behind AIS and PVI are responsible for the location of brain damage and outcome [3, 4]. In AIS, cortical-subcortical involvement is the most prominent location of damage; in PVI, the main location of damage is the periventricular white matter while the cortical areas are spared [4]. However, the corticospinal tract is often damaged, although in different locations, in the case of both types: 24–60% of cases in AIS [1, 2] and up to 80% of cases in PVI [9].

We found that although motor outcome was similar in children from both the AIS and PVI groups, the measures of cognitive ability based on K-ABC-II scores were lower in AIS compared to PVI. An earlier study by Westmacott and coworkers [14] also suggested that motor function was not linearly related to cognitive outcome and PSOM motor scores were not correlated with IQ measures. Some studies suggest, however, that overall cognitive development in perinatal stroke falls roughly within a normal range [10, 13–15], although children with PVI and AIS are often studied in one group.

Ricci and coworkers [13] have found that only one-third of children show cognitive deficit after perinatal stroke. In some other studies, children with neonatal AIS have significantly lower scores for working memory and processing speed compared to the normative population [1]. This is also the case with the measures of general cognitive ability, verbal functioning, inhibitory control and working memory [8], or the measures affecting complex cognitive skills as abstract reasoning [14]. Our data confirmed that, according to K-ABC-II, the children of the AIS group had significantly lower scores for general ability than the children of the PVI group. In addition, the former were less successful in the tasks that required higher cognitive abilities such as planning or simultaneous visual processing.

Cognitive problems in the children with PVI, all with presumed stroke, were less pronounced and only 1 of the 10

children in the study group had some mild cognitive problems. In an earlier study investigating both presumed stroke with AIS and PVI, the proportion of children with presumed perinatal stroke who had cognitive or behavioral deficits was 29% [4]. As in our study, the children with PVI had less behavioral and visual deficits than the children with a large proximal MCA stroke but they had more spasticity than the children with stroke in the anterior trunk of MCA [4]. However, adverse cognitive and behavioral outcomes were more strongly correlated with cortical involvement compared to periventricular involvement in presumed perinatal stroke [4].

4.2. Rs-fMRI Investigations. We found significant global derangements in the cognitive networks at rs-fMRI and in the cognitive function tests in the children with AIS compared to the PVI and control groups. Global neural network dysfunction can serve as a possible basis for derangements of complex cognitive functions and behavior as has also been reported in earlier stroke outcome studies [4, 10, 14]. The RSN of the children with PVI was not different from the corresponding measures for the control group.

Large-scale networks were identified in which the patients with AIS showed significantly increased functional connectivity, compared to the controls and the children with PVI, in the posterior precuneus part and the anterior frontal part of DMN, in the medial temporal component of DMN, and in the task positive network ($p < 0.01$). These networks were even increased in AIS compared to PVI ($p < 0.05$). However, after FDR correction, significantly increased functional connectivity was only found in posterior precuneus part of DMN in the AIS children compared to the controls. The DMN is deactivated during demanding cognitive tasks and is involved in episodic memory processes and self-referential mental representations [45]. The task positive network is involved in higher-order cognition and attention [45].

Earlier studies have found that most networks in children, in particular those supporting the basic motor function and sensory related processing, had a robust functional organization similar to mature adult patterns [27, 28, 43]. In contrast, DMN and the other RSN involved in the higher-order cognitive functions had immature characteristics, revealing incomplete and fragmented patterns, which indicates less developed functional connectivity, in infants [28] aged 5 to 8 years [27] and even at the age of 10–13 years [43]. A major difference between adults and children is the decomposition of DMN into several independent subsystems in children, composed of the bilateral posterior cingulate, the precuneus, the inferior parietal cortex, and the ventromedial prefrontal cortex, which are associated with the medial temporal regions [27, 29]. At the same time, the posterior precuneus region of the DMN network serves as the main hub within DMN [27]. The DMN has been found to be only weakly functionally connected in childhood but increases in connection strength over time. Therefore, an early childhood stroke that affects immature connections might have a stronger impact on functional reorganization than a stroke that affects more mature networks [29]. However, there exists also the hypothesis that damaged areas continue to support the performance of tasks involving them and the typical functional connections of these regions play an important role in preservation of normalcy after early perinatal stroke [52]. In our study significant changes in DMN and especially in the posterior precuneus part of DMN, which is the main hub within DMN, were found in the children with AIS who had also serious cognitive problems. Also, were found in the AIS and control children some derangements of the task positive network, which is part of the attention control networks. The attention control networks have generally immature characteristics in young age groups [27].

4.3. Location of Stroke and rs-fMRI Networks. Cortical involvement of damage in AIS compared to PVI with mainly periventricular damage can explain differences in network dysfunction. Increased connectivity of the networks outside the region of primary damage (DMN) can be a compensatory effect occurring after cortical brain damage in children with AIS due to brain's plasticity; in this case areas outside the lost tissue take over its functions. A similar finding was obtained by a task-based fMRI [20, 21]. The prefrontal regions, both ipsi- and contralateral to the lesion, were activated in patients but not in controls after language and visual search tasks, which may compensate for lost functions according to task-based fMRI [20]. Such contralateral activation of the language function is seen more often in younger stroke patients before the age of 2 years [21]. It is unknown whether the frontal task-based networks are activated due to alternative or compensational strategies [20].

5. Limitations of the Study

The small number of rs-fMRI examinations of perinatal stroke could limit the statistical power and generalizability of the study results. Still, our preliminary data were available for 10 children with PVI, which is close to the 12 cases of presumed PVI reported in a previous clinical-radiological study by Kirton and coworkers [4]. Although significant differences both in cognitive function and in the global networks were found in the children with AIS versus PVI, more clinical and rs-fMRI data, especially for right hemisphere strokes, would be needed to evaluate the predictive value of rs-fMRI results for establishment of cognitive deficit in these children.

On our stroke database and in the cohort of this study, the children with AIS had significantly more often epilepsy compared to the children with PVI. Epilepsy per se and/or antiepileptic treatment may have had an impact on the cognitive ability of the former. Earlier studies have also found that seizures are more frequent in children with cortical damage compared to periventricular damage in presumed perinatal stroke [4]. Cognitive impairments with lower performance in the intellectual and language measures have been found in children with perinatal stroke associated with seizures [4, 10, 11, 13, 15].

Although there were no gender differences in our stroke group compared to the controls, there were more boys in the AIS group, which could also influence the cognitive outcome.

Males with perinatal stroke performed tests significantly more poorly than a matched group of females in overall intellectual ability and in reading and processing speed [7, 14]. It should be noted that as about 60% of the children with PVI in the Estonian Perinatal Stroke Database are female [3], it was difficult to recruit male subjects with PVI to the study.

Also, we had to exclude from the study the most severe cases when the mother thought that the child would not be able to follow instructions and stay still during MRI without sedation. This could have diminished the statistical power of the rs-fMRI data for the AIS children. However, most of such cases were encountered in the AIS group with bilateral asymmetrical involvement.

6. Conclusions

Our findings demonstrate differences in the cognitive function and in the neural network profile of children with hemiparesis with left-side AIS compared to children with left-side PVI and controls matched for age and sex. The study shows that as the location of damage is different in children with AIS and PVI, also the resting-state networks and cognitive outcome are different in these groups and children with AIS and PVI should not be analyzed together in outcome studies.

Changes in the resting-state networks found in children with AIS could possibly serve as an underlying dysfunction of cognitive brain functions in perinatal stroke patients. In order to better understand the value of derangements in the brain networks in perinatal stroke patients with cognitive and behavioral problems, further studies are needed. It is important to promote early diagnosis, treatment, and rehabilitation of these children, to improve their quality of life, as well as the quality of life of their families.

Disclosure

No funding sources were used for the study design; for collection, analysis, and interpretation of the data; for the writing of the report or for the decision to submit the manuscript for publication.

Competing Interests

All the authors declare no competing interest regarding this article.

Authors' Contributions

All authors have approved the final version of the manuscript.

Acknowledgments

The study was largely conducted at Tartu University Hospital. The authors thank all patients and their parents for contribution. They are also thankful to Dr. Valentin Sander for allowing them to use the clinical information for some patients treated at Tallinn Children's Hospital. They are indebted to Ms. Pille Kool for help in the statistical analysis of the study. This study was financed by the Estonian Research Council (PUT 148, IUT3-3) by the Estonian Science Foundation (GARLA 0148P, 6627, 9016, and 5462), by targeted financing TARLA 7695, 0475, and DARLA 3144, and by Tartu University Developmental Fund.

References

[1] J. P. Boardman, V. Ganesan, M. A. Rutherford, D. E. Saunders, E. Mercuri, and F. Cowan, "Magnetic resonance image correlates of hemiparesis after neonatal and childhood middle cerebral artery stroke," *Pediatrics*, vol. 115, no. 2, pp. 321–326, 2005.

[2] B. Husson, L. Hertz-Pannier, C. Renaud et al., "Motor outcomes after neonatal arterial ischemic stroke related to early MRI data in a prospective study," *Pediatrics*, vol. 126, no. 4, pp. 912–918, 2010.

[3] P. Ilves, R. Laugesaar, D. Loorits et al., "Presumed perinatal stroke: risk factors, clinical and radiological findings," *Journal of Child Neurology*, vol. 31, no. 5, pp. 621–628, 2016.

[4] A. Kirton, G. DeVeber, A.-M. Pontigon, D. Macgregor, and M. Shroff, "Presumed perinatal ischemic stroke: vascular classification predicts outcomes," *Annals of Neurology*, vol. 63, no. 4, pp. 436–443, 2008.

[5] R. Laugesaar, A. Kolk, T. Tomberg et al., "Acutely and retrospectively diagnosed perinatal stroke: a population-based study," *Stroke*, vol. 38, no. 8, pp. 2234–2240, 2007.

[6] Y. W. Wu, C. E. Lindan, L. H. Henning et al., "Neuroimaging abnormalities in infants with congenital hemiparesis," *Pediatric Neurology*, vol. 35, no. 3, pp. 191–196, 2006.

[7] M. R. Golomb, B. P. Garg, C. Saha, F. Azzouz, and L. S. Williams, "Cerebral palsy after perinatal arteril ischemic stroke," *Journal of Child Neurology*, vol. 23, no. 3, pp. 279–286, 2008.

[8] C. A. Hajek, K. O. Yeates, V. Anderson et al., "Cognitive outcomes following arterial ischemic stroke in infants and children," *Journal of Child Neurology*, vol. 29, no. 7, pp. 887–894, 2014.

[9] A. Kirton, M. Shroff, A.-M. Pontigon, and G. DeVeber, "Risk factors and presentations of periventricular venous infarction vs arterial presumed perinatal ischemic stroke," *Archives of Neurology*, vol. 67, no. 7, pp. 842–848, 2010.

[10] A. Kolk, M. Ennok, R. Laugesaar, M.-L. Kaldoja, and T. Talvik, "Long-term cognitive outcomes after pediatric stroke," *Pediatric Neurology*, vol. 44, no. 2, pp. 101–109, 2011.

[11] J. Lee, L. A. Croen, C. Lindan et al., "Predictors of outcome in perinatal arterial stroke: a population-based study," *Annals of Neurology*, vol. 58, no. 2, pp. 303–308, 2005.

[12] E. Mercuri, M. Rutherford, F. Cowan et al., "Early prognostic indicators of outcome in infants with neonatal cerebral infarction: a clinical, electroencephalogram, and magnetic resonance imaging study," *Pediatrics*, vol. 103, no. 1, pp. 39–46, 1999.

[13] D. Ricci, E. Mercuri, A. Barnett et al., "Cognitive outcome at early school age in term-born children with perinatally acquired middle cerebral artery territory infarction," *Stroke*, vol. 39, no. 2, pp. 403–410, 2008.

[14] R. Westmacott, R. Askalan, D. Macgregor, P. Anderson, and G. deVeber, "Cognitive outcome following unilateral arterial ischaemic stroke in childhood: effects of age at stroke and lesion location," *Developmental Medicine & Child Neurology*, vol. 52, no. 4, pp. 386–393, 2010.

[15] A. O. Ballantyne, A. M. Spilkin, J. Hesselink, and D. A. Trauner, "Plasticity in the developing brain: intellectual, language and academic functions in children with ischaemic perinatal stroke," *Brain*, vol. 131, no. 11, pp. 2975–2985, 2008.

[16] A. McLinden, A. D. Baird, R. Westmacott, P. E. Anderson, and G. deVeber, "Early cognitive outcome after neonatal stroke," *Journal of Child Neurology*, vol. 22, no. 9, pp. 1111–1116, 2007.

[17] T. N. K. Raju, K. B. Nelson, D. Ferriero, and J. K. Lynch, "Ischemic perinatal stroke: summary of a workshop sponsored by the national institute of child health and human development and the national institute of neurological disorders and stroke," *Pediatrics*, vol. 120, no. 3, pp. 609–616, 2007.

[18] P. Govaert, L. Ramenghi, R. Taal, L. de Vries, and G. deVeber, "Diagnosis of perinatal stroke I: definitions, differential diagnosis and registration," *Acta Paediatrica*, vol. 98, no. 10, pp. 1556–1567, 2009.

[19] M. Staudt, C. Gerloff, W. Grodd, H. Holthausen, G. Niemann, and I. Krägeloh-Mann, "Reorganization in congenital hemiparesis acquired at different gestational ages," *Annals of Neurology*, vol. 56, no. 6, pp. 854–863, 2004.

[20] R. Everts, K. Lidzba, M. Wilke et al., "Lateralization of cognitive functions after stroke in childhood," *Brain Injury*, vol. 24, no. 6, pp. 859–870, 2010.

[21] P. Ilves, T. Tomberg, J. Kepler et al., "Different plasticity patterns of language function in children with perinatal and childhood stroke," *Journal of Child Neurology*, vol. 29, no. 6, pp. 756–764, 2014.

[22] A. R. Carter, G. L. Shulman, and M. Corbetta, "Why use a connectivity-based approach to study stroke and recovery of function?" *NeuroImage*, vol. 62, no. 4, pp. 2271–2280, 2012.

[23] E. Bullmore and O. Sporns, "Complex brain networks: graph theoretical analysis of structural and functional systems," *Nature Reviews Neuroscience*, vol. 10, pp. 186–198, 2009.

[24] C. F. Beckmann, C. E. Mackay, N. Filippini, and S. M. Smith, "Group comparison of resting-state FMRI data using multi-subject ICA and dual regression," *Neuroimage*, vol. 47, supplement 1, p. S148, 2009.

[25] I. M. Veer, C. F. Beckmann, M.-J. van Tol et al., "Whole brain resting-state analysis reveals decreased functional connectivity in major depression," *Frontiers in Systems Neuroscience*, vol. 4, article 41, pp. 1–10, 2010.

[26] C. F. Beckmann and S. M. Smith, "Probabilistic independent component analysis for functional magnetic resonance imaging," *IEEE Transactions on Medical Imaging*, vol. 23, no. 2, pp. 137–152, 2004.

[27] H. M. A. de Bie, M. Boersma, S. Adriaanse et al., "Resting-state networks in awake five- to eight-year old children," *Human Brain Mapping*, vol. 33, no. 5, pp. 1189–1201, 2012.

[28] K. P. Wylie, D. C. Rojas, R. G. Ross et al., "Reduced brain resting-state network specificity in infants compared with adults," *Neuropsychiatric Disease and Treatment*, vol. 10, pp. 1349–1359, 2014.

[29] D. A. Fair, A. L. Cohen, J. D. Power et al., "Functional brain networks develop from a 'local to distributed' organization," *PLoS Computational Biology*, vol. 5, no. 5, Article ID e1000381, 2009.

[30] K. Supekar, M. Musen, and V. Menon, "Development of large-scale functional brain networks in children," *PLoS Biology*, vol. 7, no. 7, Article ID e1000157, 2009.

[31] A. M. C. Kelly, A. Di Martino, L. Q. Uddin et al., "Development of anterior cingulate functional connectivity from late childhood to early adulthood," *Cerebral Cortex*, vol. 19, no. 3, pp. 640–657, 2009.

[32] S. Kornfeld, J. A. D. Rodríguez, R. Everts et al., "Cortical reorganisation of cerebral networks after childhood stroke: impact on outcome," *BMC Neurology*, vol. 15, no. 1, article 90, 2015.

[33] M. Dinomais, S. Groeschel, M. Staudt, I. Krägeloh-Mann, and M. Wilke, "Relationship between functional connectivity and sensory impairment: red flag or red herring?" *Human Brain Mapping*, vol. 33, no. 3, pp. 628–638, 2012.

[34] C. Papadelis, B. Ahtam, M. Nazarova et al., "Cortical somatosensory reorganization in children with spastic cerebral palsy: a multimodal neuroimaging study," *Frontiers in Human Neuroscience*, vol. 8, article 725, pp. 1–15, 2014.

[35] K. Y. Manning, D. Fehlings, R. Mesterman et al., "Resting state and diffusion neuroimaging predictors of clinical improvements following constraint-induced movement therapy in children with hemiplegic cerebral palsy," *Journal of Child Neurology*, vol. 30, no. 11, pp. 1507–1514, 2015.

[36] J. K. Saunders, *Resting-state functional magnetic resonance imaging of motor networks in perinatal stroke [Ph.D. thesis]*, Faculty of Graduate Studies in Particular Fulfillment of the Requirements for the Degree of Master of Science, 2014, http://theses.ucalgary.ca/jspui/handle/11023/1876.

[37] L. Kitchen, R. Westmacott, S. Friefeld et al., "The pediatric stroke outcome measure: a validation and reliability study," *Stroke*, vol. 43, no. 6, pp. 1602–1608, 2012.

[38] NL. Kaufman ASKaufman, *K-ABC-II. Kaufman Assessment Battery for Children. Second Edition. Manual*, American Guidance Service, Circle Pines, Minn, USA, 2004.

[39] T. D. Satterthwaite, D. H. Wolf, J. Loughead et al., "Impact of in-scanner head motion on multiple measures of functional connectivity: relevance for studies of neurodevelopment in youth," *NeuroImage*, vol. 60, no. 1, pp. 623–632, 2012.

[40] S. M. Smith, M. Jenkinson, M. W. Woolrich et al., "Advances in functional and structural MR image analysis and implementation as FSL," *NeuroImage*, vol. 23, no. 1, pp. S208–S219, 2004.

[41] M. Jenkinson, P. Bannister, J. M. Brady, and S. M. Smith, "Improved optimization for the robust and accurate linear registration and motion correction of brain images," *NeuroImage*, vol. 17, no. 2, pp. 825–841, 2002.

[42] M. Jenkinson and S. Smith, "A global optimisation method for robust affine registration of brain images," *Medical Image Analysis*, vol. 5, no. 2, pp. 143–156, 2001.

[43] L. E. Sherman, J. D. Rudie, J. H. Pfeifer, C. L. Masten, K. McNealy, and M. Dapretto, "Development of the default mode and central executive networks across early adolescence: a longitudinal study," *Developmental Cognitive Neuroscience*, vol. 10, pp. 148–159, 2014.

[44] C. F. Beckmann, M. DeLuca, J. T. Devlin, and S. M. Smith, "Investigations into resting-state connectivity using independent component analysis," *Philosophical Transactions of the Royal Society B: Biological Sciences*, vol. 360, no. 1457, pp. 1001–1013, 2005.

[45] D. M. Cole, S. M. Smith, and C. F. Beckmann, "Advances and pitfalls in the analysis and interpretation of resting-state FMRI data," *Frontiers in Systems Neuroscience*, vol. 4, article 8, 2010.

[46] D. Cordes, V. M. Haughton, K. Arfanakis et al., "Frequencies contributing to functional connectivity in the cerebral cortex in

'resting-state' data," *American Journal of Neuroradiology*, vol. 22, no. 7, pp. 1326–1333, 2001.

[47] M. J. Lowe, B. J. Mock, and J. A. Sorenson, "Functional connectivity in single and multislice echoplanar imaging using resting-state fluctuations," *NeuroImage*, vol. 7, no. 2, pp. 119–132, 1998.

[48] F. De Martino, F. Gentile, F. Esposito et al., "Classification of fMRI independent components using IC-fingerprints and support vector machine classifiers," *NeuroImage*, vol. 34, no. 1, pp. 177–194, 2007.

[49] N. Filippini, B. J. MacIntosh, M. G. Hough et al., "Distinct patterns of brain activity in young carriers of the APOE-ε4 allele," *Proceedings of the National Academy of Sciences of the United States of America*, vol. 106, no. 17, pp. 7209–7214, 2009.

[50] S. M. Smith and T. E. Nichols, "Threshold-free cluster enhancement: addressing problems of smoothing, threshold dependence and localisation in cluster inference," *NeuroImage*, vol. 44, no. 1, pp. 83–98, 2009.

[51] M. E. Thomason, E. L. Dennis, A. A. Joshi et al., "Resting-state fMRI can reliably map neural networks in children," *NeuroImage*, vol. 55, no. 1, pp. 165–175, 2011.

[52] M. H. Adhikari, A. R. Beharelle, A. Griffa et al., "Computational modeling of resting-state activity demonstrates markers of normalcy in children with prenatal or perinatal stroke," *Journal of Neuroscience*, vol. 35, no. 23, pp. 8914–8924, 2015.

Hindawi Publishing Corporation
Neural Plasticity
Volume 2016, Article ID 8583420, 11 pages
http://dx.doi.org/10.1155/2016/8583420

Research Article

Distinctive Structural and Effective Connectivity Changes of Semantic Cognition Network across Left and Right Mesial Temporal Lobe Epilepsy Patients

Xiaotong Fan,[1] Hao Yan,[2,3] Yi Shan,[4] Kun Shang,[5] Xiaocui Wang,[6] Peipei Wang,[4] Yongzhi Shan,[1] Jie Lu,[4,5,7,8] and Guoguang Zhao[1,9]

[1]*Department of Neurosurgery, Xuanwu Hospital, Capital Medical University, Beijing 100053, China*
[2]*Departments of Psychology and Linguistics, Xidian University, Xi'an 710126, China*
[3]*Neuroimaging Laboratory, School of Biomedical Engineering, Shenzhen University Health Science Center, Shenzhen 518060, China*
[4]*Department of Radiology, Xuanwu Hospital, Capital Medical University, Beijing 100053, China*
[5]*Department of Nuclear Medicine, Xuanwu Hospital, Capital Medical University, Beijing 100053, China*
[6]*Department of Biomedical Engineering, School of Life Science and Technology, Xi'an Jiaotong University, Xi'an 710049, China*
[7]*Center of Stroke, Beijing Institute for Brain Disorder, Beijing 100069, China*
[8]*Beijing Key Laboratory of Magnetic Resonance Imaging and Brain Informatics, Beijing 100053, China*
[9]*Center of Epilepsy, Beijing Institute for Brain Disorder, Beijing 100069, China*

Correspondence should be addressed to Guoguang Zhao; ggzhao@vip.sina.com

Received 10 July 2016; Accepted 20 September 2016

Academic Editor: Kevin K. W. Wang

Occurrence of language impairment in mesial temporal lobe epilepsy (mTLE) patients is common and left mTLE patients always exhibit a primary problem with access to names. To explore different neuropsychological profiles between left and right mTLE patients, the study investigated both structural and effective functional connectivity changes within the semantic cognition network between these two groups and those from normal controls. We found that gray matter atrophy of left mTLE patients was more severe than that of right mTLE patients in the whole brain and especially within the semantic cognition network in their contralateral hemisphere. It suggested that seizure attacks were rather targeted than random for patients with hippocampal sclerosis (HS) in the dominant hemisphere. Functional connectivity analysis during resting state fMRI revealed that subregions of the anterior temporal lobe (ATL) in the left HS patients were no longer effectively connected. Further, we found that, unlike in right HS patients, increased causal linking between ipsilateral regions in the left HS epilepsy patients cannot make up for their decreased contralateral interaction. It suggested that weakened contralateral connection and disrupted effective interaction between subregions of the unitary, transmodal hub of the ATL may be the primary cause of anomia in the left HS patients.

1. Introduction

Temporal lobe epilepsy (TLE) is the most common drug resistant epilepsy in adults. The majority of seizures in TLE are associated with hippocampal sclerosis (HS) or other temporal lobe abnormalities [1], which can reliably be detected in vivo by MRI [2, 3]. Patients with resection for TLE generally do not report comprehension difficulties through either clinical reports or formal testing [4] but complain of significant amnesia and anomia which reflect a semantic weakness [5–7]. A systematic review calculating pooled estimates of neuropsychological outcomes reported a 44% risk of decline in verbal memory and 34% risk of decline in naming after left-sided surgery [8]. But there are no reports of naming decline following nondominant hemisphere resection [9]. It reflects that left and right HS patients may experience distinctive functional reorganization in the nonepileptic temporal lobe under distinctive compensatory mechanisms to sustain key cognitive functions, such as language.

Semantic cognition can be decomposed into three interactive principal components implemented by separable neural networks: (1) semantic entry/exit or conceptualization (translation between sensation/motor representations and semantic knowledge); (2) the long-term representation of concepts/semantic memory; and (3) semantic control (mechanisms that interact with our vast quantity of semantic knowledge in order to generate time- and context-appropriate behavior) [10, 11]. By means of activation likelihood estimate (ALE) technique, Binder et al. reported a distinct, left-lateralized network specialized for storage and retrieval of semantic knowledge [12]. The related areas included posterior inferior parietal lobe (angular gyrus, AG; supramarginal gyrus, SMG), middle temporal gyrus (MTG), fusiform, parahippocampal gyrus, dorsomedial prefrontal cortex (dmPFC), inferior frontal gyrus (IFG), ventromedial prefrontal cortex (vmPFC), and posterior cingulate cortex (PCC). It is proposed that concepts are formed through the convergence of sensory, motor, and verbal experience via the left anterior temporal lobe (ATL), a transmodal representational hub [13] which primarily links pertinent semantic/conceptual information into the language system to produce a specific name [14]. The conclusion that the ATL is a crucial component in semantic cognition has been bolstered by contemporary basic neuroscience studies utilizing magnetoencephalography, distortion-corrected functional MRI, PET, or repetitive transcranial magnetic stimulation [15]. Meanwhile, the claim that posterior temporoparietal areas are associated with semantic control has been demonstrated in both semantic aphasia patients and healthy people [11, 16].

Concerning the common phenomenon that left HS patients, especially those after surgical resection of ATL, can perform within the normal accuracy range on standard semantic assessments but show measureable anomia [6, 17–20], we posited that a semantic-lexical disruption in the intermediate processing step that relayed retrieved semantic information on to the language system resulted in the primary problem in naming. Since temporal lobe epilepsy is considered as a network disease [21], its pathological feature requires us to examine the abnormal function of a whole network rather than a single epileptogenic region. To explore dysfunction of neural networks, functional connectivity changes in epilepsy patients have been tested by different neuroimaging modalities, such as repetitive transcranial magnetic stimulation (rTMS) [22], corticocortical evoked potentials (CCEP) [23], and EEG [24]. Although some of these techniques have the noninvasive advantage, resting state fMRI (rsfMRI) analysis possesses additional gains: resting state networks (RSNs) are highly organized in space, are reproducible from subject to subject, and differ with aging and between genders [25]. In addition, it also allows the search for significant baseline fluctuations to obtain task-free functional network information and identify epileptic circuits by providing clinicians and neurosurgeons with clues about where new or secondary epileptic foci may form, where seizures place most burden on the brain, and where are new core functional regions.

fMRI functional connectivity describes brain function and cooperation at a network level by identifying regions that make up a network of interest. It reflects the degree of signal synchrony between anatomically distant brain regions during resting state or tasks. However, these linear correlations do not provide information on the direction of influence between regions. Coefficient-based GCA is a directed functional connectivity method [26]. Given that imbalance of excitatory and inhibitory effect is a fundamental change in epilepsy [27], the GCA technique has a special advantage for investigating the pathophysiological mechanism of HS patients by means of quantifying the magnitude and direction of influence of one region time series on another [28, 29].

In sum, previous studies reported that left and right HS patients are differently impaired in semantic cognition. These patients offer the opportunity to study different impacts of focal structural lesions on functional connectivity within the semantic network. The objectives of this study were (1) to evaluate and contrast the occurrence of gray matter (GM) atrophy in patients with left and right HS in the semantic cognition network and (2) to quantify direction of influence between these anatomical regions using Granger causality analysis. We hypothesized that the presence of HS is consistent with more pronounced, diffuse GM atrophy with the semantic atrophy the most severely damaged; left HS patients' classical anomia (i.e., can provide good information about unnamed items) were caused by the unique deficit pattern of disrupted functional connectivity of the left anterior superior temporal lobe and other regions underlying semantic memory.

2. Methods

2.1. Participants. Twenty-four right-handed TLE patients (17 females, 7 males; age range 16–48 years; mean age 29.00 ± 9.57 years; epilepsy onset 12.46 ± 9.06 years; epilepsy durations 15.86 ± 7.43 years) with unilateral HS (13 left HS and 11 right HS) were recruited from Xuanwu Hospital Capital Medical University. All patients underwent a comprehensive clinical evaluation and fulfilled the following inclusion criteria: (1) typical symptoms of TLE as complex partial seizures, accompanied, or not, by simple partial seizures; some patients had aurae, like epigastric rising, hallucination, and so on; the seizure frequency was 4-5 times per day at most and 1 time per month at least; (2) standard MRI criteria for HS (hippocampal atrophy, increased T2 signal, and loss of internal hippocampal architecture) which were finally confirmed by histopathology; (3) typical EEG findings (interictal spike or sharp waves at the anterior temporal area in both wakefulness and/or sleep, various ictal rhythms including background attenuation, start-stop-start phenomenon, irregular 2–5 Hz lateralized activity, and 5–10 Hz sinusoidal waves or repetitive epileptiform discharges) [30]; (4) no other neuropsychopathic diseases like intracranial tumor, cerebral hemorrhage, infarction, trauma, schizophrenia, affective psychosis, and so on. The clinical and demographic data of all patients were shown in Table 1. Healthy adult controls (HC) without neurological or psychiatric medical history or medication known to impair memory were recruited. HC group consisted of 24 age and gender matched healthy controls (17 females, 7 males; mean age 29.50 ± 10.18 years). There was no difference

Table 1: Clinical and demographical data of the epilepsy patients.

Demographic	Left HS ($n = 13$)	Right HS ($n = 11$)
Age (mean ± SD, years)	27.3 ± 7.9	31.4 ± 11.6
Genders	5 males & 8 females	2 males & 9 females
Seizure frequency (times/week)	6.4 ± 6.4	8.4 ± 17.8
Epilepsy duration (years)	15.8 ± 8.6	15.2 ± 5.0
Seizures type	CPS	CPS
AEDs	CBZ, LTG, PHT	CBZ, LTG, PHT

CPS: complex partial seizures; AEDs: antiepileptic drugs; CBZ: carbamazepine; PHT: phenytoin; LTG: lamotrigine.

between the three groups of left HS, right HS, and normal controls ($F = 0.499$, $p = 0.611$). The local Ethics Committee approved the study and all participants gave written informed consent according to the Declaration of Helsinki prior to the study.

2.2. MRI Data Acquisition. MRI images were acquired during interictal stage with a 3.0 T scanner (MAGNETOM Tim Trio, Siemens Healthcare, Erlangen, Germany) using the 12-channel phased-array head coil supplied by the vendor. Structural images were acquired with a sagittal MP-RAGE three-dimensional T1-weighted sequence (TR = 1600 ms, TE = 2.15 ms, flip angle = 9°, thickness = 1.0 mm, and FOV = 256 mm × 256 mm). Functional images were acquired using the gradient echo-planar pulse sequence (TR = 3000 ms, TE = 30 ms, flip angle = 90°, and thickness = 3 mm). Participants were instructed to stay awake with eyes closed.

2.3. Regions of Interest (ROIs) Identification. In accordance with previous studies mentioned in the introduction part, all ROIs were defined in accordance with the AAL template, such as temporal pole of superior temporal gyrus (tpSTG) and temporal pole of middle temporal gyrus (tpMTG) that functions in conceptualization; MTG, fusiform, parahippocampal gyrus, dmPFC (medial superior frontal gyrus in AAL template), IFG, vmPFC (medial orbitofrontal gyrus in AAL template), and PCC that functions in memory storage; angular gyrus (AG) and supramarginal gyrus (SMG) that function in semantic control. Given that GM volume decrease has been reported in both ipsilateral and contralateral temporal neocortex [31–33], and mTLE patients always show atypical language lateralization [34], the current study selected 12 ROIs in each hemisphere (24 ROIs in all).

2.4. Structural Analysis. Volumetric data for cortical and subcortical structures were analyzed by optimized VBM and FIRST, parts of FSL tools, separately. The principal focus of the current study was to contrast different structural damages to the semantic cognition network in both the left and right HS patients. To make sure the severe damage to semantic cognition network was not a by-product of overall gray matter volume (GMV) loss, we also quantified structural changes of all regions between patients and controls.

The initial stages of VBM analysis included removing nonbrain tissues by Brain Extraction Tool and tissue-type segmentation with FAST4. The resulting GM partial images were then aligned to the MNI 152 template by affine-registration. A symmetric study-specific GM template was created by averaging images and flipping along the x-axis. Next, all the GM images which were nonlinearly registered to the study-specific GM template were modulated and smoothed by Gaussian kernels with a sigma of 3 mm. Regions within the semantic cognition network from WFU atlas were selected as ROIs in further two-sample t-test by randomization (5000 permutations) with TFCE implemented, between controls and left or right HS subgroups, respectively. In order to rule out the possibility that group difference was caused by the different pattern of whole brain atrophy among left and right HS patients, we added the remaining ROIs from WFU atlas in additional analyses to examine volumetric changes as aforementioned. All the volumetric results were considered statistically significant after FWE-correction at $p < 0.05$, with cluster including more than 10 continuous voxels.

FIRST was used to segment the subcortical structures, including bilateral thalamus, hippocampus, amygdala, caudate nucleus, putamen, and globus palladium. The left and right mean volume of these nucleus were extracted with fslstats. We calculate the normalized volume of subcortical structures by multiplying the scaling factor obtained from SIENAX.

2.5. Granger Causality Analysis. Functional preprocessing steps were carried out using the statistical parametric mapping (SPM5). It included the following steps: (1) slice timing correction; (2) trilinear sinc interpolation for alignment (motion correction); (3) spatial normalization based on the MNI space and resampled at 3 mm × 3 mm × 3 mm; (4) band-pass filter (0.01~0.08 Hz) spatially smoothed with a 6 mm full-width-at-half maximum (FWHM) Gaussian kernel; and (5) head motion and ventricular and white matter signal regression.

The multivariate GCA (mGCA) has been proved to be an optimal candidate to investigate the causal networks for its data-driven nature [35]. We performed mGCA on the time series of BOLD signal intensities from selected ROIs in both groups. The entire time series were averaged across voxels within each ROI picked in each group and were then normalized across subjects to form a single vector per ROI. The mGCA detected causal interactions by computing directed transfer function (DTF) from a multivariate autoregressive model of the time series [36]. We also adopted weighted DTF with partial coherence in order to emphasize direct connections and deemphasize mediated influences [36, 37]. The statistical significance of the path weights was ascertained using surrogate data. Surrogate data were generated by randomizing the phase of the original time series spectrum while retaining its magnitude. A null distribution was obtained by generating 2500 sets of surrogate data and calculating the direct directed transfer function (dDTF) from these 2500 datasets. The dDTF value obtained from the original time

series was verified using a null distribution for the one-tailed test with the significant p value of 0.01. In addition, a difference of influence (doi) term was used to assess links that showed a dominant direction of influence [38], which limits potentially spurious links caused by hemodynamic blurring [29]. The effective connectivity network of the 9 ROIs was constructed by visualizing the significant dDTF ($p < 0.01$, FDR corrected for multiple comparisons) obtained after running the statistical significant test.

The high degree nodes were considered to be the hubs of network [39]. We calculated "in-degree" (number of Granger causal efferent connections to a node) to find the central targets of network, and "out-degree" (number of Granger causal afferent connections from a node) to find the central sources [40, 41]. Further, hubs of the network were defined if the sum of "in-degree" and "out-degree" of a node was at least 1.96 standard deviations (SD) greater than the average of "in- + out-degree" of all nodes in the semantic cognition network [42].

Between-group differences in the causal connectivity graphs were determined as follows. We calculated dDTF values in all connections for every subject to explore the difference in the intensity of effective connectivity between groups, particularly with volumetric value of relevant ROI as a regressor. The links that showed between-group changes in the strength of causal influence were those whose difference in the doi term significantly differed between groups by a paired t-test ($p < 0.05$, FDR corrected).

2.6. Statistical Analysis. Analyses were performed using SPSS (IBM Corp. Released 2012. IBM SPSS Statistics, Version 21.0, Armonk, NY, USA). Volumetric comparison for normalized subcortical structures was conducted by two-sample t-test ($p < 0.05$). For each participant, a laterality index (LI) of hippocampus volume (HV) was computed using the formula [(left HV − right HV)/(left HV + right HV)]. A one-way ANOVA was used to compare LIs of left HS, right HS, and controls. Pearson's correlations were then used to examine the relationships between LI and factors such as age at epilepsy diagnosis, years since diagnosis, seizure frequency, and linking strength between ROIs in each group.

3. Results

3.1. Anatomical Changes. Group comparisons between controls and patients with left or right HS identified GMV loss confined to bilateral hemispheres (FWE corrected, $p \leq 0.05$). Specifically, in the left HS subgroup, GMV loss was found in 12 ipsilateral ROIs and 7 contralateral ROIs (Figure 1, left column); in the right HS subgroup, GMV loss was in 2 ipsilateral ROIs and 1 contralateral ROI (Figure 1, right column). Within the semantic cognition network, left HS patients showed atrophy in 4 areas of IFG, vmPFC, hippocampus, and MTG in the ipsilateral lobe, and 7 areas of IFG, vmPFC, parahippocampus, fusiform, AG, tpSTG, tpMTG, and MTG in the contralateral lobe. Meanwhile, right HS patients showed only ipsilateral MTG atrophy and no contralateral atrophy (see details in Table 2).

Table 2: Regions of GMV loss in left HS and right HS patients compared to healthy controls (FWE corrected, $p < 0.05$; cluster > 10 voxels).

Brain regions (AAL template)	Left HS ($n = 13$) voxels	Right HS ($n = 11$) voxels
Frontal_Sup_Orb_L_05	47	
Frontal_Inf_Oper_L_11	25	1
Frontal_Inf_Orb_L_15	39	
Frontal_Inf_Orb_R_16	141	
Frontal_Mid_Orb_L_25	11	
Frontal_Mid_Orb_R_26	31	
Rectus_L_27	82	
Hippocampus_L_37	75	
ParaHippocampal_R_40	57	
Occipital_Sup_L_49	146	
Occipital_Mid_L_51	368	
Postcentral_L_57	102	
Parietal_Inf_L_61	11	
Angular_R_66	61	
Thalamus_R_78		1
Heschl_L_79	65	
Temporal_Pole_Sup_R_84	329	
Temporal_Mid_L_85	315	
Temporal_Mid_R_86	351	1
Temporal_Pole_Mid_R_88	411	

Note: regions in italic are components of semantic cognition network; regions in bold are components of nonsemantic cognition network.

Further analysis showed significant difference of atrophy severity in the left and right HS patients (19/90 : 3/90; atrophy area number/network number; $p < 0.001$). In particular, the left hemisphere was more severely damaged in the left HS patients than the right ones (12/45 : 1/45; $p < 0.005$) (Figure 2(a)). In addition, atrophy severity of the semantic cognition network in the right hemisphere was more severe in the left HS patients than the right ones (7/12 : 1/12; $p < 0.05$), and patients' atrophy difference of the left nonsemantic cognition network also reached a significant level (8/33 : 0/33; $p < 0.01$) (Figure 2(b)). Even though, in the left HS patients, there was no significant differences of atrophy between left and right hemispheres (12/45 : 7/45; $p = 0.20$) or between the left and right semantic cognition network (4/12 : 7/12; $p = 0.22$), their nonsemantic networks were more severely damaged in the left hemispheres (8/33 : 0/33; $p < 0.01$) (Figure 2(c)).

3.2. Structural Asymmetry. A one-way ANOVA revealed significant differences between groups for hippocampal laterality index ($F = 12.70$, $p < 0.001$). The LI was highest (most left-lateralized) in the right HS patients (mean = 0.13, SD = 0.05), followed by the healthy controls (mean = −0.01, SD = 0.03) and the left HS group (mean = −0.21, SD = 0.05). Subsequent contrasts revealed significant differences between controls and patients with left HS ($t = 3.31$, $p = 0.002$),

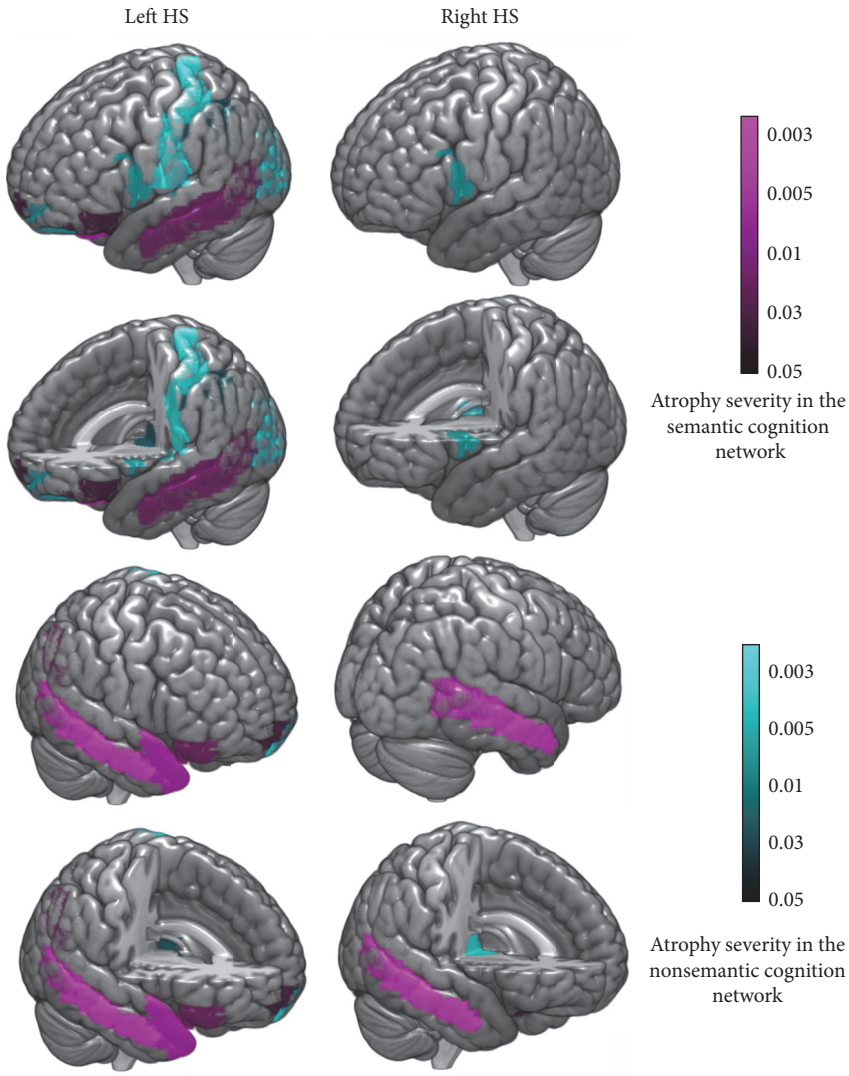

Figure 1: Gray matter volume (GMV) loss of patients with left HS or right HS (FWE corrected, $p = 0.05$; minimum cluster size 10). In the left HS subgroup, GMV loss was observed in 12 ROIs in the ipsilateral lobe (including the IFG, vmPFC, hippocampus, and MTG in the semantic cognition network) and 7 ROIs in the contralateral lobe (including the IFG, vmPFC, parahippocampus, fusiform, AG, tpSTG, tpMTG, and MTG, all of which were components of the semantic cognition network); in the right HS subgroup, GMV loss was seen in 2 ROIs in the ipsilateral lobe and the MTG in the contralateral lobe.

between controls and right HS patients ($t = -2.80$, $p < 0.01$), and between groups of left and right HS ($t = -4.27$, $p < 0.001$).

3.3. Strength Changes of Functional Connectivity in Left and Right HS Patients. A causal connectivity graph was constructed using the thickness of connecting lines to indicate the strengths of causal influences (see Figure 3). For left HS patients, right HS patients, and healthy controls, causal influences within the semantic cognition network presented strongly covarying relations (Figures 3(a), 3(b), and 3(c)). Overall, connection density among the three groups was not significantly different ($F = 0.03$, $p = 0.97$). But interconnection patterns between ATL subregions were different in the three groups: all the four subregions (left/right tpSTG and tpMTG) were significantly connected with each other in normal controls; no causal influence of the areas was found in the left HS patients; little causal influence remained in the right HS patients (colored check-boards at the bottom of each part in Figure 3).

Meanwhile, node degree analysis yielded more differences between groups. In the normal controls, the only hub of semantic cognition network was the right tpMTG. Specifically, the flow-in hub was the right dmPFC, while the right tpMTG was the only flow-out hub. In the left HS patients, the only hub was the right PCC. Specifically, the flow-in hub was the right dmPFC, while the right PCC was the only flow-out hub. However, there was no hub node in the semantic cognition network of right HS patients. Further, by comparing node degree between the left HS, right HS, and controls, we found that node degree of the right PCC was significantly different between left HS patients and controls

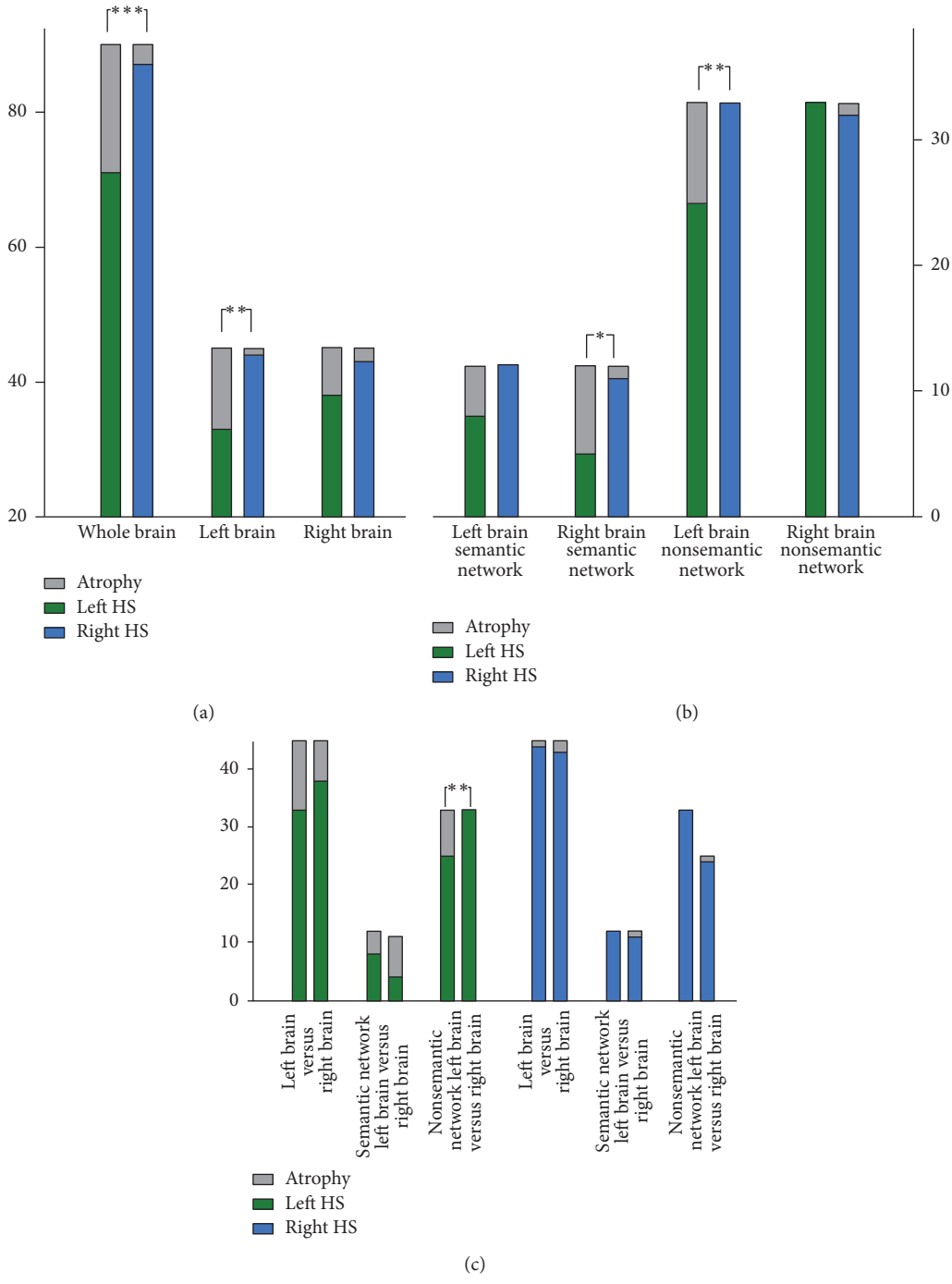

Figure 2: Comparison of atrophy severity of the left and right HS patients in both hemispheres. (i) The whole brain and especially the left hemisphere were more severely damaged in left HS patients than right HS patients. (ii) The atrophy severity of the semantic cognition network in the right hemisphere was more severe for left HS patients than right HS patients. (iii) "$*$" indicates $p < 0.05$; "$**$" indicates $p < 0.01$; "$***$" indicates $p < 0.005$.

($t = -2.23$, $p < 0.05$), and node degree of the right MTG was significantly different between right HS patients and controls ($t = 3.42$, $p < 0.002$). By comparing in-degree and out-degree between the left HS and controls, we found that the out-degree of right PCC ($t = -2.25$, $p < 0.05$), right IFG ($t = 2.67$, $p < 0.02$), left MTG ($t = 2.20$, $p < 0.05$), and left tpMTG ($t = -2.07$, $p < 0.05$) was significantly different. In contrast, by comparing in-degree and out-degree between the right HS and controls, we found that both the in-degree and out-degree of right MTG ($t = 3.03$, $p < 0.005$; $t = 2.63$, $p < 0.02$) were significantly different.

Between-group analysis showed increased driving effect between nodes in ipsilateral structures and decreased driving effect between nodes of contralateral structures in left HS

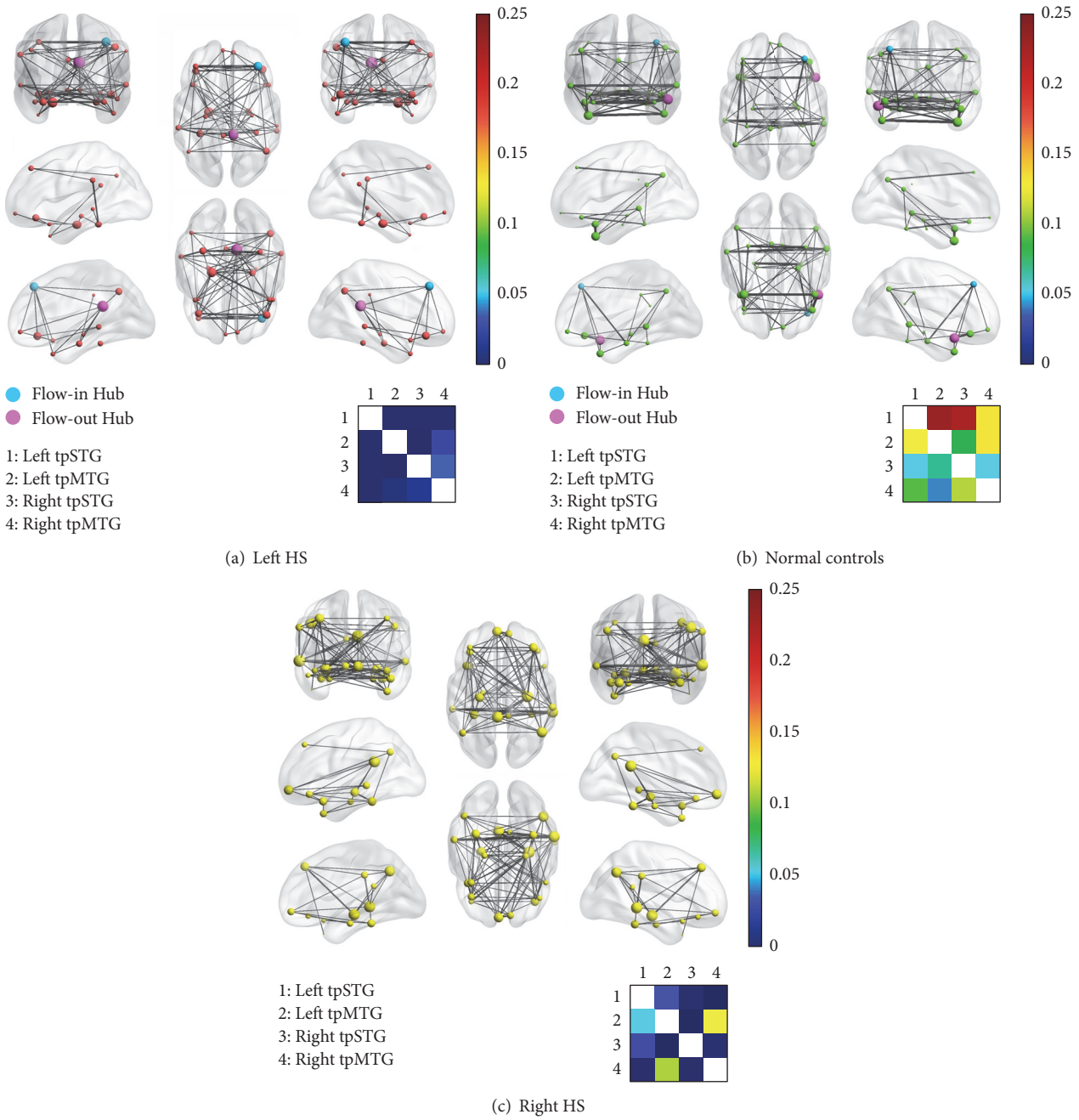

FIGURE 3: Causal influence of effective connectivity between ROIs in the semantic cognition network. (i) Connection density among the three groups of left HS patients, right HS patients, and normal controls was not significantly different from each other. (ii) The network hub in the normal controls was the right tpMTG (the flow-in hub the right dmPFC and the flow-out hub the right tpMTG), and the network hub in the left HS patients was the right PCC (the flow-in hub the right dmPFC and the flow-out hub the right PCC), but there was no hub node in the semantic cognition network of patients with right HS. (iii) Subregions of the anterior temporal lobe (ATL) in the bilateral hemispheres were strongly connected in normal controls but partially interconnected in right HS patients and not interconnected in left HS patients.

patients compared with normal controls. In detail, increased causal effects were found in the interactions from right AG to right parahippocampal gyrus, from right AG to right SMG, from left MTG to left parahippocampal gyrus, from left tpMTG to left PCC, and from left tpMTG to left MTG; decreased causal effects were found in the interactions from right PCC to left vmPFC, from right fusiform to left fusiform, and from left tpSTG to right tpSTG. There were also 3 exceptions where the causal effect from right vmPFC to right PCC and from left hippocampus to left parahippocampal gyrus decreased and where from right tpMTG to left MTG increased (see Figure 4(a)). By contrast, directional interaction weight changes between right HS patients and the controls seemed rather systematic. Increased interaction between

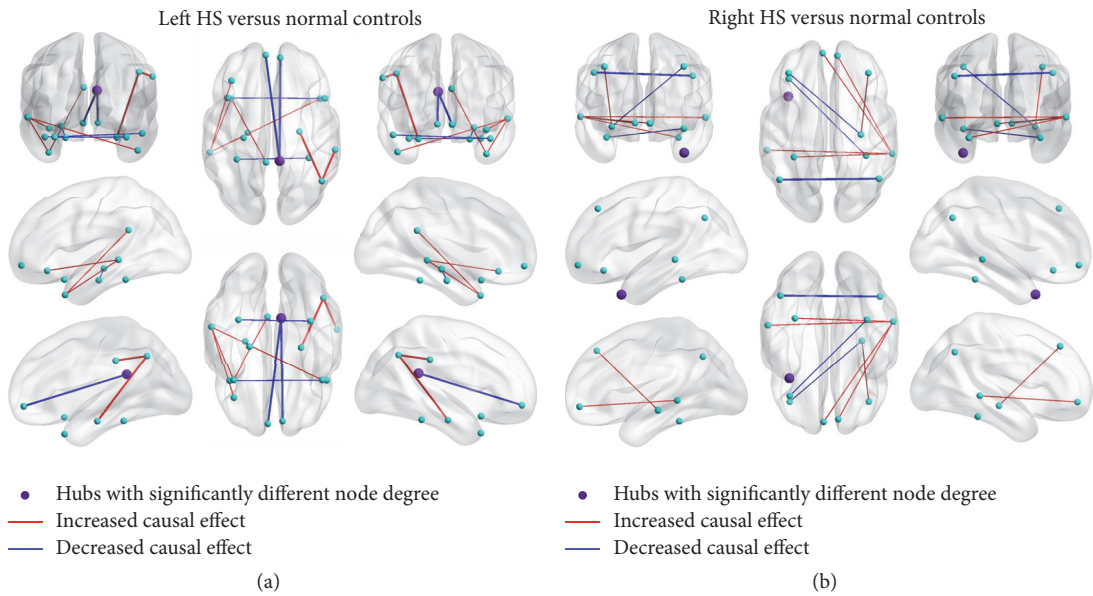

Figure 4: Changes of the driving effect between nodes in the semantic cognition network between the left HS, right HS, and normal controls. (i) The driving effect between nodes in ipsilateral structures increased and it decreased between nodes of contralateral structures in patients with left HS. (ii) Directional interaction weight changes between normal and patients with right HS seemed rather systematic, as an increased causal connectivity change was accompanied with a decreased intensity change and vice versa. (iii) The node degree of the right PCC was significantly different between patients with left HS and controls, and the node degree of the right MTG was significantly different between patients with right HS and controls.

ipsilateral ROIs originated from right vmPFC to right MTG; decreased intrahemisphere interaction originated from right hippocampus to right dmPFC. Increased interaction between contralateral ROIs originated from right AG to left AG, from left vmPFC to right MTG, and from right hippocampus to left dmPFC; decreased interhemisphere interaction originated from left fusiform to right MTG, from right fusiform to left IFG, and from right MTG to left MTG (see Figure 4(b)).

3.4. Correlation between Hippocampal LI and Epilepsy Onset Time, Duration, Frequency, and Strength of Causal Influence. There was significant correlation between hippocampus LI and changed path weights of effectively interconnected ROIs. The linking intensity from right AG to right parahippocampal gyrus in the left HS patients was negatively correlated with hippocampal LI ($r = -0.56$, $p < 0.05$), while the linking intensity from right AG to right SMG was positively correlated with hippocampal LI ($r = -0.61$, $p < 0.05$). No significant correlation was found between hippocampus LI and epilepsy onset time, duration, and frequency in both groups.

4. Discussion

To explore disrupted conceptualization in mTLE patients with HS, the current study focused on identifying structural and effective connectivity changes of the semantic cognition network. We found that the gray matter was significantly reduced in in both left and right HS patients. Even though the two hemispheres were equally damaged in mTLE patients with left HS, all the 7 regions that showed atrophy in the contralateral hemisphere were semantic cognition network components. Meanwhile, significant increased linking intensity changes between ipsilateral regions and decreased linking intensity changes between contralateral regions (particularly in the ATL area) were only found in the left mTLE group. The consistent anatomical and functional connectivity changes suggested that the breakdown of effective connectivity between left and right hemispheres, possibly caused by the severely damaged contralateral hemisphere, was the reason of more severe language impairment of left HS patients.

4.1. "Targeted Attacks" Affected the Contralateral Hemisphere of Left HS Patients Mostly. Previous quantitative MRI volumetric and voxel-based morphometry (VBM) studies have identified atrophy of the hippocampus [43] along with distributed abnormalities in neighboring and distant structures including the entorhinal cortex [43–45], parahippocampal gyrus [43], basal ganglia [46], lateral temporal cortex, frontal lobe, and cerebellum [47]. This distributed atrophy indicated influence of seizure propagation on the whole brain. Our findings were consistent with previous findings concerning the effect of epilepsy duration on gray matter volume in VBM studies [48, 49]. The altered topologies can be attributed to the seizure-dependent reinforcement of an epileptogenic configuration of the brain network.

Our findings also revealed different seizure propagation effects in the two patient groups. In the left HS patients, more regions in the whole brain, especially the dominant hemisphere, were injured. It was manifested that the left HS patients were more easily affected and may experience more serious hippocampal injuries, as their hippocampal LI varied

more from normal controls. One theory about mechanisms underlying brain damage in mTLE hypothesizes that seizure propagation determines the distribution of damage [33]. Our findings matched such a theory, since left HS patients were more easily affected.

In addition, we specifically found that all the 7 atrophy regions in the right hemisphere in left HS patients were within the semantic cognition network. It indicated that left HS patients also displayed a higher vulnerability to seizure attacks in the potential compensatory semantic networks. We postulated that more serious anatomical changes in the left semantic cognition network and a disrupted compensatory mechanism in the contralateral hemisphere, which received "targeted attack" with higher vulnerability to disease, lead to more severe language impairment in the left HS patients.

4.2. Breakdown of Interhemisphere Connection, Especially in ATL, Induced More Severe Language Impairment in Left HS Patients. The results of the Granger causality analyses using functional ROIs showed no significantly different connection density among the left HS patients, right HS patients, and normal controls. However, node degree analysis revealed that hubs of patients' semantic cognition network changed. The right tpMTG was the only hub center in normal controls. Its importance was best manifested in the outflow condition. In contrast, the ATL was not the longer semantic cognition network hub in both left and right HS patients.

In particular, subregions of the ATLs (tpSTG and tpMTG) in the left and right hemispheres were causally affected by each other in normal controls. It was in stark contrast with semantic cognition networks in patients with left and right HS, in which connections between ATL subregions were all disrupted in left HS patients while only the bidirectional causal connection between left and right tpMTG remained in right HS patients. Patterson et al. [50] propose that bilateral anterior temporal lobes are amodal, abstract conceptual hubs that bind modality-specific properties, which are grounded in the sensory-motor system. Pobric et al. [51] used repetitive transcranial magnetic stimulation (rTMS) to disrupt neural processing temporarily in the left or right temporal poles and reported that rTMS disrupted semantic processing for words and pictures with the same degree. Their work illustrated that left and right anterior temporal lobes are critical in forming concepts of both words and pictures. Our findings suggested that even the residual weak interhemisphere interactions can sustain a relatively normal semantic network (in the right HS patients). Moreover, the integrating role of the semantic network hub in ATL (the right tpMTG) cannot be compensated by other region (such as the right PCC in the left HS patients), even though it may also be effectively connected with many areas in the network. It implicated that left and right ATLs functioned as a transmodal hub via mutual interconnections.

Changes in interregional functional coupling are thought to represent compensatory mechanisms secondary to structural pathology and seizure-related activity [52]. In terms of compensation strategies, patients with left HS showed that causal linking between nodes in ipsilateral structures increased, while causal effects between nodes of contralateral structures decreased. In contrast, patients with right HS showed a balanced change where the number of significantly increased interhemisphere and intrahemisphere causal interactions was the same as that of decreased interhemisphere and intrahemisphere causal interactions. The equal occurrence rate of altered effective changes may be a coincidence. However, it also indicates that if effective connections between ipsilateral and contralateral regions were damaged, patients with right HS were able to form a compensatory one to sustain a relatively normal semantic competence. It may owe to their less severe structural changes. In other words, the severe targeted atrophy in the contralateral hemisphere in patients with left HS caused disrupted interconnection between hemispheres and cannot be substituted for by intensified connection between regions in the same hemisphere. Thus, the breakdown of interhemisphere connections, especially those across left and right ATLs, leads to naming disability.

4.3. Hippocampal Sclerosis Was Accompanied with Reduced Causal Influence from the AG. The two significant correlations between hippocampus LI and the path weights of the semantic cognition network both originated from the right AG in left HS patients. Since gray matter of the right AG was also significantly reduced, the structural change of the right AG may influence the power flowing out from it. It was consistent with the conclusion that the AG occupies a position at the top of a processing hierarchy underlying concept retrieval and conceptual integration [12]. As impaired semantic control was associated with deregulated access to knowledge, patients may have difficulty directing activation towards the target and away from irrelevant prepotent associations [10].

5. Conclusions and Limitation

By comparing structural changes of left and right mTLE patients with healthy controls, the current study suggested that left HS patients had a higher vulnerability to seizure attacks, which may affect their compensation strategy. The interrupted effective connectivity between subregions of the ATL across hemispheres, which performs a unitary, homogeneous, transmodal representation for conceptual information, may be the primary reason why left HS patients displayed severe name finding difficulties but relevant good comprehension ability. In sum, our study revealed that the severe and targeted anatomical changes resulted in failed compensatory strategy in left HS patients, which was characterized by increased intrahemisphere causal interaction but decreased interhemisphere causal links.

The primary limitation in the current study is the small number of left and right HS patients. Our intention was to maintain uniformity across patients, even if it means sacrificing sample size. Incorporating patients with a loose standard may reduce detectability of group difference. However, it may also lead to no significant correlation between the magnitude of Granger causality interaction and patients' clinical data, such as disease onset time, duration, or seizure frequency.

Competing Interests

The authors declare that there are no competing interests regarding the publication of this paper.

Authors' Contributions

Xiaotong Fan and Hao Yan contributed equally to this work.

Acknowledgments

The project was supported by the National Natural Science Foundation of China (81522021, 31400962, 81371201, and 31371026), the Beijing Municipal Science & Technology Commission (Z141100002114034), and the China Postdoctoral Science Foundation (2015M582400).

References

[1] J. H. Margerison and J. A. N. Corsellis, "Epilepsy and the temporal lobesa clinical, electroencephalographic and neuropathological study of the brain in epilepsy, with particular reference to the temporal lobes," *Brain*, vol. 89, no. 3, pp. 499–530, 1966.

[2] F. Cendes, "MRS and FMRI in partial epilepsies," *Arquivos de Neuro-Psiquiatria*, vol. 61, supplement 1, pp. 78–82, 2003.

[3] H. G. Wieser, "ILAE Commission Report. Mesial temporal lobe epilepsy with hippocampal sclerosis," *Epilepsia*, vol. 45, no. 6, pp. 695–714, 2004.

[4] G. Glosser, A. E. Salvucci, and N. D. Chiaravalloti, "Naming and recognizing famous faces in temporal lobe epilepsy," *Neurology*, vol. 61, no. 1, pp. 81–86, 2003.

[5] B. D. Bell, B. P. Hermann, A. R. Woodard et al., "Object naming and semantic knowledge in temporal lobe epilepsy," *Neuropsychology*, vol. 15, no. 4, pp. 434–443, 2001.

[6] S. M. Antonucci, P. M. Beeson, D. M. Labiner, and S. Rapcsak, "Lexical retrieval and semantic knowledge in patients with left inferior temporal lobe lesions," *Aphasiology*, vol. 22, no. 3, pp. 281–304, 2008.

[7] D. L. Drane, G. A. Ojemann, E. Aylward et al., "Category-specific naming and recognition deficits in temporal lobe epilepsy surgical patients," *Neuropsychologia*, vol. 46, no. 5, pp. 1242–1255, 2008.

[8] E. M. S. Sherman, S. Wiebe, T. B. Fay-Mcclymont et al., "Neuropsychological outcomes after epilepsy surgery: systematic review and pooled estimates," *Epilepsia*, vol. 52, no. 5, pp. 857–869, 2011.

[9] D. S. Sabsevitz, S. J. Swanson, T. A. Hammeke et al., "Use of preoperative functional neuroimaging to predict language deficits from epilepsy surgery," *Neurology*, vol. 60, no. 11, pp. 1788–1792, 2003.

[10] E. Jefferies, "The neural basis of semantic cognition: converging evidence from neuropsychology, neuroimaging and TMS," *Cortex*, vol. 49, no. 3, pp. 611–625, 2013.

[11] E. Jefferies and M. A. Lambon Ralph, "Semantic impairment in stroke aphasia versus semantic dementia: a case-series comparison," *Brain*, vol. 129, no. 8, pp. 2132–2147, 2006.

[12] J. R. Binder, R. H. Desai, W. W. Graves, and L. L. Conant, "Where is the semantic system? A critical review and meta-analysis of 120 functional neuroimaging studies," *Cerebral Cortex*, vol. 19, no. 12, pp. 2767–2796, 2009.

[13] T. T. Rogers, M. A. Lambon Ralph, P. Garrard et al., "Structure and deterioration of semantic memory: a neuropsychological and computational investigation," *Psychological Review*, vol. 111, no. 1, pp. 205–235, 2004.

[14] M. A. Lambon Ralph, K. Sage, R. W. Jones, and E. J. Mayberry, "Coherent concepts are computed in the anterior temporal lobes," *Proceedings of the National Academy of Sciences of the United States of America*, vol. 107, no. 6, pp. 2717–2722, 2010.

[15] M. A. Lambon Ralph, "Neurocognitive insights on conceptual knowledge and its breakdown," *Philosophical Transactions of the Royal Society of London B: Biological Sciences*, vol. 369, no. 1634, pp. 265–279, 2014.

[16] K. A. Noonan, E. Jefferies, M. Visser, and M. A. Lambon Ralph, "Going beyond inferior prefrontal involvement in semantic control: evidence for the additional contribution of dorsal angular gyrus and posterior middle temporal cortex," *Journal of Cognitive Neuroscience*, vol. 25, no. 11, pp. 1824–1850, 2013.

[17] D. Tranel, "The left temporal pole is important for retrieving words for unique concrete entities," *Aphasiology*, vol. 23, no. 7-8, pp. 867–884, 2009.

[18] M. A. Lambon Ralph, L. Cipolotti, F. Manes, and K. Patterson, "Taking both sides: do unilateral anterior temporal lobe lesions disrupt semantic memory?" *Brain*, vol. 133, no. 11, pp. 3243–3255, 2010.

[19] D. Kemmerer, D. Rudrauf, K. Manzel, and D. Tranel, "Behavioral patterns and lesion sites associated with impaired processing of lexical and conceptual knowledge of actions," *Cortex*, vol. 48, no. 7, pp. 826–848, 2012.

[20] K. Tsapkini, C. E. Frangakis, and A. E. Hillis, "The function of the left anterior temporal pole: evidence from acute stroke and infarct volume," *Brain*, vol. 134, no. 10, pp. 3094–3105, 2011.

[21] S. S. Spencer, "Neural networks in human epilepsy: evidence of and implications for treatment," *Epilepsia*, vol. 43, no. 3, pp. 219–227, 2002.

[22] W. N. Löscher, J. Dobesberger, C. Szubski, and E. Trinka, "rTMS reveals premotor cortex dysfunction in frontal lobe epilepsy," *Epilepsia*, vol. 48, no. 2, pp. 359–365, 2007.

[23] R. Matsumoto, D. R. Nair, E. LaPresto et al., "Functional connectivity in the human language system: a cortico-cortical evoked potential study," *Brain*, vol. 127, no. 10, pp. 2316–2330, 2004.

[24] J. Montplaisir, T. Nielsen, J. Côté, D. Boivin, I. Rouleau, and G. Lapierre, "Interhemispheric EEG coherence before and after partial callosotomy," *Clinical EEG Electroencephalography*, vol. 21, no. 1, pp. 42–47, 1990.

[25] B. B. Biswal, M. Mennes, X. N. Zuo et al., "Toward discovery science of human brain function," *Proceedings of the National Academy of Sciences of the United States of America*, vol. 107, no. 10, pp. 4734–4739, 2010.

[26] G. Chen, J. P. Hamilton, M. E. Thomason, I. H. Gotlib, Z. S. Saad, and R. W. Cox, "Granger causality via vector auto-regression tuned for fMRI data analysis," *Proceedings of International Society for Magnetic Resonance in Medicine*, vol. 17, p. 1718, 2009.

[27] D. W. Cope, G. Di Giovanni, S. J. Fyson et al., "Enhanced tonic $GABA_A$ inhibition in typical absence epilepsy," *Nature Medicine*, vol. 15, no. 12, pp. 1392–1398, 2009.

[28] R. Goebel, A. Roebroeck, D.-S. Kim, and E. Formisano, "Investigating directed cortical interactions in time-resolved fMRI data using vector autoregressive modeling and Granger causality mapping," *Magnetic Resonance Imaging*, vol. 21, no. 10, pp. 1251–1261, 2003.

[29] A. Roebroeck, E. Formisano, and R. Goebel, "Mapping directed influence over the brain using Granger causality and fMRI," *NeuroImage*, vol. 25, no. 1, pp. 230–242, 2005.

[30] M. M. Jan, M. Sadler, and S. R. Rahey, "Electroencephalographic features of temporal lobe epilepsy," *Canadian Journal of Neurological Sciences*, vol. 37, no. 4, pp. 439–448, 2010.

[31] N. F. Moran, L. Lemieux, N. D. Kitchen, D. R. Fish, and S. D. Shorvon, "Extrahippocampal temporal lobe atrophy in temporal lobe epilepsy and mesial temporal sclerosis," *Brain*, vol. 124, no. 1, pp. 167–175, 2001.

[32] N. Bernasconi, S. Duchesne, A. Janke, J. Lerch, D. L. Collins, and A. Bernasconi, "Whole-brain voxel-based statistical analysis of gray matter and white matter in temporal lobe epilepsy," *NeuroImage*, vol. 23, no. 2, pp. 717–723, 2004.

[33] F. Riederer, R. Lanzenberger, M. Kaya, D. Prayer, W. Serles, and C. Baumgartner, "Network atrophy in temporal lobe epilepsy: a voxel-based morphometry study," *Neurology*, vol. 71, no. 6, pp. 419–425, 2008.

[34] D. W. Loring, K. J. Meador, G. P. Lee et al., "Cerebral language lateralization: evidence from intracarotid amobarbital testing," *Neuropsychologia*, vol. 28, no. 8, pp. 831–838, 1990.

[35] O. Demirci, M. C. Stevens, N. C. Andreasen et al., "Investigation of relationships between fMRI brain networks in the spectral domain using ICA and Granger causality reveals distinct differences between schizophrenia patients and healthy controls," *NeuroImage*, vol. 46, no. 2, pp. 419–431, 2009.

[36] R. Stilla, G. Deshpande, S. LaConte, X. Hu, and K. Sathian, "Posteromedial parietal cortical activity and inputs predict tactile spatial acuity," *The Journal of Neuroscience*, vol. 27, no. 41, pp. 11091–11102, 2007.

[37] G. Deshpande, K. Sathian, and X. Hu, "Effect of hemodynamic variability on Granger causality analysis of fMRI," *NeuroImage*, vol. 52, no. 3, pp. 884–896, 2010.

[38] J. Lu, H. Liu, M. Zhang et al., "Focal pontine lesions provide evidence that intrinsic functional connectivity reflects polysynaptic anatomical pathways," *The Journal of Neuroscience*, vol. 31, no. 42, pp. 15065–15071, 2011.

[39] E. Bullmore and O. Sporns, "Complex brain networks: graph theoretical analysis of structural and functional systems," *Nature Reviews Neuroscience*, vol. 10, no. 3, pp. 186–198, 2009.

[40] D. Sridharan, D. J. Levitin, and V. Menon, "A critical role for the right fronto-insular cortex in switching between central-executive and default-mode networks," *Proceedings of the National Academy of Sciences of the United States of America*, vol. 105, no. 34, pp. 12569–12574, 2008.

[41] M. C. Stevens, G. D. Pearlson, and V. D. Calhoun, "Changes in the interaction of resting-state neural networks from adolescence to adulthood," *Human Brain Mapping*, vol. 30, no. 8, pp. 2356–2366, 2009.

[42] Z. Liu, Y. Zhang, L. Bai et al., "Investigation of the effective connectivity of resting state networks in Alzheimer's disease: A functional MRI study combining independent components analysis and multivariate Granger causality analysis," *NMR in Biomedicine*, vol. 25, no. 12, pp. 1311–1320, 2012.

[43] N. Bernasconi, A. Bernasconi, Z. Caramanos, S. B. Antel, F. Andermann, and D. L. Arnold, "Mesial temporal damage in temporal lobe epilepsy: a volumetric MRI study of the hippocampus, amygdala and parahippocampal region," *Brain*, vol. 126, part 2, pp. 462–469, 2003.

[44] T. Salmenperä, R. Kälviäinen, K. Partanen, and A. Pitkänen, "Hippocampal and amygdaloid damage in partial epilepsy: a cross-sectional MRI study of 241 patients," *Epilepsy Research*, vol. 46, no. 1, pp. 69–82, 2001.

[45] L. Bonilha, C. Rorden, J. J. Halford et al., "Asymmetrical extrahippocampal grey matter loss related to hippocampal atrophy in patients with medial temporal lobe epilepsy," *Journal of Neurology, Neurosurgery and Psychiatry*, vol. 78, no. 3, pp. 286–294, 2007.

[46] S. Dreifuss, F. J. G. Vingerhoets, F. Lazeyras et al., "Volumetric measurements of subcortical nuclei in patients with temporal lobe epilepsy," *Neurology*, vol. 57, no. 9, pp. 1636–1641, 2001.

[47] E. K. Sandok, T. J. O'Brien, C. R. Jack, and E. L. So, "Significance of cerebellar atrophy in intractable temporal lobe epilepsy: a quantitative MRI study," *Epilepsia*, vol. 41, no. 10, pp. 1315–1320, 2000.

[48] J. Natsume, N. Bernasconi, F. Andermann, and A. Bernasconi, "MRI volumetry of the thalamus in temporal, extratemporal, and idiopathic generalized epilepsy," *Neurology*, vol. 60, no. 8, pp. 1296–1300, 2003.

[49] C. Á. Szabó, J. L. Lancaster, S. Lee et al., "MR imaging volumetry of subcortical structures and cerebellar hemispheres in temporal lobe epilepsy," *American Journal of Neuroradiology*, vol. 27, no. 10, pp. 2155–2160, 2006.

[50] K. Patterson, P. J. Nestor, and T. T. Rogers, "Where do you know what you know? The representation of semantic knowledge in the human brain," *Nature Reviews Neuroscience*, vol. 8, no. 12, pp. 976–987, 2007.

[51] G. Pobric, E. Jefferies, and M. A. Lambon Ralph, "Category-specific versus category-general semantic impairment induced by transcranial magnetic stimulation," *Current Biology*, vol. 20, no. 10, pp. 964–968, 2010.

[52] B. C. Bernhardt, S. J. Hong, A. Bernasconi, and N. Bernasconi, "Imaging structural and functional brain networks in temporal lobe epilepsy," *Frontiers in Human Neuroscience*, vol. 7, article 624, 14 pages, 2013.

Hindawi Publishing Corporation
Neural Plasticity
Volume 2016, Article ID 6238575, 11 pages
http://dx.doi.org/10.1155/2016/6238575

Clinical Study

Ipsilesional High Frequency Repetitive Transcranial Magnetic Stimulation Add-On Therapy Improved Diffusion Parameters of Stroke Patients with Motor Dysfunction: A Preliminary DTI Study

Zhiwei Guo,[1] Yu Jin,[1] Haitao Peng,[1] Guoqiang Xing,[1,2] Xiang Liao,[1] Yunfeng Wang,[3] Huaping Chen,[1] Bin He,[1] Morgan A. McClure,[1] and Qiwen Mu[1,4]

[1]*Department of Imaging and Imaging Institute of Rehabilitation and Development of Brain Function, The Second Clinical Medical College of North Sichuan Medical College, Nanchong Central Hospital, Nanchong 637000, China*
[2]*Lotus Biotech.Com LLC., John Hopkins University-MCC, Rockville, MD, USA*
[3]*Department of Neurology, The Second Clinical Medical College of North Sichuan Medical College, Nanchong Central Hospital, Nanchong 637000, China*
[4]*Peking University Third Hospital, Beijing, China*

Correspondence should be addressed to Qiwen Mu; muqiwen99@yahoo.com

Received 7 July 2016; Accepted 31 August 2016

Academic Editor: Lin Ai

Purpose. The aim of this study was to evaluate the effects of high frequency repetitive transcranial magnetic stimulation (HF-rTMS) on stroke patients with motor dysfunction and to investigate the underlying neural mechanism. *Methods*. Fifteen stroke patients were assigned to the rTMS treatment (RT) group and conventional treatment (CT) group. Patients in the RT received 10 Hz rTMS stimulation on the ipsilesional primary motor cortex for 10 days plus conventional treatment of CT, which consisted of acupuncture and antiplatelet aggregation medication. Difference in fractional anisotropy (FA) between pretreatment and posttreatment and between two groups was determined. Correlations between FA values and neurological assessments were also calculated. *Results*. Both groups significantly improved the neurological function after treatment. rTMS-treated patients showed better improvement in Fugl-Meyer Assessment (FMA) score and increased FA value in motor-related white matter and gray matter cortices compared with CT-treated patients and pretreatment status. Besides, the increased FA value in the ipsilesional posterior limb of the internal capsule in RT group was significantly correlated with the improved FMA score. *Significance*. HF-rTMS could be a supplement therapy to CT in improving motor recovery in patients with stroke. And this benefit effect may be achieved through modulating the ipsilesional corticospinal tracts and motor-related gray matter cortices.

1. Introduction

Stroke is the major cause of adult disability worldwide. Up to 80% of the stroke patients endure motor deficits that severely lowers the quality of their daily lives [1, 2]. Most of the stroke survivors could obtain a certain degree of motor improvement after various therapies, including medication, acupuncture, movement training, and other types of interventions. So far, however, the effectiveness of these interventions remains unsatisfactory.

The neural mechanisms of motor recovery following stroke remain unknown. Recent studies indicate that the functional plasticity and structural remodeling of white microstructure could underlie the poststroke recovery process [3–6]. Transcranial magnetic stimulation (TMS) is a safe, painless, and noninvasive strategy that was first reported by Barker et al. in 1985 [7, 8]. Repetitive TMS (rTMS) is a new method that can alert activity in cortex and induce lasting effects on neuroplasticity in the cortex, and it has been used to treat depression, Parkinson's disease, stroke, and other

neurological diseases in recent years. The rTMS therapy for motor recovery following stroke aims to augment neural plasticity and improve motor function based on the interhemispheric competition model, which states that inhibitory rTMS on contralesional hemisphere increases excitability in the ipsilesional motor cortex by reducing excessive interhemispheric inhibition from the contralesional motor cortex [9–11], whereas excitatory rTMS over the affected hemisphere directly increases the excitability of the ipsilesional motor cortex [11–14].

Previous plastic studies of rTMS had focused mainly on functional brain mapping. Currently, diffusion tensor imaging (DTI) has been widely used as a noninvasive tool to investigate and measure the integrity of white matter in vivo [15]. Fractional anisotropy (FA), one of DTI parameters, can quantify the degree of water diffusion and reliably visualize the microstructural status, but it is susceptible to axonal myelination as well as density and orientational coherence [16]. Reduced FA has been reported in Wallerian degeneration or destruction of white matter integrity [17] and in people with motor impairments [18]. Several DTI-based studies that evaluated the FA values along the ipsilesional corticospinal tracts (CST) suggest a decreased FA value following stroke [19–21]. After the interventions of different treatments, the progressively increased FA values in the ipsilesional CST were found positively correlated with the functional recovery of the stroke patients as measured by the Fugl-Meyer Assessment (FMA) [4, 5, 22]. Several related studies also reported that the stroke motor recovery is positively and significantly associated with the changes of FA in the contralesional hemisphere after unilateral infract [23–25]. Besides, previous low frequency rTMS studies also have shown obvious effects in improving motor function via inhibiting contralesional motor cortex and exciting the ipsilesional cortex [26, 27]. To date the research on rTMS-induced white matter modification after stroke is limited, and it is not clear if high frequency rTMS could also lead to an improvement in motor function and remodeling of white microstructures in stroke patients with motor dysfunction.

The present study aimed at determining whether high frequency rTMS-induced excitability of the ipsilesional hemisphere would cause plastic changes in the microstructure of white matter of stroke patients with motor dysfunction and the correlation with motor recovery.

2. Methods

2.1. Participants. Fifteen acute ischemic stroke patients with left hemisphere infarctions were recruited for this study from March to December 2015 at the Second Clinical Medical College of North Sichuan Medical College, Nanchong, China, with the following inclusion criteria: (1) first-ever stroke patients with a unilateral hemisphere infarct within seven days of onset; (2) the lesion being subcortical with its focal point confirmed by diffusion weighted imaging (DWI); (3) National Institutes of Health Stroke Scale (NIHSS) scores ≥2; (4) mild to moderate motor impairment lasting at least 48 hours; (5) age from 50 to 80 years; and (6) being without seizure, dysgnosia, psychosis, or other coexistent neurological/psychiatric disease. All study procedures were conducted in accordance with the Helsinki Declaration of 1975 and were approved by Institutional Review Board of the North Sichuan Medical College. Informed consent was obtained from all participants prior to enrollment into the study.

A total of 15 patients were assigned to two groups: 7 to the rTMS treatment (RT) group and 8 to the conventional treatment (CT) group. The patients in the RT group received 10 Hz rTMS treatment over the ipsilesional motor cortex for 10 days plus conventional treatment, whereas patients in CT group underwent conventional treatment including acupuncture and antiplatelet aggregation drugs medication.

2.2. MRI Procedure and Neurological Evaluation. Each patient received the neurological functional assessments and MRI scans two times: prior to the first rTMS session and immediately after the end of rTMS treatments (10 days of rTMS stimulation). All patients received the same medical therapy including anticoagulant (low molecular weight heparin or aspirin), brain protection (piracetam), and blood circulation protection (*Salvia miltiorrhiza*).

2.3. Clinical Assessment. All patients were assessed by Fugl-Meyer Assessment (FMA), NIHSS, and Barthel Index scale (BI) to evaluate the severity of stroke and functional disability by trained and experienced neurologists before MRI examination. The FMA measurement consists of the motor function assessment items on upper limb and lower limb. BI is often used to evaluate the activity ability of daily living of stroke patient. For both of FMA and BI scales, a higher score reveals a better motor function or activity ability. On the contrary, a higher score of NIHSS, a comprehensive assessment to estimate the degree of neurological impairment, reflects a more serious stroke-related disability. Behavioral assessment and MRI examination were both conducted on the same day. To minimize operator-dependent bias, the neurologists were blinded to the patient grouping. The differences in clinical assessment scores between the RT and CT groups and before the first session and after the end of treatment were analysed by using the SPSS 22.0 software (Statistical Package for Social Sciences, Chicago, IL, USA). The results were considered significant at $p < 0.05$.

2.4. Resting Motor Threshold. For the rTMS treatment, the TMS coil was placed on the ipsilesional motor cortex. To determine the stimulation intensity, the resting motor threshold (RMT), defined as the minimal output of stimulation that could evoke muscle twitch of the contralateral first dorsal interosseous (FDI) or elicited a motor evoked potential (MEP) of at least an amplitude of 50 μV in at least half of 10 consecutive stimuli recorded by electromyography [28], was determined for each patient by connecting the rTMS stimulator to an electromyogram apparatus (Dantec Keypoint System, Skovlunde, Denmark). The MEP signal was recorded from the surface Ag/AgCI electrodes placed on the FDI hand muscles.

2.5. rTMS Protocols. Patients in the RT group received 10 daily sessions of rTMS over the hand area of the ipsilesional primary motor cortex (M1) for a duration of 15 minutes using a Mag Pro butterfly-shape coil stimulator (MagVenture, Lucernemarken, Denmark). Each session of rTMS involved 30 trains of 50 pulses with 25-second intervals at 10 Hz and 90% RMT (total 1500 pulses/day). The stimulated motor cortex was determined and defined as the location that could elicit muscle twitch and the largest MEP of the contralateral FDI. As the ipsilesional hemisphere remained nonresponsive to TMS stimulation, the exact site of stimulation was defined as the location homologous to the contralesional motor cortex. Besides, during the rTMS treatment, the coil was positioned tangentially to the scalp of the stimulation target at a 45° angle from the midsagittal plane.

2.6. Acupuncture Strategy. Acupuncture was performed at the bilateral Fengchi acupoint and ipsilesional Baihui, Xuanzhong, Quchi, Hegu, Zusanli, and Sanyinjiao acupoints, with Baihui and Fengchi forward flat spines 0.5–1.5 inch, obliquely to the tip of the nose direction of the wind pool, and the remaining acupoints down to levels of 0.8–2.0 inches. The twisting angle was less than 90 degrees. The acupuncture treatment was performed by experienced and licensed acupuncturists. Each patient received thirty minutes of acupuncture treatment per day following rTMS treatment. Patients in both the RT and CT groups were also given antiplatelet aggregation drugs to improve blood circulation.

2.7. MRI Acquisition. All MRI data were acquired on a GE Signa HDxt 1.5 Tesla MR scanner (General Electric Medical System, Milwaukee, WI, USA) by using an 8-channel head coil. The DTI acquisition was performed by using a single-shot echo-planar imaging (EPI) sequence with the following parameters: TR/TE = 8500/96 ms, flip angle = 90°, field of view = 240 mm × 240 mm, matrix = 256 × 256, voxel sizes = $0.94 \times 0.94 \times 5.0\ \text{mm}^3$, 32 axial slices with no gap, and acquisition time = 4 minutes and 50 seconds. The diffusion sensitive gradients were applied along 30 noncollinear directions with b value = $1000\ \text{s/mm}^2$ to obtain the weighted images and one unweighted B0 image with b value = $0\ \text{s/mm}^2$.

Along with the diffusion tensor imaging scan, high resolution anatomical T1-weighted images were also acquired for each subject using a three-dimensional-spoiled gradient recalled (3D-SPGR) sequence: TR/TE = 9.1/2.9 ms, flip angle = 20°, field of view = 240 mm × 240 mm, matrix = 256 × 256, voxel sizes = $0.94 \times 0.94 \times 1.2\ \text{mm}^3$, and 124 slices with no gap.

2.8. Image Processing. SPM8 software (statistical parametric mapping, http://www.fil.ion.ucl.ac.uk/spm/) was used for preprocessing of DTI datasets to remove the head motion by aligning 30 diffusion weighted images to B0 image. Eddy current distortions were corrected by affine registration to the reference B0 image. Whole brain fiber tracking and reconstruction of the diffusion parameter images were evaluated in the DTI native space using interpolated streamline propagation algorithm with Diffusion Toolkit Software (http://trackvis.org/). Three eigenvalues ($\lambda 1$, $\lambda 2$, and $\lambda 3$) and the maps of MD and FA were produced for each subject.

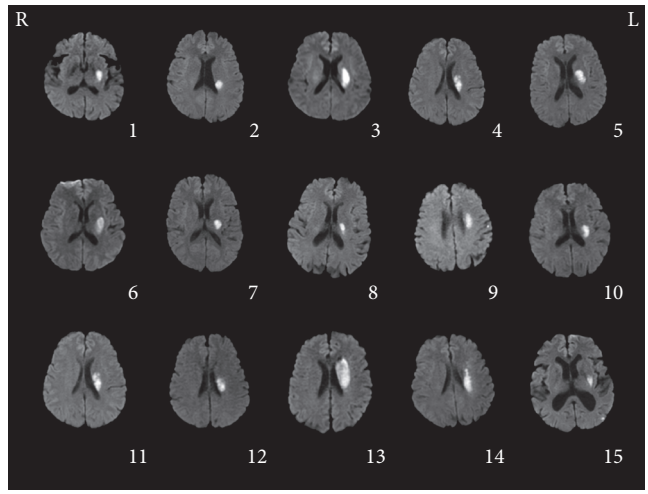

Figure 1: Individual diffusion weighted images in the axial view. The panel shows the slice with maximum infarct volume. Each subject is coded by the same serial number as the first row in Table 1.

During fiber tracking, if the FA value was lower than 0.2 or if the angle was less than 40°, the path tracking was stopped. All of the maps were normalized to the Montreal Neurological Institute (MNI) coordinate system and reinterpolated into isotropic voxels of 3.0 mm × 3.0 mm × 3.0 mm. Finally, to improve the signal-to-noise ratio of the maps, an isotropic Gaussian kernel (FWHM = 8 mm) was applied to complete the spatial smooth filtering. To detect the alteration of MD and FA values after the rTMS treatment, a paired t-test was adopted with a statistical significant level of $p < 0.05$. The two-sample t-test was also used to compare the images between the patients from RT and CT groups. To minimize the possible impact on the findings, age, gender, and duration of stroke were used as covariates in all statistical analyses.

2.9. Correlation Analysis. After comparing the FA maps between pre- and post-rTMS treatments, the motor-related brain regions, which revealed significant differences, were selected as regions of interest (ROI) to investigate the potential relationships between the alteration of diffusion parameters in these ROIs and clinical assessment improvement. Each ROI was defined as a cluster composed of 27 voxels around the peak coordinate of the difference area. For each ROI, the extracted values were manually checked and confirmed before the average value of the 27 voxels was obtained. Finally, Pearson correlation analysis was conducted between the diffusion parameters and clinical assessments including FM and BI to estimate their homogeneity.

3. Results

Table 1 shows the demographic and clinical characteristics of the included stroke patients. No significant differences in age, gender, type of stroke, duration, or baseline behavioral scores were observed between the RT and CT groups at baseline. Figure 1 illustrates the lesion location from the slice of maximum infarct volume on DWI images for each

Table 1: Clinical data of included stroke patients.

Group	Number	Age (years)	Duration (days)	Gender	Lesion location	NIHSS		FM		BI	
						Pre	Post	Pre	Post	Pre	Post
RT	1	72	5	F	L_IC, BG	8	5	10	42	50	60
	2	63	5	M	L_IC, BG	6	4	13	34	60	70
	3	79	3	M	L_IC, BG	10	6	38	69	35	55
	4	64	6	F	L_IC, BG	11	3	77	89	25	70
	5	64	6	F	L_IC, BG	11	9	67	77	25	30
	6	74	3	F	L_IC, BG	6	3	32	60	65	80
	7	58	4	M	L_IC, BG	9	5	22	51	25	45
		67.71 ± 7.4	**4.57 ± 1.27**			**8.71 ± 2.14**	**5.00 ± 2.08***	**37.00 ± 26.00**	**60.29 ± 19.54*△**	**40.71 ± 17.42**	**58.57 ± 17.00***
CT	8	56	4	F	L_IC	10	8	20	22	25	30
	9	76	3	M	L_IC, BG, CR	5	3	60	64	50	65
	10	53	6	F	L_IC, BG	9	7	14	35	40	55
	11	75	7	M	L_IC, BG	10	7	40	41	25	50
	12	61	5	F	L_IC, BG	9	6	22	27	30	40
	13	67	5	F	L_IC, BG, CR	7	3	63	69	80	90
	14	77	4	M	L_IC, BG, CR	11	5	11	18	20	30
	15	68	6	M	L_IC, BG	5	3	20	24	60	70
		66.63 ± 9.24	**5.00 ± 1.30**			**8.25 ± 2.32**	**5.25 ± 2.05***	**31.25 ± 20.56**	**37.5 ± 19.37***	**41.25 ± 20.83**	**53.75 ± 20.83***

BG: basal ganglia; BI: Barthel Index; CT: conventional treatment; CR: corona radiate; FM: Fugl-Meyer Assessment; L_IC: left internal capsule; NIHSS: National Institutes of Health Stroke Scale; RT: repetitive transcranial magnetic stimulation treatment; $*$ represents the significant difference between preclinical and postclinical scores ($p < 0.05$); △ represents the significant difference between the clinical scores of RT and CT groups.

Table 2: Brain regions with significant clusters and peak voxel coordinates showing FA difference between pre- and post-rTMS treatment.

Brain region	MNI coordinates (x, y, z)	t value	Voxel number
Post > pre			
Supp_motor_area_R	7, −23, 60	4.89	77
Frontal_mid_R	36, 10, 51	3.18	48
Precentral_L	−38, −2, 48	4.67	55
Precentral_R	27, −20, 54	4.22	73
Thalamus_L	−23, −23, 6	7.56	39
Temporal_inf_L	−59, −20, −30	6.89	31
Post < pre			
Precuneus_R	5, −68, 53	−4.74	32
Parietal_sup_R	27, −49, 51	−5.58	54
Angular_L	−44, −61, 48	−2.84	28

MNI: Montreal Neurological Institute; L: left; R: right.

Table 3: Brain regions with significant clusters and peak voxel coordinates showing FA difference between rTMS group and control group.

Brain region	MNI coordinates (x, y, z)	t value	Voxel number
RT > CT			
Supp_motor_area_L	0, −1, 61	7.91	294
Precentral_L	−44, −13, 60	3.63	75
Precentral_R	36, −23, 58	3.56	51
Postcentral_L	−48, −26, 54	2.78	59
Paracentral_lobule_L	−2, −31, 60	4.13	162
Precuneus_L	−2, −47, 60	3.9	372
Frontal_inf_tri_R	49, 32, 7	4.13	58
Thalamus_L	−23, −20, 6	2.68	51
Insula_R	45, 6, 9	2.96	46
Frontal_sup_medial_R	2, 59, 3	3.63	286
Temporal_mid_R	65, −36, 3	3.56	76
Occipital_sup_R	11, −96, 4	2.61	42
RT < CT			
Frontal_mid_R	29, 53, 3	−4.23	122
Caudate_L	−13, 17, 10	−2.39	58
Frontal_sup_L	−14, 67, 2	−2.76	50
Frontal_mid_L	−30, 10, 51	−3.1	29

MNI: Montreal Neurological Institute; L: left; R: right; RT: repetitive transcranial magnetic stimulation treatment; CT: conventional treatment.

participant. All of the patients completed the 10 treatment sessions without reporting any adverse effects.

3.1. Behavioral Outcomes. Table 1 shows the descriptive pretreatment and posttreatment data for all clinical measures for both RT and CT groups. NIHSS, FMA, and BI scores showed significant changes after the treatment in both groups (NIHSS: RT: $p = 0.003$; CT: $p = 0.001$; FMA: RT: $p = 0.001$; CT: $p = 0.026$; BI: RT: $p = 0.012$, CT: $p = 0.001$). Additionally, the increase in FMA was significantly greater in the RT than in the CT group after the treatment ($p = 0.041$).

3.2. Factional Anisotropy Improvement. Paired comparisons between pre- and post-rTMS conditions revealed that the quantitative diffusion FA values of patients in the RT had increased significantly in the ipsilesional posterior limb of internal capsule (PLIC), M1, contralesional supplementary motor area (SMA), middle frontal gyrus (MFG), bilateral CST at the level of corona radiate (CR), and contralesional PLIC after 10 days of rTMS intervention ($p < 0.05$, uncorrected). The significant differences were demonstrated in Figure 2 and detailed information of significant clusters and peak voxels was recorded in Table 2. No significant changes were observed in the CT after a 10-day acupuncture and conventional medication treatment. Moreover, the quantitative diffusion FA value in the bilateral PLIC, M1, and SMA was significantly different between the RT and CT groups after rTMS and conventional treatment ($p < 0.05$, uncorrected) (Figure 3 and Table 3).

3.3. Relationship between Motor Improvement and White Microstructure. To evaluate the relationship between the quantitative FA values and the functional clinical recovery, we detected a significant and positive correlation between the altered FA value in the ipsilesional PLIC and changes in FMA scores in RT group ($r = 0.78$, $p = 0.039$) (Figure 4). For the CT group, although positive correlation was found, it was not significant ($r = 0.27$, $p = 0.52$). No significant correlation was observed in other areas.

4. Discussion

In this study, 10-day successive sessions of exciting high frequency (10 Hz) rTMS over the ipsilesional motor cortex were evaluated in acute ischemic stroke patients, as an add-on therapy to current therapy for its effect on motor function recovery. Voxel-based diffusion parameter analysis was applied to investigate the microstructural alteration after this treatment. The investigation showed that both RT plus CT (including acupuncture and medication) and CT alone improved the motor function of the affected limb. Furthermore, the improvement was greater in the RT + CT group than in the CT alone group as measured by FM score (Table 1). The significantly improved microstructural properties of motor-related white fibers and gray matter areas, which included the PLIC, M1, SMA, MFG, and CR, were also observed in the RT + CT group. The FA changes in the ipsilesional PLIC of rTMS-treated patients but not in that of control patients showed a linear relationship with the functional motor gains, suggesting a potential modulation of the motor function recovery and motor-related neural systems as well as the interhemispheric communication by repeated rTMS treatment in stroke patients. The results of this study also demonstrated that high frequency rTMS was

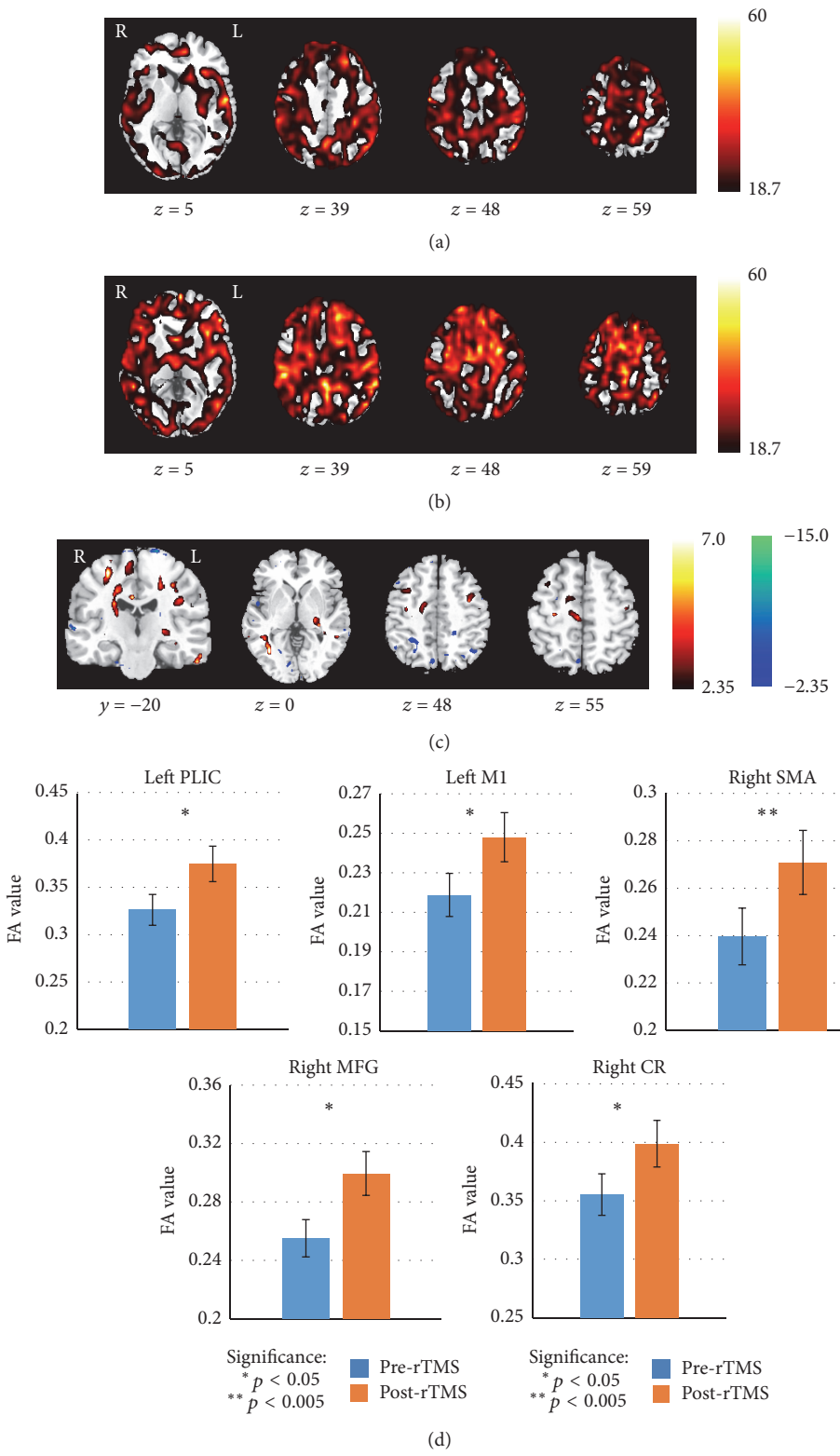

Figure 2: Comparison of FA maps between pre- and post-rTMS treatment for stroke patients in RT group. The FA results of one-sample t-test for stroke patients of pre- (a) and post-rTMS treatment (b). (c) Significantly changed brain areas are superimposed on the che2bet hemisphere of the Montreal Neurological Institute template brain in the three-view drawing ($p < 0.05$). The warm and cold tones separately indicate the increased and decreased FA value after rTMS treatment. (d) Bars represent the mean FA values. Vertical bars indicate estimated standard errors. Compared with the pre-rTMS treatment, the mean FA showed a significant increase after rTMS treatment in bilateral posterior limb of internal capsule (PLIC), left precentral gyrus (PG), right supplementary motor area (SMA), right middle frontal gyrus (MFG), and right corona radiate (CR).

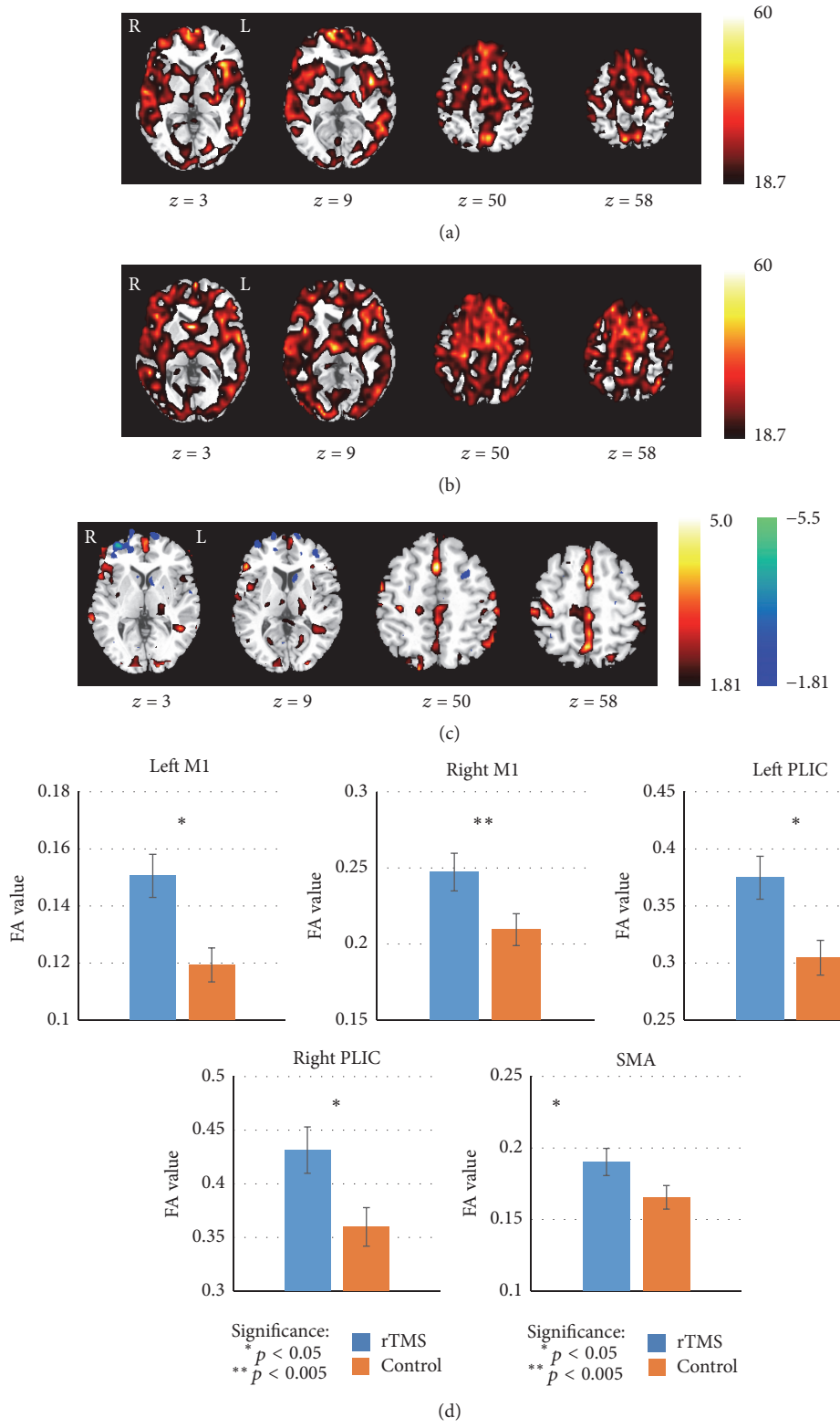

Figure 3: Comparison of FA maps between patients of RT and CT groups after treatment. The FA results of one-sample t-test for stroke patients of post-CT (a) and post-rTMS treatment (b). (c) Significantly changed brain areas are superimposed on the che2bet hemisphere of the Montreal Neurological Institute template brain in the three-view drawing ($p < 0.05$). The warm and cold tones separately indicate the increased and decreased FA value of RT. (d) Bars represent the mean FA values. Vertical bars indicate estimated standard errors. Compared with the CT, the mean FA value showed a significant increase after rTMS treatment in bilateral posterior limb of internal capsule (PLIC), primary motor area (M1), and supplementary motor area (SMA) in RT.

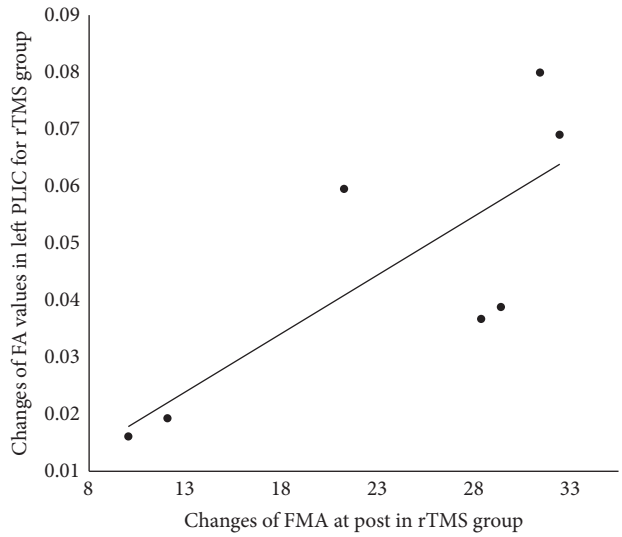

Figure 4: Relationship between changes of FA value in the ipsilesional posterior limb of internal capsule and changes of FMA score after rTMS treatment in the RT group (correlation coefficient $r = 0.78$, $p = 0.039$).

a safe and tolerable add-on therapy for acute ischemic stroke patients.

Previous studies showed that rTMS alone was effective for motor recovery in stroke patients [14, 29–32]. In these studies, both single session [14, 29] and multiple sessions [30–32] of rTMS over affected hemisphere facilitated and enhanced motor recovery in stroke patients, in terms of movement accuracy [14], movement time [14], frequency of finger tapping [29], grip strength [30–32], and other motor aspects of motor function. However, so far, no study has reported FMA as a potential mechanism underlying high frequency rTMS-induced motor rehabilitation after stroke.

In this study, rTMS add-on therapy significantly increased FA values in the ipsilesional and contralesional PLIC and bilateral CR of stroke patients and this increase in the ipsilesional PLIC was positively correlated with the alteration of FMA scores. Although similar imaging results were observed in the CT group, they did not reach a significant level. These findings would reflect a boosting effect of rTMS on motor function recovery after stroke. Recent studies have shown that PLIC is mainly comprised of CST which control voluntary movement and is commonly used as the regions to the analysis of the integrity of CST [33, 34]. Compared to other brain regions, PLIC would have a closer relationship with motor function. In addition, studies on stroke patients observed that degree of damage to the PLIC (reflected as reductions in FA values) is correlated with poor motor function [21], and the regional FA changes of PLIC could predict changes of motor impairment [35]. Thus, an increased FMA score would represent improved motor ability, and the positive correlation may indicate that the bigger FA value increased the better motor recovery of the patients.

There is evidence that PLIC and CR were mainly comprised of CST which project from the motor cortex to the PLIC [34, 36, 37] and to brain stem [33]. Previous diffusion microstructural studies have showed significantly decreased FA values in ipsilesional [5, 38, 39] and contralesional [24, 40] PLIC and CST after stroke. The degree of FA reduction in PLIC was also correlated with the damage of motor ability [5, 24]. During rehabilitation, the FA value of both the affected [21, 41] and unaffected CST increased significantly [42], and it has been used to predict the long-term motor outcome after stroke [21, 43]. Furthermore, a 7-day HF-rTMS reduced the infarct volumes, improved glucose metabolism, and inhibited neuronal apoptosis in lesional area in mice with acute experimental stroke [44]. In our study, we placed high frequency rTMS stimulation over the ipsilesional M1 area which is the origin of CST. Therefore, the neuromodulation of rTMS is possibly associated with or modulated through this structural pathway that involved improved energy metabolism.

Except for the white matter structures, we also observed increased FA value in several motor-related gray matter areas including the bilateral M1, SMA, ipsilesional thalamus, paracentral lobule, and contralesional MFG after rTMS treatment. It is known that the brain motor network, consisting of the M1, SMA, and paracentral lobule [45, 46], is crucially involved in the voluntary motor control [47]. Although MFG is not part of the motor network, previous functional MRI studies illustrated that MFG may monitor and reinforce motor performance and cognitive and executive functions during stroke recovery [48–51]. Besides, thalamus is involved in the modulation of motor function [52].

The cortical interhemispheric competition theory suggests a dual facilitation and inhibition modulation mechanism of the excitability of motor cortex between bilateral hemispheres that may underlie the recovery of motor dysfunction [53]. Indeed, increased FA value in CST and the transcallosal M1-M1 tracts was reported during stroke rehabilitation [35, 38], supporting that both are associated with subsequent motor recovery. A recent study of low frequency rTMS (LF-rTMS) on contralesional hemisphere in stroke patients with motor dysfunction suggests that LF-rTMS could increase FA value of transcallosal motor fibers and modulate and assist adaptive neuroplastic changes in stroke patients [54]. Together with this study's findings of FA value increased in bilateral M1 and motor-related cortex, it can be inferred that these findings may reflect the neuromodulation and therapeutic effects of rTMS on microstructural plasticity in stroke patients.

There are several limitations in the present study. First, only a small number of patients were included in each group that reduced the analysis power in statistical analysis. Second, regarding the behavioral assessment, only FMA, NIHSS, and BI were used to evaluate rTMS-induced motor recovery. Because FMA is mainly for motor function assessment, whereas NIHSS and BI are too general to evaluate specific motor ability, more refined and targeted motor measurement could produce more detailed findings. Third, the potential effects of acupuncture treatment and medication received by both RT and CT groups cannot be excluded. In addition, the longer-term effects of rTMS treatment were not evaluated.

Although both RT and CT improved the neurological scores, motor function, and daily activity ability, a greater

improvement in FMA scores was observed in RT group than in the CT group, suggesting a specific effect of HF-rTMS in this regard. A recent DTI study showed that a 4-week acupuncture treatment with conventional medication could improve the FMA score and white matter diffusion parameters compared to medication alone in stroke patients with unilateral motor deficits [55]. Thus, the lack of clear-cut different results between the RT + CT group and CT group in this study may have been obscured by the potential therapeutic effect of acupuncture present in both treatment groups, or the greater improvement in FMA score in the RT + CT group may still reflect additional beneficial effects of rTMS over CT on motor recovery. Future studies with separate controls of rTMS, acupuncture, and medication are needed to verify this possibility.

To our knowledge, this study is the first to have evaluated the effectiveness of high frequency rTMS add-on therapy in acute stroke patients with motor dysfunction using voxel-based diffusion parameter analysis. rTMS treatment plus CT for 10 days improved diffusion microstructures in motor-related white matter and gray matter brain regions that correlated with the behavioral recovery in stroke patients. Our results also suggest that change in FA values of the ipsilesional PLIC could be a potential biomarker for motor recovery in stroke patient that deserves further investigation.

Competing Interests

The authors declare no competing interests regarding the publication of this paper.

Acknowledgments

This work was supported by the National Natural Science Foundation of China (no. 81271559) and the State Administration of Foreign Experts Affairs, China (nos. SZD201516 and SZD201606). The authors thank Professor Cheng Luo for his professional suggestion to their research.

References

[1] F. E. Buma, E. Lindeman, N. F. Ramsey, and G. Kwakkel, "Functional neuroimaging studies of early upper limb recovery after stroke: a systematic review of the literature," *Neurorehabilitation and Neural Repair*, vol. 24, no. 7, pp. 589–608, 2010.

[2] L. Liu, D. Wang, K. S. Lawrence Wong, and Y. Wang, "Stroke and stroke care in China huge burden, significant workload, and a national priority," *Stroke*, vol. 42, no. 12, pp. 3651–3654, 2011.

[3] A. K. Rehme and C. Grefkes, "Cerebral network disorders after stroke: evidence from imaging-based connectivity analyses of active and resting brain states in humans," *The Journal of Physiology*, vol. 591, no. 1, pp. 17–31, 2013.

[4] C. Grefkes and N. S. Ward, "Cortical reorganization after stroke: how much and how functional?" *The Neuroscientist*, vol. 20, no. 1, pp. 56–70, 2014.

[5] J. D. Schaechter, Z. P. Fricker, K. L. Perdue et al., "Microstructural status of ipsilesional and contralesional corticospinal tract correlates with motor skill in chronic stroke patients," *Human Brain Mapping*, vol. 30, no. 11, pp. 3461–3474, 2009.

[6] G. Liu, C. Dang, X. Chen et al., "Structural remodeling of white matter in the contralesional hemisphere is correlated with early motor recovery in patients with subcortical infarction," *Restorative Neurology and Neuroscience*, vol. 33, no. 3, pp. 309–319, 2015.

[7] A. T. Barker, R. Jalinous, and I. L. Freeston, "Non-invasive magnetic stimulation of human motor cortex," *The Lancet*, vol. 325, no. 8437, pp. 1106–1107, 1985.

[8] M. Hallett, "Transcranial magnetic stimulation and the human brain," *Nature*, vol. 406, no. 6792, pp. 147–150, 2000.

[9] N. Takeuchi, T. Tada, M. Toshima et al., "Inhibition of the unaffected motor cortex by 1 Hz repetitive transcranial magnetic stimulation enhances motor performance and training effect of the paretic hand in patients with chronic stroke," *Journal of Rehabilitation Medicine*, vol. 40, no. 4, pp. 298–303, 2008.

[10] N. Takeuchi, T. Chuma, Y. Matsuo, I. Watanabe, and K. Ikoma, "Repetitive transcranial magnetic stimulation of contralesional primary motor cortex improves hand function after stroke," *Stroke*, vol. 36, no. 12, pp. 2681–2686, 2005.

[11] F. Fregni, P. S. Boggio, C. G. Mansur et al., "Transcranial direct current stimulation of the unaffected hemisphere in stroke patients," *NeuroReport*, vol. 16, no. 14, pp. 1551–1555, 2005.

[12] F. Hummel, P. Celnik, P. Giraux et al., "Effects of non-invasive cortical stimulation on skilled motor function in chronic stroke," *Brain*, vol. 128, no. 3, pp. 490–499, 2005.

[13] V. Di Lazzaro, P. Profice, F. Pilato et al., "Motor cortex plasticity predicts recovery in acute stroke," *Cerebral Cortex*, vol. 20, no. 7, pp. 1523–1528, 2010.

[14] Y.-H. Kim, S. H. You, M.-H. Ko et al., "Repetitive transcranial magnetic stimulation-induced corticomotor excitability and associated motor skill acquisition in chronic stroke," *Stroke*, vol. 37, no. 6, pp. 1471–1476, 2006.

[15] L. J. Lanyon, "Diffusion tensor imaging: structural connectivity insights, limitations and future directions," in *Neuroimaging-Methods*, pp. 137–162, 2012.

[16] P. J. Basser and C. Pierpaoli, "Microstructural and physiological features of tissues elucidated by quantitative-diffusion-tensor MRI," *Journal of Magnetic Resonance, Series B*, vol. 111, no. 3, pp. 209–219, 1996.

[17] M. Møller, J. Frandsen, G. Andersen, A. Gjedde, P. Vestergaard-Poulsen, and L. Østergaard, "Dynamic changes in corticospinal tracts after stroke detected by fibretracking," *Journal of Neurology, Neurosurgery, and Psychiatry*, vol. 78, no. 6, pp. 587–592, 2007.

[18] J. Puig, S. Pedraza, G. Blasco et al., "Acute damage to the posterior limb of the internal capsule on diffusion tensor tractography as an early imaging predictor of motor outcome after stroke," *American Journal of Neuroradiology*, vol. 32, no. 5, pp. 857–863, 2011.

[19] A. Sterr, P. J. A. Dean, A. J. Szameitat, A. B. Conforto, and S. Shen, "Corticospinal tract integrity and lesion volume play different roles in chronic hemiparesis and its improvement through motor practice," *Neurorehabilitation and Neural Repair*, vol. 28, no. 4, pp. 335–343, 2014.

[20] S.-H. Cho, D. G. Kim, D.-S. Kim, Y.-H. Kim, C.-H. Lee, and S. H. Jang, "Motor outcome according to the integrity of the corticospinal tract determined by diffusion tensor tractography in the early stage of corona radiata infarct," *Neuroscience Letters*, vol. 426, no. 2, pp. 123–127, 2007.

[21] E. H. Kim, J. Lee, and S. H. Jang, "Motor outcome prediction using diffusion tensor tractography of the corticospinal tract in

large middle cerebral artery territory infarct," *NeuroRehabilitation*, vol. 32, no. 3, pp. 583–590, 2013.

[22] S. H. Jang, K. Kim, S. H. Kim, S. M. Son, W. H. Jang, and H. G. Kwon, "The relation between motor function of stroke patients and diffusion tensor imaging findings for the corticospinal tract," *Neuroscience Letters*, vol. 572, pp. 1–6, 2014.

[23] Z. Liu, Y. Li, X. Zhang, S. Savant-Bhonsale, and M. Chopp, "Contralesional axonal remodeling of the corticospinal system in adult rats after stroke and bone marrow stromal cell treatment," *Stroke*, vol. 39, no. 9, pp. 2571–2577, 2008.

[24] C. Granziera, H. Ay, S. P. Koniak, G. Krueger, and A. G. Sorensen, "Diffusion tensor imaging shows structural remodeling of stroke mirror region: results from a pilot study," *European Neurology*, vol. 67, no. 6, pp. 370–376, 2012.

[25] E. M. Andrews, S.-Y. Tsai, S. C. Johnson et al., "Human adult bone marrow-derived somatic cell therapy results in functional recovery and axonal plasticity following stroke in the rat," *Experimental Neurology*, vol. 211, no. 2, pp. 588–592, 2008.

[26] C. G. Mansur, F. Fregni, P. S. Boggio et al., "A sham stimulation-controlled trial of rTMS of the unaffected hemisphere in stroke patients," *Neurology*, vol. 64, no. 10, pp. 1802–1804, 2005.

[27] F. Fregni, P. S. Boggio, A. C. Valle et al., "A sham-controlled trial of a 5-day course of repetitive transcranial magnetic stimulation of the unaffected hemisphere in stroke patients," *Stroke*, vol. 37, no. 8, pp. 2115–2122, 2006.

[28] S. Groppa, A. Oliviero, A. Eisen et al., "A practical guide to diagnostic transcranial magnetic stimulation: report of an IFCN committee," *Clinical Neurophysiology*, vol. 123, no. 5, pp. 858–882, 2012.

[29] M. Ameli, C. Grefkes, F. Kemper et al., "Differential effects of high-frequency repetitive transcranial magnetic stimulation over ipsilesional primary motor cortex in cortical and subcortical middle cerebral artery stroke," *Annals of Neurology*, vol. 66, no. 3, pp. 298–309, 2009.

[30] E. M. Khedr, A. E. Etraby, M. Hemeda, A. M. Nasef, and A. A. E. Razek, "Long-term effect of repetitive transcranial magnetic stimulation on motor function recovery after acute ischemic stroke," *Acta Neurologica Scandinavica*, vol. 121, no. 1, pp. 30–37, 2010.

[31] W. H. Chang, Y.-H. Kim, O. Y. Bang, S. T. Kim, Y. H. Park, and P. K. W. Lee, "Long-term effects of rTMS on motor recovery in patients after subacute stroke," *Journal of Rehabilitation Medicine*, vol. 42, no. 8, pp. 758–764, 2010.

[32] M. P. Malcolm, W. J. Triggs, K. E. Light et al., "Repetitive transcranial magnetic stimulation as an adjunct to constraint-induced therapy: an exploratory randomized controlled trial," *American Journal of Physical Medicine and Rehabilitation*, vol. 86, no. 9, pp. 707–715, 2007.

[33] J. K. Park, B. S. Kim, G. Choi et al., "Evaluation of the somatotopic organization of corticospinal tracts in the internal capsule and cerebral peduncle: results of diffusion-tensor MR tractography," *Korean Journal of Radiology*, vol. 9, no. 3, pp. 191–195, 2008.

[34] K. A. Potter-Baker, N. M. Varnerin, D. A. Cunningham et al., "Influence of corticospinal tracts from higher order motor cortices on recruitment curve properties in stroke," *Frontiers in Neuroscience*, vol. 10, article 79, 2016.

[35] R. Lindenberg, L. L. Zhu, T. Rüber, and G. Schlaug, "Predicting functional motor potential in chronic stroke patients using diffusion tensor imaging," *Human Brain Mapping*, vol. 33, no. 5, pp. 1040–1051, 2012.

[36] D. A. Cunningham, A. Machado, D. Janini et al., "Assessment of inter-hemispheric imbalance using imaging and noninvasive brain stimulation in patients with chronic stroke," *Archives of Physical Medicine and Rehabilitation*, vol. 96, no. 4, pp. S94–S103, 2015.

[37] A. I. Holodny, D. M. Gor, R. Watts, P. H. Gutin, and A. M. Ulug, "Diffusion-tensor MR tractography of somatotopic organization of corticospinal tracts in the internal capsule: initial anatomic results in contradistinction to prior reports," *Radiology*, vol. 234, no. 3, pp. 649–653, 2005.

[38] Y.-T. Fan, K.-C. Lin, H.-L. Liu, Y.-L. Chen, and C.-Y. Wu, "Changes in structural integrity are correlated with motor and functional recovery after post-stroke rehabilitation," *Restorative Neurology and Neuroscience*, vol. 33, no. 6, pp. 835–844, 2015.

[39] Y. Li, P. Wu, F. Liang, and W. Huang, "The microstructural status of the corpus callosum is associated with the degree of motor function and neurological deficit in stroke patients," *PLoS ONE*, vol. 10, no. 4, Article ID e0122615, 2015.

[40] S. Y. Kwak, S. S. Yeo, B. Y. Choi, C. H. Chang, and S. H. Jang, "Corticospinal tract change in the unaffected hemisphere at the early stage of intracerebral hemorrhage: a diffusion tensor tractography study," *European Neurology*, vol. 63, no. 3, pp. 149–153, 2010.

[41] Y. Takenobu, T. Hayashi, H. Moriwaki, K. Nagatsuka, H. Naritomi, and H. Fukuyama, "Motor recovery and microstructural change in rubro-spinal tract in subcortical stroke," *NeuroImage: Clinical*, vol. 4, pp. 201–208, 2014.

[42] K. Marumoto, T. Koyama, M. Hosomi et al., "Diffusion tensor imaging predicts the outcome of constraint-induced movement therapy in chronic infarction patients with hemiplegia: a pilot study," *Restorative Neurology and Neuroscience*, vol. 31, no. 4, pp. 387–396, 2013.

[43] J. Puig, G. Blasco, J. Daunis-I-Estadella et al., "Decreased corticospinal tract fractional anisotropy predicts long-term motor outcome after stroke," *Stroke*, vol. 44, no. 7, pp. 2016–2018, 2013.

[44] F. Gao, S. Wang, Y. Guo et al., "Protective effects of repetitive transcranial magnetic stimulation in a rat model of transient cerebral ischaemia: a microPET study," *European Journal of Nuclear Medicine and Molecular Imaging*, vol. 37, no. 5, pp. 954–961, 2010.

[45] F. A. Middleton and P. L. Strick, "Basal ganglia and cerebellar loops: motor and cognitive circuits," *Brain Research Reviews*, vol. 31, no. 2-3, pp. 236–250, 2000.

[46] R. P. Dum and P. L. Strick, "Motor areas in the frontal lobe of the primate," *Physiology & Behavior*, vol. 77, no. 4-5, pp. 677–682, 2002.

[47] H. Nakata, K. Sakamoto, A. Ferretti et al., "Negative BOLD effect on somato-motor inhibitory processing: an fMRI study," *Neuroscience Letters*, vol. 462, no. 2, pp. 101–104, 2009.

[48] J. Camchong, A. W. MacDonald III, C. Bell, B. A. Mueller, and K. O. Lim, "Altered functional and anatomical connectivity in schizophrenia," *Schizophrenia Bulletin*, vol. 37, no. 3, pp. 640–650, 2011.

[49] K. Öneş, E. Y. Yalçinkaya, B. C. Toklu, and N. Caglar, "Effects of age, gender, and cognitive, functional and motor status on functional outcomes of stroke rehabilitation," *NeuroRehabilitation*, vol. 25, no. 4, pp. 241–249, 2009.

[50] A. W. S. Leung, S. K. W. Cheng, A. K. Y. Mak, K.-K. Leung, L. S. W. Li, and T. M. C. Lee, "Functional gain in hemorrhagic stroke patients is predicted by functional level and cognitive abilities

measured at hospital admission," *NeuroRehabilitation*, vol. 27, no. 4, pp. 351–358, 2010.

[51] C.-H. Park, W. H. Chang, S. H. Ohn et al., "Longitudinal changes of resting-state functional connectivity during motor recovery after stroke," *Stroke*, vol. 42, no. 5, pp. 1357–1362, 2011.

[52] M. R. DeLong, M. D. Crutcher, and A. P. Georgopoulos, "Primate globus pallidus and subthalamic nucleus: functional organization," *Journal of Neurophysiology*, vol. 53, no. 2, pp. 530–543, 1985.

[53] A. C. Vidal, P. Banca, A. G. Pascoal, G. Cordeiro, J. Sargento-Freitas, and M. Castelo-Branco, "Modulation of cortical interhemispheric interactions by motor facilitation or restraint," *Neural Plasticity*, vol. 2014, Article ID 210396, 8 pages, 2014.

[54] A. Demirtas-Tatlidede, M. Alonso-Alonso, R. P. Shetty, I. Ronen, A. Pascual-Leone, and F. Fregni, "Long-term effects of contralesional rTMS in severe stroke: safety, cortical excitability, and relationship with transcallosal motor fibers," *NeuroRehabilitation*, vol. 36, no. 1, pp. 51–59, 2015.

[55] Y. Li, Y. Wang, H. Zhang, P. Wu, and W. Huang, "The effect of acupuncture on the motor function and white matter microstructure in ischemic stroke patients," *Evidence-Based Complementary and Alternative Medicine*, vol. 2015, Article ID 164792, 10 pages, 2015.

Hindawi Publishing Corporation
Neural Plasticity
Volume 2016, Article ID 9265621, 12 pages
http://dx.doi.org/10.1155/2016/9265621

Review Article

MRI Biomarkers for Hand-Motor Outcome Prediction and Therapy Monitoring following Stroke

U. Horn,[1] M. Grothe,[2] and M. Lotze[1]

[1]*Functional Imaging Unit, Department of Diagnostic Radiology and Neuroradiology, University Medicine, University of Greifswald, Greifswald, Germany*
[2]*Department of Neurology, University Medicine, University of Greifswald, Greifswald, Germany*

Correspondence should be addressed to M. Lotze; martin.lotze@uni-greifswald.de

Received 12 July 2016; Accepted 23 August 2016

Academic Editor: Lijun Bai

Several biomarkers have been identified which enable a considerable prediction of hand-motor outcome after cerebral damage already in the subacute stage after stroke. We here review the value of MRI biomarkers in the evaluation of corticospinal integrity and functional recruitment of motor resources. Many of the functional imaging parameters are not feasible early after stroke or for patients with high impairment and low compliance. Whereas functional connectivity parameters have demonstrated varying results on their predictive value for hand-motor outcome, corticospinal integrity evaluation using structural imaging showed robust and high predictive power for patients with different levels of impairment. Although this is indicative of an overall higher value of structural imaging for prediction, we suggest that this variation be explained by structure and function relationships. To gain more insight into the recovering brain, not only one biomarker is needed. We rather argue for a combination of different measures in an algorithm to classify fine-graded subgroups of patients. Approaches to determining biomarkers have to take into account the established markers to provide further information on certain subgroups. Assessing the best therapy approaches for individual patients will become more feasible as these subgroups become specified in more detail. This procedure will help to considerably save resources and optimize neurorehabilitative therapy.

1. The Challenge: Preparing the Field

Stroke continues to be the leading cause for long-term disabilities. Worldwide, about 5 million people who have suffered from a stroke remain permanently impaired [1], leaving a majority of patients with disturbances in the motor abilities [2]. About 75% of those who experience stroke have lingering upper limb impairment [3]. As restoring hand-motor abilities is crucial in improving the patients' daily lives, the efficiency of training strategies is essential. In contrast to lower limb training, which only focuses on pure repetition of gait movements [4], upper limb motor function training needs to combine different aspects of motor abilities to rehabilitate the everyday requirements [5]. Plasticity research has also suggested that repetitions close to the individual output limit improve motor ability more than the number of overall repetitions alone [6]. It is therefore crucial to adjust the therapy to the functional requirements of each patient.

The therapeutic success depends on the amount of lesioned brain resources and the capability of affected systems to adapt to alternative intact resources. In addition, the time after stroke is a relevant factor for plasticity: specifically, the acute and subacute phases after stroke are characterized by augmented plasticity, which can last up to 3 or 4 months [7]. In these early stages, therapeutic intervention may lead to functionally relevant improvements whereas, in the chronic stage, the potential to recover basic functions is limited (e.g., [8, 9]).

Figure 1 provides an overview of the different stages after stroke for the adult patient.

So far, it has not been possible to properly assess individual recovery processes. Based on clinical presentation alone, it is difficult to estimate which patients will recover their upper limb function [10]. Prognostic measures are needed to identify the individual potential for improvement and to

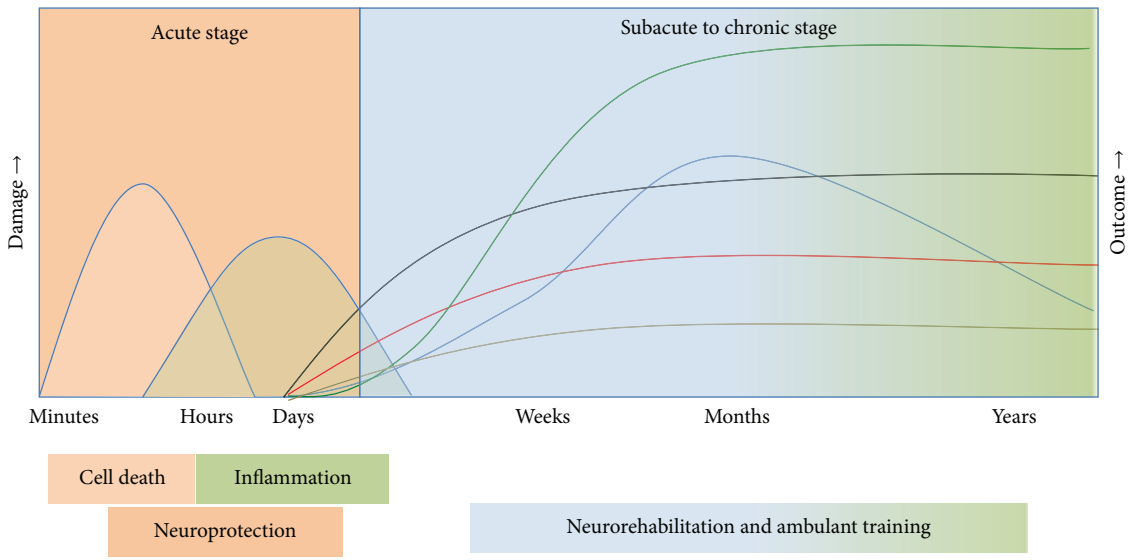

Figure 1: This graph illustrates the need for prognostic assessment tools, especially for the clinically important subacute stage. In the acute stage, cell death and inflammation are associated with worse outcome, and the therapeutic goal therefore is neuroprotection. In the subacute to chronic stage, neurorehabilitation individually improves clinical outcome.

predict the individual outcome after stroke. Imaging techniques can complement the clinical assessment and provide an insight into the patient's individual plasticity processes and offer appropriate therapy. The diagram was modified after [11].

2. Outcome Assessment

The definition of a unified motor outcome assessment is difficult and the choice of the outcome parameter is highly dependent on the patient group being investigated: patients with low outcome are not able to perform more demanding tests, while those with high motor outcome show ceiling effects in less demanding tests. There also seems to be a discrepancy between the outcome measurement used in the rehabilitative phase and the real life relevance of this motor performance. Different scores can rate the different abilities recovering over time, for example, measuring strength, aiming, pinch grip, and tapping tasks. For instance, motor training in healthy participants modulates four independent motor abilities: aiming, speed, steadiness, and visuomotor tracking [13]. It would be desirable to represent these four different motor abilities in outcome scores more specifically. Another suggestion for optimizing outcome measurements is to apply an objective measurement for the usage of the affected hand in activity of daily living (ADL), for instance, with accelerometers [14]. Data gained by accelerometers as outcome measures might also solve the problems of interrater variability and the nonparametric distribution of scores. Measuring different outcome scores at once, which are highly associated, causes a multiple comparison problem. To solve this problem, large sample sizes are necessary to differentiate predictors for several performance outcome parameters. Rather than averaging over different scores, a certain parameter which depicts the relevant motor ability most accurately seems desirable.

It is possible to summarize those measures which illustrate the recovery best, for example, by building a composed score with principal component analyses (PCA) [15–17]. However, the composed recovery score does not reveal which component leads to the measured improvement, and the PCA scores are also dependent on the specific data set, which varies with different studies.

For a single patient, the outcome parameters can be set individually, depending on the requirements of and relevance to the patient. In prediction studies, however, it is necessary to assess several abilities which might be relevant to the outcome of the specific group. PCA therefore are able to assess the main effects of the group rather than the individual when several variables might influence the outcome.

3. Contributions of Imaging on Neural Substrates of Motor Recovery

Different imaging strategies have been developed addressing functional loss in different stages after stroke.

Specifically, structural imaging has been important in determining the outcome and understanding of functional loss. However, most of these approaches are poorly standardized and usually expert knowledge is required to estimate the exact localization or extent of the damage. There are some approaches simplifying the research methods to assess structural damage of the white matter (e.g., for the pyramidal tract [18]).

In contrast, functional imaging has so far only partially contributed to the understanding of the neural mechanisms of recovered hand-motor function and has gained almost no access to clinical routine over the past decades. We will

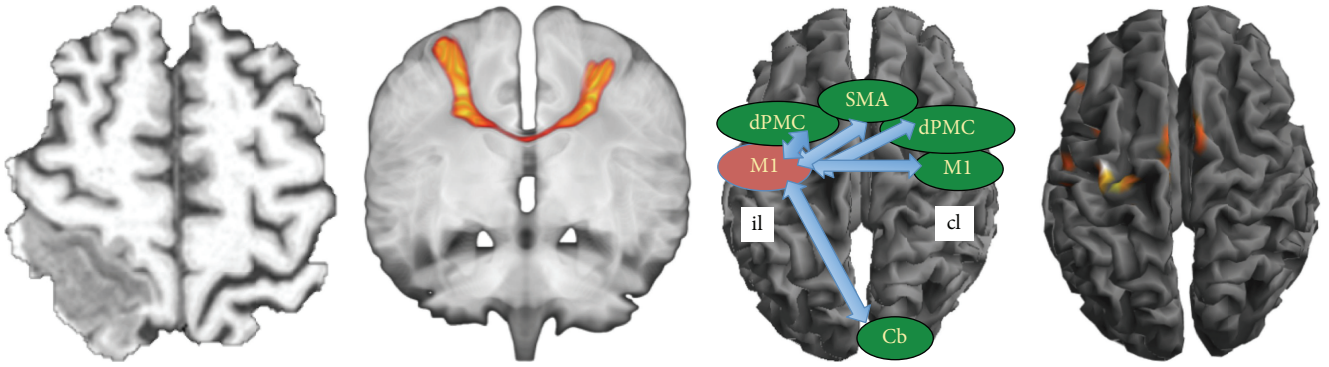

Figure 2: Two structural and two functional imaging methods applied in monitoring and predicting hand-motor outcome after stroke. From left to right: lesion mapping on a T1 weighted imaging dataset; diffusion-weighted imaging measuring structural connectivity, demonstrated here with probabilistic tracking between the bilateral primary motor cortices; resting-state fMRI (rs-fMRI) assessing functional connectivity between different regions of interest (Cb: cerebellar anterior hemisphere; dPMC: dorsal premotor cortex; SMA: supplementary motor area); and activation fMRI during active grip strength task with the affected right hand.

discuss some problems that the frequently used imaging techniques are facing and what is necessary to overcome those issues.

Figure 2 provides an overview of the most frequently used imaging techniques for stroke motor imaging.

3.1. Structural Imaging. The clinically most important contribution of MRI to the evaluation of hand-motor outcome is the precise quantification of the damaged neural resources. Particularly, the lesion location and the amount of damage of parts of hand movement representation and their white matter connections are critical parameters assessed with structural imaging (e.g., [19]). Additional impairment (e.g., somatosensory impairment [20]) might decrease the outcome of conventional motor training. It is crucial to add this information in prognostic decisions to allow for more specified training. In addition, some patients with certain lesion locations show extremely good functional recovery (e.g., anterior cerebellar hemisphere lesion), whereas others have almost no recovery potential (e.g., with brain stem or cerebellar vermis lesions). The evaluation of motor impairment, outcome, and therapy approaches is usually based on the experience of the neurologist. However, it usually is difficult to predict the clinical outcome based only on this information. Apart from the individual clinical information like age, concomitant diseases, or education, the anatomical position of the lesion is the most important information. On the other hand, the functional relevance of this anatomical area might be different among different patients, depending, for example, on other lesioned structures as well. Voxel-wise statistics in groups of lesioned patients were able to extend this knowledge [21]. Therefore, lesion mapping is about to find its way in prognostic algorithms in clinical settings and might contribute to prediction of stroke recovery.

To more accurately examine the contribution of white matter damage on motor performance, diffusion-weighted imaging (DWI) strategies have been developed in the last decade, which may exceptionally be integrated into the current clinical routine [18]. DWI-evaluation strategies for motor research are usually limited on tracts connecting areas processing motor control. The standard for hand-motor function is the pyramidal tract running through the posterior limb of the internal capsule (PLIC).

The intactness of the corticospinal tract (CST) can be assessed with axonal or radial diffusivity [22], as well as with fractional anisotropy (FA) [23] within the PLIC. Whereas the usage of axial and radial diffusivity has been criticized [24], the FA is the most robust and most widely applied parameter. FA in the PLIC represents a rather global measure, since tracts from the dorsal premotor cortex (dPMC) and the SMA and the primary motor cortex (M1) and primary somatosensory cortex (S1) and parietal cortex pass through the PLIC.

A decrease in FA in the first days after stroke goes along with the temporal evolution of Wallerian degeneration. Using an ischemic rat model, Wallerian degeneration has been demonstrated to occur during the first days after stroke [25]. In order to assess a robust FA parameter for prognostic considerations, it is recommended to measure DWI not earlier than five days after stroke. Predictability could be improved if DWI is measured after at least two weeks [26].

The intactness of the CST, as tested with diffusion-weighted imaging, has proved very useful for the prediction of hand-motor outcome, especially in more severely affected patients, for example, [27–33]. Parameters assessed with DWI predict the long-term motor outcome better than lesion volume [34]. These parameters can also be used to predict treatment gains in the subacute or chronic stage [35–37].

Besides the corticospinal tract, which has been most frequently assessed, alternate corticofugal fibers and corticocortical connections have recently attracted more attention (for a synopsis, see, e.g., [38]). White matter integrity of noncrossing fibers between M1 and M1 can predict training-induced performance gains in chronic patients [37]. For subacute patients with mild hand-motor impairment, we found a predictive value of $M1^{il}$ to $M1^{cl}$ diffusivity

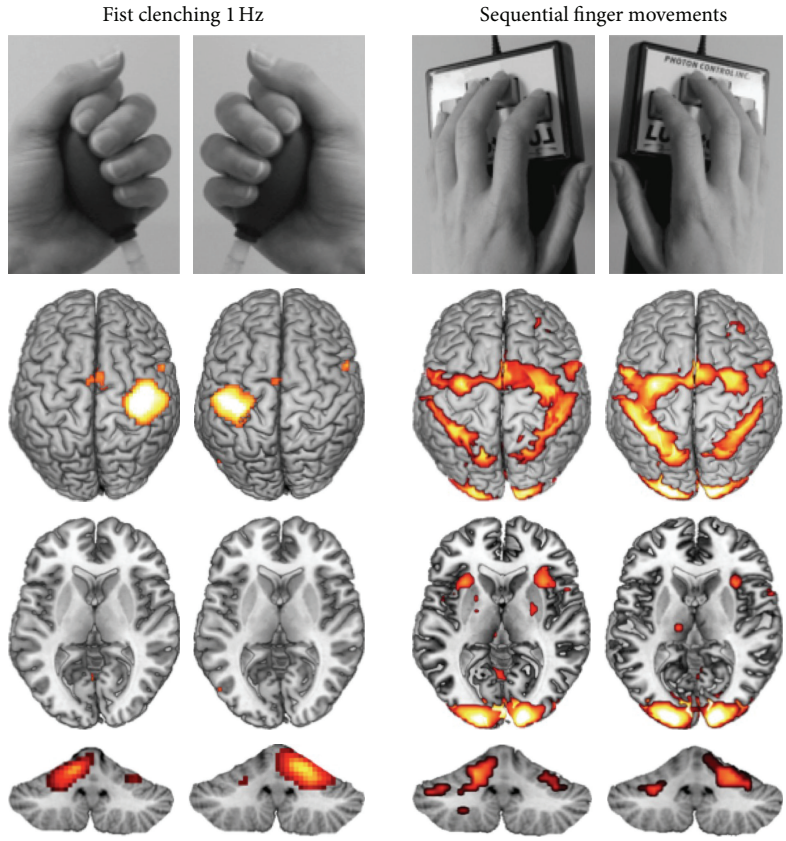

Figure 3: Task characteristics have a crucial impact on fMRI results. Unilateral hand and finger movements performed with left and right hand in a group of 15 right-handed young participants (group results for the premeasurement of the training paradigm reported in [12]). Whereas the fist clenching task shows high lateralization in the cortical and cerebellar representation sites, unilateral finger sequence movements are bilaterally represented. In addition, finger sequences involve basal ganglia and inferior cerebellar hemisphere, at least when performed with the nondominant left hand.

for three- and six-month motor outcome, as tested with the Box and Block test [39]. Especially for tasks requiring bihemispheric resources, such as grasping and transferring objects, these interhemispheric tracts are important, since they enable a bihemispheric coordination of sensorimotor activation [40].

Therefore, structural imaging not only provides stable biomarkers which have become clinically more relevant in predicting motor outcome but also offers enormous potential for developing further parameters to describe the structural intactness of patients in detail.

3.2. Activation fMRI: Activation Representation and Network

3.2.1. Tasks Applied for Activation fMRI after Stroke. Despite the focal damage of a stroke incident, the impact of the lesion leads to local and global changes in brain function. Activation or task-based fMRI has been applied to assess these changes in functional representation after stroke. Two hand-motor tasks are most frequently applied, both allowing a precise control for force and frequency: hand grip using visual feedback of strength [41, 42] and finger sequence using MRI-compatible keyboards [43].

Figure 3 shows typical representation maps for the hand grip modulation and the finger sequence task in a group of healthy young volunteers.

3.2.2. General Findings for Activation fMRI after Stroke. In general, patients showed increased diffuse activation in several areas including motor areas in comparison to healthy controls during different motor tasks. When patients move their affected hand, the lateralization and focus on the contralateral primary sensorimotor cortex during simple unilateral movements (Figure 3) are less expressed than in healthy controls [41]. The increased activation in motor areas of both the damaged hemisphere (ipsilesional) and the unaffected hemisphere (contralesional) has been repeatedly reported (e.g., [44]; meta-analysis by [45]). This increase in activation fMRI in motor areas during simple hand movements often diminishes if recovery is successful. If the increase sustains in later stages, it is often associated with greater motor impairment [41, 46]. The increased use of secondary motor areas can be associated with less functionality of the arm as assessed with accelerometers [47].

In contrast, good motor recovery is related to near-normal activation patterns [48, 49]. One main marker for

good recovery seems to be the focused recruitment of the ipsilesional M1 during movement of the affected hand [50–52]. This high recruitment of neural resources of the somatotopic hand representation as a positive sign for well recovered hand-motor function is also characteristic of motor recovery after traumatic brain injury [53].

A prognostic marker for less motor outcome might therefore be assigned to the activation of the contralesional M1 [54] during movements with the affected hand. This hypothesis is supported by a study showing more activity in patients with more severe impairments [55].

Nonetheless, some processes seem to contradict this near to normal hypothesis. The focus on the $M1^{il}$ does not necessarily imply good recovery [56], and even good recovering patients may show $M1^{cl}$ activation [57–60]. The importance of the contralesional hemisphere is not completely understood, but for some patients it may be indicative of involvement of recovered motor function [43]. While lateralization of cortical activation obtained with fMRI is associated with motor impairment in the chronic stage [40], it is not a relevant predictor of change scores resulting from training [61].

In addition, specifically the dorsal premotor cortex (dPMC) has been shown to be profoundly activated in stroke patients [62], and improved motor performance has often been associated with increased dPMC activation in the damaged hemisphere [63]. The dPMC in both hemispheres might have functional significance for patients with partial recovery after stroke [64]. There is also evidence for an enhanced involvement of the ventral premotor cortex (vPMC) [65] and the supplementary motor area (SMA) [63] in restoring motor functions.

3.2.3. Activation fMRI Network Analysis. To elucidate the role of the different regions involved in recovery processes activation, fMRI also enables network analyses to gain information about the interaction of motor areas. There are different methods to assess connectivity between regions, such as dynamic causal modelling (DCM) and structural equation modelling (SEM). An overview of connectivity in stroke networks is provided in [66]. The main results from activation studies are confirmed in network analyses: good recovery is accompanied by network parameters similar to healthy controls. If premotor and supplementary motor areas interact at a lower level with the ipsilesional motor cortex, this decrease is associated with impairment [67–69]. In addition, an inhibitory influence of $M1^{cl}$ to $M1^{il}$ at later stages of recovery is associated with poorer motor outcome [67, 68], which is congruent with the model of suppression of the ipsilesional hemisphere by the contralesional side [70]. Overall, patients that show good recovery have a high integration of $M1^{il}$ in the motor network, for example, [71].

Although network analyses might give more insight into the underlying processes of recovery, they are rarely integrated in prediction analyses. This is mainly due to the hypothesis-driven character of the analyses, focusing only on some aspects of the motor network rather than on its entire complexity. As recovery and the resulting changes in the motor network are highly individual, the same clinical outcome could be driven by different network changes. The methods are therefore promising for assessing individual changes in the motor network over time but are more difficult to apply on inhomogeneous patient groups because different aspects of the motor network are of interest in various recovery courses. In addition, due to the ongoing development of these network analyses, some results are highly dependent on the analysis software [72]. Up to now, more time is needed to establish robust methods before integrating them to prognostic schemes.

3.2.4. Problems with Activation fMRI for Stroke. Whereas the investigation of the functionality of the injured brain during certain motor tasks is promising, there are some difficulties with fMRI protocols.

Since the results obtained in an activation task are dependent on the task and the compliance of the participant to fulfill the protocol, it is crucial to control for task performance; otherwise, performance cannot be distinguished from altered representation. Especially for longitudinal studies, the performance and the effort between the measurements have to be balanced [15]. Performance control during imaging is essential, since movement parameters such as force, amplitude, and frequency are associated with the magnitude of activation fMRI [15, 73, 74]. In addition, especially for large lesions, the question of mirrored movements with the unaffected hand is of high importance, decreasing lateralization of representation to the ipsilesional hemisphere.

Even in healthy subjects, there are major differences in brain activation, depending on the task type (Figure 3), movement patterns involved, task difficulty, or attention. This variance in tasks tested, in addition to the different measures of hand function, makes it more difficult to compare the results of different studies. It is therefore necessary to assess this variance in healthy controls, especially in people of various ages, as the experienced task difficulty and the resulting activation fMRI patterns have been shown to strongly depend on age [75].

Even so, it is often questionable which task depicts the recovery process most accurately. The task has to be accurate enough to capture the impairment effects but simple enough to be carried out by all investigated patients. It is difficult to compare the activation patterns of patients with different severities of stroke. If differences in brain activation only illustrate the task not being executed properly, the usefulness for stroke prediction is low (see, e.g., [76] for compliance of swallowing performance in stroke patients). Therefore, only patients who are able to perform the task can be investigated.

Another problem arises when analyzing movements involving the proximal upper limb (e.g., in aiming tasks), as these increase movement artifacts and are therefore of limited use.

Increased associated head movements in stroke patients who struggle to fulfill the protocol are a general problem, also in other tasks. These head movements exclude a significant number of patients from group analyses, leading to a preselection, and biasing, of patient population.

When examining stroke recovery with fMRI, major problems arise from the interpretation of differences in activation patterns between individuals and the variation within an individual during the recovery course. Therefore, it is difficult to assign the outcome to the activation of a certain region. For example, a diminishing activation of premotor areas in well recovering patients is a good prognostic sign, but patients with more damage to the tracts might profit from dPMC activation which supports motor output. Many factors, such as lesion size, lesion location, age, structural damage, potential for plasticity, previous training experience, and motivation, affect the recovery course and thus the functional activation during motor tasks. In addition, patients in different studies are measured at different time points after stroke. Ward and colleagues have claimed that the depicted changes are more likely a function of recovery than of time [15]. This explains why different patients, even when measured at the same time after stroke, can show different activation patterns.

Activation fMRI analyses can therefore be useful when depicting an individual recovery course over time, as plasticity processes can be observed in direct relation to the motor functions of interest. In examining groups, it is challenging to balance the task requirements over all subjects. Passive tasks may be suited to be used in early stages after stroke, but they do not always reflect the various differences in motor recovery in detail [42].

Therefore, task-based fMRI can be of importance to assess slight differences in compensational areas or lateralization between hemispheres if the patients are preselected according to their ability to fulfill the protocol.

3.2.5. Can Knowledge of Changes in Functional Representation during Short- and Long-Term Training Procedures by Healthy Participants Help to Understand Motor Recovery in Patients after Stroke? One approach to understanding the processes of motor recovery in patients is the transfer of knowledge of plasticity processes during training in healthy controls. Representational changes after short- and long-term hand-motor training in healthy volunteers show characteristic differences. Short-term training is characterized by an increase in fMRI magnitude in anterior cerebellar hemisphere and the dorsomedial basal ganglia and a decrease in dorsolateral prefrontal cortical representation [77]. In addition to further cortical economization, long-term training is characterized by increased dorsolateral basal ganglia activation and contralateral M1/S1 activation and decreased cerebellar activation [77] (for extremely long trained instrumentalists, see [78]). When performing training protocols developed for stroke patients (arm ability training [79]), healthy young volunteers showed cortical economization in a finger sequence task after two weeks of training for the nondominant upper limb. In a hand grip task with visual feedback, these subjects showed a focused activation pattern in contralateral putamen and ipsilateral anterior cerebellum [12]. In contrast, using the same training strategy to increase hand-motor performance in patients in the subacute stage after stroke, representational changes in visual feedback hand-strength modulation task have only been located in the ventral premotor cortex (vPMC; [42]). Here, the knowledge about fMRI representation of long-term training in healthy volunteers appeared to be of limited value for the training in patients after stroke. In stroke patients there are many reorganization processes, including general recovery processes, task-specific training effects, and compensatory processes [80]. In addition, different lesion locations have different impacts on network disturbances, which might alter short-term and long-term training processes. Overall, processes observed during the recovery of motor ability in patients are difficult to equate with the changes taking place during motor training in healthy volunteers, but assessing training processes in healthy subjects can help to differentiate the various processes involved in stroke recovery.

3.3. Resting-State fMRI. In the light of the difficulties of activation of fMRI discussed above, resting-state fMRI (rs-fMRI) seems promising, since it requires little compliance. Rs-fMRI can therefore be conducted in the acute (0–24 hours after stroke onset) to subacute (24 h to 6 weeks after stroke) phase after stroke, comparable to structural MRI [81]. With respect to hand-motor function after stroke, specifically the functional connectivity (FC) of rs-fMRI between cortical motor areas has been described to be associated with motor impairment [82]. Overall, stroke patients with motor impairment show initially decreased interhemispheric M1 connectivity and increased connectivity between ipsilesional M1 and secondary motor areas, particularly in the ipsilesional hemisphere [83].

Indeed, for patients with motor impairment after stroke, an initially decreased rsFC between $M1^{il}$ and $M1^{cl}$ in comparison to healthy age-matched controls is the most consistent finding reported in resting-state studies on stroke patients [69, 82–86]. Previous studies measuring rsFC at the subacute stage found significant associations with motor performance at time of fMRI [82, 84]. This reduced interhemispheric rsFC between the primary motor cortices showed an increase over a period of three months [85] and is associated with motor improvements when increasing up to the level of healthy controls [87]. Park and colleagues [86] investigated rs-fMRI in 12 subacute stroke patients to estimate the value of rsFC for predicting motor outcome. They found a positive association between six-month motor outcome measured with Fugl-Meyer score and rsFC of the $M1^{il}$ with the contralesional thalamus, supplementary motor area (SMA), and medial frontal gyrus.

In contrast, investigating rsFC in the subacute stage, Lindow and colleagues [39] found no predictive value for early or late outcomes. They only observed associations with the motor function at the same time of recovery after mild hand-motor impairment and interpreted the lack of prognostic findings in the highly fluctuating character of rsFC after stroke as previously documented by [85]. The latter authors investigated 31 stroke patients with motor impairment within the first 24 hours and after 7 and after 90 days and found that the reduced interhemispheric sensorimotor (SM1) rsFC normalized over time. Their work is an excellent example of how rsFC can vary after stroke, and this variability may well

be the reason why long-term motor outcome prediction is problematic using this measurement.

In the light of different individual recovery curves (see Figure 1), a measurement variable with high predictive value should provide constant parameters in the clinically most interesting subacute phase (which is the case, e.g., with FA measured with DTI). For monitoring the impact of a therapeutic intervention on changes in the motor network, a highly responsive parameter indicating individual changes over time might be more suitable. This has recently been demonstrated with rs-fMRI for monitoring changes induced by transcranial direct current stimulation (TDCS [88]).

3.4. Combining Measurements. Each of the methods described here is to some extent suitable for hand-motor outcome prediction, depending on the outcome parameters, time point of measurement, patient group, and so forth. This raises the question of whether different methods might depict associated characteristics or whether they have a different predictive value. Whereas DTI or lesion maps define structural deficits, task-based and task-free fMRIs depict a functionality of the motor network. Therefore, different measures might complement each other.

Some studies included multiple methods to predict motor outcome of stroke patients. DTI and resting-state fMRI have both been assessed to evaluate motor impairment [84, 89] or to predict recovery [39]. In other studies, DTI and activation of fMRI measures also constitute a good combination to detect structural and functional markers for stroke prediction or monitoring of impairment status [61, 90–92]. In addition, transcranial magnetic stimulation (TMS) is frequently used to complement imaging methods [16, 29, 61, 93]. Whereas TMS has a higher positive predictive power, DWI of the pyramidal tract has a higher negative predictive power [94].

The overall results of the various methods were replicated here, but some of the measurements are correlated with each other. For instance, it has been observed that CST damage and rsFC are associated [84, 89, 95]. fMRI measures are also related to the tract damage [40, 92, 96–98]. In general, functional and structural connectivity are often correlated, but functional connectivity can also be present if there is a rather indirect than direct structural connection [99].

Although some potential associations exist, different parameters usually depict different aspects. DTI parameters do not necessarily correlate with TMS measures of tract projections [40] because they may depend on other aspects such as distance of motor neurons stimulated from the scalp (e.g., [100]) or interactions of the motor network.

Similarly, functional parameters such as rsFC and activation of fMRI show no relevant associations [101]. Carter and colleagues found an interesting association between the rsFC and the observed motor outcome [84]. Measuring 23 stroke patients in the subacute stage with resting-state and DTI, they observed that rsFC was only associated with motor outcome when CST damage was low. This study is a good example of the prognostic value of a functional biomarker depending on the structural level.

This hierarchical structure needs to be kept in mind when investigating stroke recovery and searching for biomarkers. It is illustrated in Figure 4 that stroke results in structural brain damage; the more brain structures representing motor function are destroyed, the lower the probability to recover motor function is.

After stroke, the primary goal is to regain motor function. Can the desired function be achieved? If the answer is no, the next question is, is there at least a potential for functionality? If the answer is no again, the following question is, is the structure at least as intact as needed for compensatory processes?

These questions are asked by the predicting recovery potential (PREP) algorithm [30] to assess hand-motor outcome after stroke. Biomarkers are used at each level to answer how the patient's status can be described. At the motor output level, the assessment via SAFE score (sum of the shoulder abduction and finger extension) distinguishes patients with already good functionality of the hand and arm from those without. For the latter group, TMS then helps to determine whether there is a potential for functionality and subsequent recovery (i.e., motor-evoked potential (MEP) present/absent). In case of a lack of MEP, a further distinction between patients can be made on a structural level by DWI measurements. The FA parameter in the PLIC described above can give information about the structural damage in terms of an asymmetry index between the affected and unaffected hemisphere. Here imaging methods complement the established assessments to classify patients in groups for therapeutic decisions.

When focusing on motor function, the PREP algorithm makes a meaningful classification. Because in a clinical setting even more fine-grained classifications are needed; the potential for more biomarkers is clear, especially in patients with notable recovery potential, who constitute a rather diverse group.

When evaluating the functionality of a structure, the presence of a MEP is a rather rough measure. It would be interesting to know which regions have retained their functionality. As mentioned before, the restoration of the lesioned motor network is crucial for the recovery of motor performance. If the contralesional hemisphere is involved in simple unilateral movements of the affected hand, prognostic signs are worse. The contralesional hemisphere may interfere with the recovery process of the ipsilesional hemisphere by suppressing the motor output of this hemisphere [70]. Therefore, the functional level could be assessed in more detail, for example, with TMS silent period or resting state determining the balance between hemispheres. If there is a strong interhemispheric imbalance, additional modulations are desirable.

In some groups, a further classification can also be useful, especially regarding therapy decisions. For example, determining the amount of structural damage in other structures apart from the PLIC is valuable in assessing the precise potential for motor recovery or compensation processes. With a more fine-grained classification, better therapy decisions can be made.

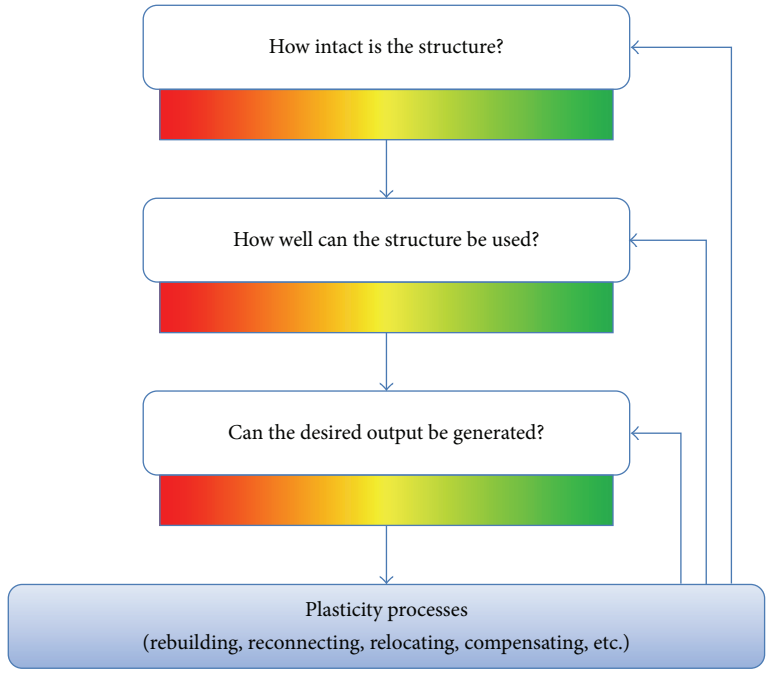

Figure 4: The processes in the brain after stroke can be separated into different hierarchical levels: structural damage (from severe to nearly none) is caused by the stroke incident. Functional recovery potential is usually related to the spared resources of the affected network. The more severe the damage is, the less likely it is to achieve a certain level of functionality. A lack of functionality in turn leads to a poor outcome. Different strategies of the brain, such as compensation with other areas, try to tackle these problems early after stroke. Plasticity processes can start at any of these levels. Note that the intactness and usability of a structure depend on the structural integrity and functionality of various regions and connections, which are important in different ways for generating a certain motor output.

It is therefore of utmost importance to investigate certain predefined groups to differentiate them further and to assess multiple parameters early after stroke. Apart from a few exceptions (e.g., [29, 30, 39, 93]), there is a striking lack of prediction studies in acute patients using different modalities. Of course this is due to the high effort when imaging with different measures in a clinical setting. With a stepwise algorithm, however, only a few parameters need to be assessed for each patient, since, for most of the less impaired patients, imaging biomarkers are not necessary. One strategy to cope with the need for decision diagrams is pooling data and establishing large databases. This way, shaping the subgroups may become easier because patients with comparable structural damage can be assessed together. Databases such as PLORAS for the language network are also a promising prototype for motor recovery databases [102]. Specifically, structural imaging or rs-fMRI can complement the existing methods in acute stroke patients, as these methods are easier to implement in the clinical setting than task-based fMRI.

Early measurements can also provide a basis for simulations of how the functionality will probably be affected by certain structural deficits. One approach is implemented in The Virtual Brain (TVB), a novel application for modelling brain dynamics that simulates an individual's brain activity by integrating his own neuroimaging data with local biophysical models [103]. Those biophysical models have to be underpinned with data on the relationship of different measures and an understanding of the processes at different hierarchical levels. However, this understanding still needs to be improved, as most of the methods are still not fully understood, and basic research is necessary to assess all factors influencing the imaging results.

Imaging can add information in the therapeutic decision process if the type of functional deficit can be assessed as early as possible. As mentioned, the hierarchy ends with a certain function on which our assessment is based. It is therefore useful to know which function will be in deficit and needs to be prioritized. Many stroke patients show neuropsychological impairments like aphasia, apraxia, ataxia, neglect, and depression. The relative risk of these impairments might be detected by lesion mapping comparing the location of lesion to probability maps of large data sets of patients functionally investigated. Specifically, those with a high probability of additional impairment need further specific testing. For instance, a patient with neglect needs specific therapy for this concern in addition to motor therapy. In addition, it would be helpful to know and predict the interference among different impairments, for example, with neuropsychological deficits and motor impairments.

Another approach to assessing stroke recovery is apparent from Figure 4: the ongoing process of plasticity applies to every stage of the structure-function hierarchy. As already mentioned, the depicted changes are more likely a function of recovery than of time [15]. Besides the possibility of combining imaging methods, there is the need to measure recovery process longitudinally to assess plasticity processes

in detail. This multilayered assessment of individual patients will deepen our understanding of the processes during recovery, which is an important step in the intervention and support with therapy programs.

The mentioned problems regarding the high intersubject variance in methods such as task-based or rest fMRI can be circumvented by using imaging markers as monitoring parameters [15, 88]. In prediction algorithms, imaging can not only help to assess the potential for a certain outcome, but also extend the knowledge predicting the different recovery stages, which may allow us to identify additional factors that contribute to the course of events.

4. Conclusion

Procedures with a low level of instruction, low need for patient compliance, short imaging time, and standardized data evaluation strategies are especially promising for both the monitoring and prognosis of hand-motor performance after stroke or brain damage after traumatic brain injury. Over the last years, brain imaging procedures have made a significant step towards becoming a standardized approach, enabling the clinical usage of tools that were previously limited to scientific use. Whereas predictive parameters should be robust and stable over time (such as structural imaging parameters), monitoring needs more sensitive methods for functional changes under intervention (e.g., resting-state fMRI).

In the light of the high prognostic and monitoring effects of nonimaging procedures such as testing motor performance (arm extension) or motor-evoked potentials of hand muscles, the role of the methodologically more challenging imaging procedures is optimally utilized in an algorithm. Currently, the PREP algorithm is the most promising step in this direction. Future extensions will focus on certain subgroups as determined by imaging parameters and assess the best therapy approaches for individual patients. This procedure will help to considerably save resources and optimize neurorehabilitative therapy.

Competing Interests

The authors declare that there is no conflict of interests regarding the publication of this paper.

Acknowledgments

M. Lotze was supported by a grant from the German Research Foundation (DFG Lo795/7-1). U. Horn was financed by a graduate scholarship from the state of Mecklenburg-Vorpommern. U. Horn and M. Lotze were supported by an interaction project of the North-German Universities (VNU; 2016).

References

[1] V. L. Feigin, M. H. Forouzanfar, R. Krishnamurthi et al., "Global and regional burden of stroke during 1990–2010: findings from the Global Burden of Disease Study 2010," *The Lancet*, vol. 383, no. 9913, pp. 245–255, 2014.

[2] G. Kwakkel, B. J. Kollen, and R. C. Wagenaar, "Long term effects of intensity of upper and lower limb training after stroke: a randomised trial," *Journal of Neurology Neurosurgery and Psychiatry*, vol. 72, no. 4, pp. 473–479, 2002.

[3] E. S. Lawrence, C. Coshall, R. Dundas et al., "Estimates of the prevalence of acute stroke impairments and disability in a multiethnic population," *Stroke*, vol. 32, no. 6, pp. 1279–1284, 2001.

[4] M. Pohl, C. Warner, M. Holzgraefe et al., "Repetitive locomotor training and physiotherapy improve walking and basic activities of daily living after stroke: a single-blind, randomized multicentre trial (DEutsche GAngtrainerStudie, DEGAS)," *Clinical Rehabilitation*, vol. 21, no. 1, pp. 17–27, 2007.

[5] C. J. Winstein, S. L. Wolf, A. W. Dromerick et al., "Effect of a task-oriented rehabilitation program on upper extremity recovery following motor stroke: the ICARE randomized clinical trial," *The Journal of the American Medical Association*, vol. 315, no. 6, pp. 571–581, 2016.

[6] C. Brogårdh, F. W. Johansson, F. Nygren, and B. H. Sjölund, "Mode of hand training determines cortical reorganisation: arandomized controlled study in healthy adults," *Journal of Rehabilitation Medicine*, vol. 42, no. 8, pp. 789–794, 2010.

[7] J. W. Krakauer, S. T. Carmichael, D. Corbett, and G. F. Wittenberg, "Getting neurorehabilitation right: what can be learned from animal models?" *Neurorehabilitation and Neural Repair*, vol. 26, no. 8, pp. 923–931, 2012.

[8] G. Kwakkel, R. C. Wagenaar, J. W. R. Twisk, G. J. Lankhorst, and J. C. Koetsier, "Intensity of leg and arm training after primary middle-cerebral-artery stroke: a randomised trial," *The Lancet*, vol. 354, no. 9174, pp. 191–196, 1999.

[9] G. Kwakkel, B. J. Kollen, J. Van der Grond, and A. J. H. Prevo, "Probability of regaining dexterity in the flaccid upper limb: impact of severity of paresis and time since onset in acute stroke," *Stroke*, vol. 34, no. 9, pp. 2181–2186, 2003.

[10] C. Stinear, "Prediction of recovery of motor function after stroke," *The Lancet Neurology*, vol. 9, no. 12, pp. 1228–1232, 2010.

[11] B. H. Dobkin and S. T. Carmichael, "The specific requirements of neural repair trials for stroke," *Neurorehabilitation and Neural Repair*, vol. 30, no. 5, pp. 470–478, 2016.

[12] A. D. Walz, K. Doppl, E. Kaza, S. Roschka, T. Platz, and M. Lotze, "Changes in cortical, cerebellar and basal ganglia representation after comprehensive long term unilateral hand motor training," *Behavioural Brain Research*, vol. 278, pp. 393–403, 2015.

[13] T. Platz, S. Roschka, M. I. Christel, F. Duecker, J. C. Rothwell, and A. Sack, "Early stages of motor skill learning and the specific relevance of the cortical motor system—a combined behavioural training and theta burst TMS study," *Restorative Neurology and Neuroscience*, vol. 30, no. 3, pp. 199–211, 2012.

[14] B. H. Dobkin, "Wearable motion sensors to continuously measure real-world physical activities," *Current Opinion in Neurology*, vol. 26, no. 6, pp. 602–608, 2013.

[15] N. S. Ward, M. M. Brown, A. J. Thompson, and R. S. J. Frackowiak, "Neural correlates of motor recovery after stroke: a longitudinal fMRI study," *Brain*, vol. 126, no. 11, pp. 2476–2496, 2003.

[16] E. B. Quinlan, L. Dodakian, J. See et al., "Neural function, injury, and stroke subtype predict treatment gains after stroke," *Annals of Neurology*, vol. 77, no. 1, pp. 132–145, 2015.

[17] R. Schulz, P. Koch, M. Zimerman et al., "Parietofrontal motor pathways and their association with motor function after stroke," *Brain*, vol. 138, no. 7, pp. 1949–1960, 2015.

[18] M. A. Petoe, W. D. Byblow, E. J. M. De Vries et al., "A template-based procedure for determining white matter integrity in the internal capsule early after stroke," *NeuroImage: Clinical*, vol. 4, pp. 695–700, 2014.

[19] S. J. Page, L. V. Gauthier, and S. White, "Size doesn't matter: cortical stroke lesion volume is not associated with upper extremity motor impairment and function in mild, chronic hemiparesis," *Archives of Physical Medicine and Rehabilitation*, vol. 94, no. 5, pp. 817–821, 2013.

[20] E. Abela, J. Missimer, R. Wiest et al., "Lesions to primary sensory and posterior parietal cortices impair recovery from hand paresis after stroke," *PLoS ONE*, vol. 7, no. 2, Article ID e31275, 2012.

[21] C. Rorden and H.-O. Karnath, "Using human brain lesions to infer function: a relic from a past era in the fMRI age?" *Nature Reviews Neuroscience*, vol. 5, no. 10, pp. 813–819, 2004.

[22] L. van Dokkum, I. Hauret, D. Mottet, J. Froger, J. Métrot, and I. Laffont, "The contribution of kinematics in the assessment of upper limb motor recovery early after stroke," *Neurorehabilitation and Neural Repair*, vol. 28, no. 1, pp. 4–12, 2014.

[23] R. Schulz, C.-H. Park, M.-H. Boudrias, C. Gerloff, F. C. Hummel, and N. S. Ward, "Assessing the integrity of corticospinal pathways from primary and secondary cortical motor areas after stroke," *Stroke*, vol. 43, no. 8, pp. 2248–2251, 2012.

[24] C. A. M. Wheeler-Kingshott and M. Cercignani, "About 'axial' and 'radial' diffusivities," *Magnetic Resonance in Medicine*, vol. 61, no. 5, pp. 1255–1260, 2009.

[25] H. Iizuka, K. Sakatani, and W. Young, "Neural damage in the rat thalamus after cortical infarcts," *Stroke*, vol. 21, no. 5, pp. 790–794, 1990.

[26] Y. H. Kwon, Y. J. Jeoung, J. Lee et al., "Predictability of motor outcome according to the time of diffusion tensor imaging in patients with cerebral infarct," *Neuroradiology*, vol. 54, no. 7, pp. 691–697, 2012.

[27] J. Konishi, K. Yamada, O. Kizu et al., "MR tractography for the evaluation of functional recovery from lenticulostriate infarcts," *Neurology*, vol. 64, no. 1, pp. 108–113, 2005.

[28] M. Nelles, J. Gieseke, S. Flacke, L. Lachenmayer, H. H. Schild, and H. Urbach, "Diffusion tensor pyramidal tractography in patients with anterior choroidal artery infarcts," *American Journal of Neuroradiology*, vol. 29, no. 3, pp. 488–493, 2008.

[29] W. D. Byblow, C. M. Stinear, P. A. Barber, M. A. Petoe, and S. J. Ackerley, "Proportional recovery after stroke depends on corticomotor integrity," *Annals of Neurology*, vol. 78, no. 6, pp. 848–859, 2015.

[30] C. M. Stinear, P. A. Barber, M. Petoe, S. Anwar, and W. D. Byblow, "The PREP algorithm predicts potential for upper limb recovery after stroke," *Brain*, vol. 135, no. 8, pp. 2527–2535, 2012.

[31] B. N. Groisser, W. A. Copen, A. B. Singhal, K. K. Hirai, and J. D. Schaechter, "Corticospinal tract diffusion abnormalities early after stroke predict motor outcome," *Neurorehabilitation and Neural Repair*, vol. 28, no. 8, pp. 751–760, 2014.

[32] T. Koyama, M. Tsuji, H. Miyake, T. Ohmura, and K. Domen, "Motor outcome for patients with acute intracerebral hemorrhage predicted using diffusion tensor imaging: an application of ordinal logistic modeling," *Journal of Stroke and Cerebrovascular Diseases*, vol. 21, no. 8, pp. 704–711, 2012.

[33] Y. Kusano, T. Seguchi, T. Horiuchi et al., "Prediction of functional outcome in acute cerebral hemorrhage using diffusion tensor imaging at 3T: a prospective study," *American Journal of Neuroradiology*, vol. 30, no. 8, pp. 1561–1565, 2009.

[34] J. Puig, S. Pedraza, G. Blasco et al., "Acute damage to the posterior limb of the internal capsule on diffusion tensor tractography as an early imaging predictor of motor outcome after stroke," *American Journal of Neuroradiology*, vol. 32, no. 5, pp. 857–863, 2011.

[35] J. D. Riley, V. Le, L. Der-Yeghiaian et al., "Anatomy of stroke injury predicts gains from therapy," *Stroke*, vol. 42, no. 2, pp. 421–426, 2011.

[36] J. Song, V. A. Nair, B. M. Young et al., "DTI measures track and predict motor function outcomes in stroke rehabilitation utilizing BCI technology," *Frontiers in Human Neuroscience*, vol. 9, article 195, 2015.

[37] R. Lindenberg, L. L. Zhu, T. Rüber, and G. Schlaug, "Predicting functional motor potential in chronic stroke patients using diffusion tensor imaging," *Human Brain Mapping*, vol. 33, no. 5, pp. 1040–1051, 2012.

[38] P. Koch, R. Schulz, and F. C. Hummel, "Structural connectivity analyses in motor recovery research after stroke," *Annals of Clinical and Translational Neurology*, vol. 3, no. 3, pp. 233–244, 2016.

[39] J. Lindow, M. Domin, M. Grothe, U. Horn, S. B. Eickhoff, and M. Lotze, "Connectivity-based predictions of hand motor outcome for patients at the subacute stage after stroke," *Frontiers in Human Neuroscience*, vol. 10, article 101, 2016.

[40] M. Lotze, W. Beutling, M. Loibl et al., "Contralesional motor cortex activation depends on ipsilesional corticospinal tract integrity in well-recovered subcortical stroke patients," *Neurorehabilitation and Neural Repair*, vol. 26, no. 6, pp. 594–603, 2012.

[41] N. S. Ward, M. M. Brown, A. J. Thompson, and R. S. J. Frackowiak, "Neural correlates of outcome after stroke: a cross-sectional fMRI study," *Brain*, vol. 126, no. 6, pp. 1430–1448, 2003.

[42] U. Horn, S. Roschka, K. Eyme, A. D. Walz, T. Platz, and M. Lotze, "Increased ventral premotor cortex recruitment after arm training in an fMRI study with subacute stroke patients," *Behavioural Brain Research*, vol. 308, pp. 152–159, 2016.

[43] M. Lotze, J. Markert, P. Sauseng, J. Hoppe, C. Plewnia, and C. Gerloff, "The role of multiple contralesional motor areas for complex hand movements after internal capsular lesion," *The Journal of Neuroscience*, vol. 26, no. 22, pp. 6096–6102, 2006.

[44] P. M. Rossini, C. Calautti, F. Pauri, and J.-C. Baron, "Post-stroke plastic reorganisation in the adult brain," *The Lancet Neurology*, vol. 2, no. 8, pp. 493–502, 2003.

[45] A. K. Rehme, S. B. Eickhoff, C. Rottschy, G. R. Fink, and C. Grefkes, "Activation likelihood estimation meta-analysis of motor-related neural activity after stroke," *NeuroImage*, vol. 59, no. 3, pp. 2771–2782, 2012.

[46] L. J. Volz, A.-S. Sarfeld, S. Diekhoff et al., "Motor cortex excitability and connectivity in chronic stroke: a multimodal model of functional reorganization," *Brain Structure & Function*, vol. 220, no. 2, pp. 1093–1107, 2015.

[47] K. J. Kokotilo, J. J. Eng, M. J. McKeown, and L. A. Boyd, "Greater activation of secondary motor areas is related to less arm use after stroke," *Neurorehabilitation and Neural Repair*, vol. 24, no. 1, pp. 78–87, 2010.

[48] S. C. Cramer, "Functional imaging in stroke recovery," *Stroke*, vol. 35, no. 11, supplement 1, pp. 2695–2698, 2004.

[49] D. Tombari, I. Loubinoux, J. Pariente et al., "A longitudinal fMRI study: in recovering and then in clinically stable sub-cortical stroke patients," *NeuroImage*, vol. 23, no. 3, pp. 827–839, 2004.

[50] S. C. Cramer, A. Mark, K. Barquist et al., "Motor cortex activation is preserved in patients with chronic hemiplegic stroke," *Annals of Neurology*, vol. 52, no. 5, pp. 607–616, 2002.

[51] T. Askim, B. Indredavik, T. Vangberg, and A. Håberg, "Motor network changes associated with successful motor skill relearning after acute ischemic stroke: a longitudinal functional magnetic resonance imaging study," *Neurorehabilitation and Neural Repair*, vol. 23, no. 3, pp. 295–304, 2009.

[52] C. Calautti, P. S. Jones, M. Naccarato et al., "The relationship between motor deficit and primary motor cortex hemispheric activation balance after stroke: longitudinal fMRI study," *Journal of Neurology, Neurosurgery and Psychiatry*, vol. 81, no. 7, pp. 788–792, 2010.

[53] M. Lotze, W. Grodd, F. A. Rodden et al., "Neuroimaging patterns associated with motor control in traumatic brain injury," *Neurorehabilitation and Neural Repair*, vol. 20, no. 1, pp. 14–23, 2006.

[54] Y. Dong, B. H. Dobkin, S. Y. Cen, A. D. Wu, and C. J. Winstein, "Motor cortex activation during treatment may predict therapeutic gains in paretic hand function after stroke," *Stroke*, vol. 37, no. 6, pp. 1552–1555, 2006.

[55] R. S. Marshall, E. Zarahn, L. Alon, B. Minzer, R. M. Lazar, and J. W. Krakauer, "Early imaging correlates of subsequent motor recovery after stroke," *Annals of Neurology*, vol. 65, no. 5, pp. 596–602, 2009.

[56] A. Feydy, R. Carlier, A. Roby-Brami et al., "Longitudinal study of motor recovery after stroke: recruitment and focusing of brain activation," *Stroke*, vol. 33, no. 6, pp. 1610–1617, 2002.

[57] H. Foltys, T. Krings, I. G. Meister et al., "Motor representation in patients rapidly recovering after stroke: a functional magnetic resonance imaging and transcranial magnetic stimulation study," *Clinical Neurophysiology*, vol. 114, no. 12, pp. 2404–2415, 2003.

[58] C. M. Bütefisch, R. Kleiser, B. Körber et al., "Recruitment of contralesional motor cortex in stroke patients with recovery of hand function," *Neurology*, vol. 64, no. 6, pp. 1067–1069, 2005.

[59] D. G. Nair, S. Hutchinson, F. Fregni, M. Alexander, A. Pascual-Leone, and G. Schlaug, "Imaging correlates of motor recovery from cerebral infarction and their physiological significance in well-recovered patients," *NeuroImage*, vol. 34, no. 1, pp. 253–263, 2007.

[60] A. Riecker, K. Gröschel, H. Ackermann, S. Schnaudigel, J. Kassubek, and A. Kastrup, "The role of the unaffected hemisphere in motor recovery after stroke," *Human Brain Mapping*, vol. 31, no. 7, pp. 1017–1029, 2010.

[61] C. M. Stinear, P. A. Barber, P. R. Smale, J. P. Coxon, M. K. Fleming, and W. D. Byblow, "Functional potential in chronic stroke patients depends on corticospinal tract integrity," *Brain*, vol. 130, no. 1, pp. 170–180, 2007.

[62] S. Bestmann, O. Swayne, F. Blankenburg et al., "The role of contralesional dorsal premotor cortex after stroke as studied with concurrent TMS-fMRI," *Journal of Neuroscience*, vol. 30, no. 36, pp. 11926–11937, 2010.

[63] H. Johansen-Berg, H. Dawes, C. Guy, S. M. Smith, D. T. Wade, and P. M. Matthews, "Correlation between motor improvements and altered fMRI activity after rehabilitative therapy," *Brain*, vol. 125, no. 12, pp. 2731–2742, 2002.

[64] H. Johansen-Berg, M. F. S. Rushworth, M. D. Bogdanovic, U. Kischka, S. Wimalaratna, and P. M. Matthews, "The role of ipsilateral premotor cortex in hand movement after stroke," *Proceedings of the National Academy of Sciences of the United States of America*, vol. 99, no. 22, pp. 14518–14523, 2002.

[65] I. Loubinoux, S. Dechaumont-Palacin, E. Castel-Lacanal et al., "Prognostic value of fMRI in recovery of hand function in subcortical stroke patients," *Cerebral Cortex*, vol. 17, no. 12, pp. 2980–2987, 2007.

[66] A. K. Rehme and C. Grefkes, "Cerebral network disorders after stroke: evidence from imaging-based connectivity analyses of active and resting brain states in humans," *Journal of Physiology*, vol. 591, no. 1, pp. 17–31, 2013.

[67] C. Grefkes, D. A. Nowak, S. B. Eickhoff et al., "Cortical connectivity after subcortical stroke assessed with functional magnetic resonance imaging," *Annals of Neurology*, vol. 63, no. 2, pp. 236–246, 2008.

[68] A. K. Rehme, S. B. Eickhoff, L. E. Wang, G. R. Fink, and C. Grefkes, "Dynamic causal modeling of cortical activity from the acute to the chronic stage after stroke," *NeuroImage*, vol. 55, no. 3, pp. 1147–1158, 2011.

[69] L. Wang, C. Yu, H. Chen et al., "Dynamic functional reorganization of the motor execution network after stroke," *Brain*, vol. 133, no. 4, pp. 1224–1238, 2010.

[70] N. S. Ward and L. G. Cohen, "Mechanisms underlying recovery of motor function after stroke," *Archives of Neurology*, vol. 61, no. 12, pp. 1844–1848, 2004.

[71] R. Schulz, A. Buchholz, B. M. Frey et al., "Enhanced effective connectivity between primary motor cortex and intraparietal sulcus in well-recovered stroke patients," *Stroke*, vol. 47, no. 2, pp. 482–489, 2016.

[72] S. Frässle, K. E. Stephan, K. J. Friston et al., "Test-retest reliability of dynamic causal modeling for fMRI," *NeuroImage*, vol. 117, pp. 56–66, 2015.

[73] T. H. Dai, J. Z. Liu, V. Saghal, R. W. Brown, and G. H. Yue, "Relationship between muscle output and functional MRI-measured brain activation," *Experimental Brain Research*, vol. 140, no. 3, pp. 290–300, 2001.

[74] S. C. Cramer, R. M. Weisskoff, J. D. Schaechter et al., "Motor cortex activation is related to force of squeezing," *Human Brain Mapping*, vol. 16, no. 4, pp. 197–205, 2002.

[75] M. Loibl, W. Beutling, E. Kaza, and M. Lotze, "Non-effective increase of fMRI-activation for motor performance in elder individuals," *Behavioural Brain Research*, vol. 223, no. 2, pp. 280–286, 2011.

[76] P. G. Mihai, M. Otto, M. Domin, T. Platz, S. Hamdy, and M. Lotze, "Brain imaging correlates of recovered swallowing after dysphagic stroke: a fMRI and DWI study," *NeuroImage: Clinical*, 2016.

[77] E. Dayan and L. G. Cohen, "Neuroplasticity subserving motor skill learning," *Neuron*, vol. 72, no. 3, pp. 443–454, 2011.

[78] M. Lotze, G. Scheler, H.-R. M. Tan, C. Braun, and N. Birbaumer, "The musician's brain: functional imaging of amateurs and professionals during performance and imagery," *NeuroImage*, vol. 20, no. 3, pp. 1817–1829, 2003.

[79] T. Platz, T. Winter, N. Muller, C. Pinkowski, C. Eickhof, and K.-H. Mauritz, "Arm ability training for stroke and traumatic brain injury patients with mild arm paresis: a single-blind, randomized, controlled trial," *Archives of Physical Medicine and Rehabilitation*, vol. 82, no. 7, pp. 961–968, 2001.

[80] J. W. Krakauer, "Motor learning: its relevance to stroke recovery and neurorehabilitation," *Current Opinion in Neurology*, vol. 19, no. 1, pp. 84–90, 2006.

[81] G. Di Pino, G. Pellegrino, G. Assenza et al., "Modulation of brain plasticity in stroke: a novel model for neurorehabilitation," *Nature Reviews Neurology*, vol. 10, no. 10, pp. 597–608, 2014.

[82] A. R. Carter, S. V. Astafiev, C. E. Lang et al., "Resting interhemispheric functional magnetic resonance imaging connectivity predicts performance after stroke," *Annals of Neurology*, vol. 67, no. 3, pp. 365–375, 2010.

[83] A. K. Rehme, L. J. Volz, D. L. Feis et al., "Identifying neuroimaging markers of motor disability in acute stroke by machine learning techniques," *Cerebral Cortex*, vol. 25, no. 9, pp. 3046–3056, 2015.

[84] A. R. Carter, K. R. Patel, S. V. Astafiev et al., "Upstream dysfunction of somatomotor functional connectivity after corticospinal damage in stroke," *Neurorehabilitation and Neural Repair*, vol. 26, no. 1, pp. 7–19, 2012.

[85] A.-M. Golestani, S. Tymchuk, A. Demchuk, and B. G. Goodyear, "Longitudinal evaluation of resting-state fMRI after acute stroke with hemiparesis," *Neurorehabilitation and Neural Repair*, vol. 27, no. 2, pp. 153–163, 2013.

[86] C.-H. Park, W. H. Chang, S. H. Ohn et al., "Longitudinal changes of resting-state functional connectivity during motor recovery after stroke," *Stroke*, vol. 42, no. 5, pp. 1357–1362, 2011.

[87] H. Xu, W. Qin, H. Chen, L. Jiang, K. Li, and C. Yu, "Contribution of the resting-state functional connectivity of the contralesional primary sensorimotor cortex to motor recovery after subcortical stroke," *PLoS ONE*, vol. 9, no. 1, Article ID e84729, 2014.

[88] J. L. Chen and G. Schlaug, "Increased resting state connectivity between ipsilesional motor cortex and contralesional premotor cortex after transcranial direct current stimulation with physical therapy," *Scientific Reports*, vol. 6, Article ID 23271, 2016.

[89] J. L. Chen and G. Schlaug, "Resting state interhemispheric motor connectivity and white matter integrity correlate with motor impairment in chronic stroke," *Frontiers in Neurology*, vol. 4, article 178, 2013.

[90] M. Qiu, W. G. Darling, R. J. Morecraft, C. C. Ni, J. Rajendra, and A. J. Butler, "White matter integrity is a stronger predictor of motor function than BOLD response in patients with stroke," *Neurorehabilitation and Neural Repair*, vol. 25, no. 3, pp. 275–284, 2011.

[91] M.-H. Milot, S. J. Spencer, V. Chan et al., "Corticospinal excitability as a predictor of functional gains at the affected upper limb following robotic training in chronic stroke survivors," *Neurorehabilitation and Neural Repair*, vol. 28, no. 9, pp. 819–827, 2014.

[92] J. Song, B. M. Young, Z. Nigogosyan et al., "Characterizing relationships of DTI, fMRI, and motor recovery in stroke rehabilitation utilizing brain-computer interface technology," *Frontiers in Neuroengineering*, vol. 7, article 31, 2014.

[93] S. H. Jang, S. H. Ahn, J. Sakong et al., "Comparison of TMS and DTT for predicting motor outcome in intracerebral hemorrhage," *Journal of the Neurological Sciences*, vol. 290, no. 1-2, pp. 107–111, 2010.

[94] Y. H. Kwon, S. M. Son, J. Lee, D. S. Bai, and S. H. Jang, "Combined study of transcranial magnetic stimulation and diffusion tensor tractography for prediction of motor outcome in patients with corona radiata infarct," *Journal of Rehabilitation Medicine*, vol. 43, no. 5, pp. 430–434, 2011.

[95] J. Liu, W. Qin, J. Zhang, X. Zhang, and C. Yu, "Enhanced interhemispheric functional connectivity compensates for anatomical connection damages in subcortical stroke," *Stroke*, vol. 46, no. 4, pp. 1045–1051, 2015.

[96] F. Hamzei, C. Dettmers, M. Rijntjes, and C. Weiller, "The effect of cortico-spinal tract damage on primary sensorimotor cortex activation after rehabilitation therapy," *Experimental Brain Research*, vol. 190, no. 3, pp. 329–336, 2008.

[97] L. E. Wang, M. Tittgemeyer, D. Imperati et al., "Degeneration of corpus callosum and recovery of motor function after stroke: a multimodal magnetic resonance imaging study," *Human Brain Mapping*, vol. 33, no. 12, pp. 2941–2956, 2012.

[98] W. Wei, L. Bai, J. Wang et al., "A longitudinal study of hand motor recovery after sub-acute stroke: a study combined FMRI with diffusion tensor imaging," *PLoS ONE*, vol. 8, no. 5, Article ID e64154, 2013.

[99] J. S. Damoiseaux and M. D. Greicius, "Greater than the sum of its parts: a review of studies combining structural connectivity and resting-state functional connectivity," *Brain Structure and Function*, vol. 213, no. 6, pp. 525–533, 2009.

[100] M. Lotze, R. J. Kaethner, M. Erb, L. G. Cohen, W. Grodd, and H. Topka, "Comparison of representational maps using functional magnetic resonance imaging and transcranial magnetic stimulation," *Clinical Neurophysiology*, vol. 114, no. 2, pp. 306–312, 2003.

[101] J. Zhang, L. Meng, W. Qin, N. Liu, F.-D. Shi, and C. Yu, "Structural damage and functional reorganization in Ipsilesional M1 in well-recovered patients with subcortical stroke," *Stroke*, vol. 45, no. 3, pp. 788–793, 2014.

[102] M. L. Seghier, E. Patel, S. Prejawa et al., "The PLORAS database: a data repository for predicting language outcome and recovery after stroke," *NeuroImage*, vol. 124, pp. 1208–1212, 2016.

[103] M. I. Falcon, J. D. Riley, V. Jirsa et al., "The virtual brain: modeling biological correlates of recovery after chronic stroke," *Frontiers in Neurology*, vol. 6, article 228, 2015.